Universitat Autònoma de Barcelona

# Evolution of swine influenza virus associated with vaccination

**Álvaro López Valiñas**

# Evolution of swine influenza virus associated with vaccination

Álvaro López Valiñas

PhD Thesis

Bellatera, 2022

Universitat Autònoma de Barcelona

# Evolution of swine influenza virus associated with vaccination

Tesis doctoral presentada por **Álvaro López Valiñas** para acceder al grado de Doctor en el marco del programa de Doctorado en *Medicina i Sanitat Animals de la Facultat de Veterinària de la Universitat Autònoma de Barcelona*, bajo la dirección de Dr. **Jóse Ignacio Núñez Garrote** y Dr. **Ayub Darji,** y la tutoría del Dr. **Joaquim Segalés**.

Bellaterra, 2022

IRTA CReSA
Centre de Recerca en Sanitat Animal

The research carried out in the present manuscript has been funded by grant AGL2016–75280-R from Ministerio de Ciencia, Innovación y Universidades from the Spanish government.

Álvaro López Valiñas has a pre-doctoral fellowship FPI 2017 from Ministerio de Ciencia, Innovación y Universidades from the Spanish government.

Cover design: Lorena López Valiñas

El Dr. **Jóse Ignacio Núñez Garrote**, investigador del *Institut de Recerca i Tecnologia Agroalimentàries - Centre de Recerca en Sanitat Animal* (IRTA-CReSA), el Dr. **Ayub Darji** investigador del IRTA-CReSA y el Dr. **Joaquim Segalés Coma**, profesor catedrático del *Departament de Sanitat i d'Anatomia Animals* de la *Facultat de Veterinària* de la *Universidad Autónoma de Barcelona (*UAB*)* e investigador adscrito al IRTA-CReSA.

Certifican que:

Que la memoria titulada "*Evolution of swine influenza virus associated with vaccination*", presentada por **Álvaro López Valiñas** para la obtención del Grado de Doctor en *Medicina i Sanitat Animals* se ha realizado bajo la dirección y tutoría, y autorizan su presentación a fin de ser evaluada por la comisión correspondiente.

Y porque así conste y tenga los efectos que correspondan, firman el presente certificado en Bellaterra (Barcelona), 18 de noviembre de 2022.

Directores Tutor

Dr. Jose Ignacio Núñez Garrote Dr. Ayub Darji Dr. Joaquim Segalés

Doctorando

Álvaro López Valiñas

*A miña familia*

*Un bico ao ceo*

**Table of contents**

# List of abbreviations

**A**

AIV(s): avian influenza virus(es)

ANOVA: analysis of variance

ANT3: adenine nucleotide translocator 3

**B**

BALF: Broncho alveolar lavage fluid

BSL-3: biosafety level 3

**C**

CDC: Centers for Disease Control and Prevention

cH1N1 classic H1N1

CPSF: cleavage and polyadenylation specificity

cRNP: complementary ribonucleoprotein

Ct: threshold cycle

**D**

DMEM: Dulbecco's modified Eagle's medium

dpi: days post infection

dpv: days post vaccination

**E**

EA: Eurasia

ED: Effector Domain

eIF4G1: eukaryotic translation initiation factor 4G1

ELISA: Enzyme-linked immunosorbent assay

EU: European union

**F**

FAO: Food and Agriculture Organization

FBS: fetal bovine serum

G

Genotype 4: G4

H

HA: hemagglutinin

HA1: hemagglutinin subunuit 1

HA2: hemagglutinin subunit 2

HAU: hemagglutination units

HE: hematoxylin-eosin

HI: Hemagglutination inhibition

HLA-B7: human leukocyte antigen B7

I

IA: image analysis

IAV(s): Influenza A virus (es)

IBV(s): Influenza B virus (es)

ICV(s): Influenza C virus (es)

ID: identification

IDV(s): Influenza D virus (es)

IFN: Interferon

IgG: immunoglobulin G

IHC: immunohistochemistry

In.: Inoculumn

L

LR: linker region

M

M: matrix

M1: Matrix protein

M2: Ion channel

MDCK: Madin–Darby Canine Kidney

MOI: Multiplicity of infection

mRNA: messenger RNA

N

NA: Neuraminidase

Neg.: Negative

NEP: nuclear export protein

NGS: Next generation sequencing

NP: Nucleoprotein

NS1: Nonstructural protein 1

NS2: Nonstructural protein 2

NSPs: non-structural proteins

NT: Nasal turbinate.

O

ORF: open reading frame

P

PA: polymerase acid protein

PB1: polymerase basic 1

PB2: polymerase basic 2

PBS: phosphate buffered saline

PCR: polymerase chain reaction.

PCV2: porcine circovirus type 2

PRCV: porcine respiratory coronavirus

PRDC: Porcine respiratory disease complex

PRRSV: porcine reproductive and respiratory syndrome virus

R

RBC(s): red blood cell(s)

RBD: Receptor binding domain

RdRp: RNA-dependent RNA polymerase

RNA BD: RNA binding domain

RT-qPCR: quantitative reverse transcription-polymerase chain reaction

S

SA: sialic acid

SIV(s): Swine Influenza Virus (es)

SLA-B7: human leukocyte antigen B7

SNV(s): single nucleotide variant(s)

ss: single stranded

T

$TCID_{50}$: 50% tissue culture infection dose

TR: triple reassortant

TRIM22: tripartite motif 22

V

VAERD: Vaccine-associated enhanced respiratory disease.

VDAC1: anion channel 1

vRNA: viral RNA

vRNP: viral ribonucleoprotein

W

WHO: World Health Organization

WOAH: World Organisation for Animal Health

Π

$\pi$: nucleotide diversity

$\pi_N$: nonsynonymous nucleotide diversity

$\pi_S$: synonymous nucleotide diversity

**Abstract**

Influenza A virus (IAV) is a worldwide distributed pathogen able to infect many species of avian and mammals, including humans and pigs. Its genome is characterized by having 8 RNA negative sense segments: the polymerases (PB2, PB1, and PA), the hemagglutinin (HA), the nucleoprotein (NP), the neuraminidase (NA), matrix (M), and the segment that code for the non-structural proteins (NS). IAV polymerases, such as other RNA viruses, have a low proofreading activity, thus virus genome accumulates a great deal of point mutation on a short time scale. Besides, genomic reassortment events are feasible when two different IAV subtypes simultaneously coinfect the same host. These genetic mechanisms are a source of high genetic diversity, which provides plasticity to the virus, being able to quickly adapt in changing environments. Virus evolution can make that virus achieve new antigenic patterns, being no longer recognized by the previous host immunity, generating seasonal epidemic and pandemic IAVs. In 2009 a swine-origin A(H1N1)pdm09 strain arose, harbouring swine, human and avian influenza segments, and caused the last IAV pandemic. This outbreak, highlighted the hypothesis of pigs as "mixing vessels", playing an important role in the adaptation of avian viruses to humans, as pigs could be infected by both IAVs. Currently, there are 3 dominant subtypes of swine influenza virus (SIV) circulating in pigs: H1N1, H3N2, and H1N2. To control SIV, the most widely used strategy in Europe, although limited, is the application of trivalent vaccines. The immunity provided by this vaccine is not complete, allowing virus replication and hence evolving, which could generate escape mutants. Therefore, SIV poses a continuous threat to both, animal and human health, since its evolution can affect its antigenicity, host range, virulence, antiviral resistance, and pathogenesis.

Due to all these antecedents, in this doctoral thesis, the evolutionary dynamics of SIV viral populations have been studied in a pig model with pre-existing immunity against the virus by next sequencing technology. The first study evaluates the evolution of the Eurasian "avian-like" (EA) H1N1 virus in vaccinated and nonvaccinated animals. Positive selection was the main evolution force detected in samples collected from vaccinated animals, where important mutations were reported in HA, NS1, and NP. In the second study, the evolution of the "human-like" H3N2 virus was analyzed in vaccinated and nonvaccinated animals that had previously recovered from an unexpected natural infection with the A(H1N1)pdm09 virus. In both scenarios, natural selection was influencing virus evolution, finding proportionally more nonsynonymous substitutions in HA and NA in viruses recovered from vaccinated animals. In the last chapter, the impact of the vaccine on genome reassortment and genetic drift during an

experimental coinfection with H1N1 EA and H3N2 “human-like” has been studied. Results showed a minor possibility of reassortment events in vaccinated animals. On the other hand, the greatest genetic diversification was detected in H1N1 subtype in vaccinated animals, reporting substitutions that may play an important role in the evasion of the immune response in the HA and NA.

The results obtained in this doctoral thesis corroborate the enormous capacity of mutation and adaptation of SIV. Different evolutionary patterns found in vaccinated and nonvaccinated animals were detected, providing a novel insight of SIV evolution under different scenarios.

**Resumen**

El virus de la influenza A (IAV) es un patógeno mundialmente distribuido que puede infectar a multitud de especies de aves y de mamíferos, incluidos cerdos y humanos. Se trata de un virus de ARN cadena negativa, cuyo genoma está fragmentado en 8 segmentos; las polimerasas (PB2, PB1 y PA), la hemaglutinina (HA), la nucleoproteína (NP), la neuraminidasa (NA), la matriz (M) y el segmento que codifica para las proteínas no estructurales (NS). La polimerasa del IAV, como la de otros virus de ARN, se caracteriza por su baja fidelidad durante la replicación, que hace que se acumulen muchas mutaciones en el genoma de IAV en una escala temporal corta. Además, se pueden producir intercambios de segmentos entre distintos subtipos cuando simultáneamente coinfectan al mismo huésped. Estos mecanismos genéticos son una fuente de diversidad genética elevada, que otorga al virus mucha plasticidad ante ambientes cambiantes. La evolución del virus puede hacer que estos adquieran nuevos perfiles antigénicos, no siendo reconocidos por la inmunidad previa existente, generando gripes estacionales endémicas y pandémicas. En el año 2009, la cepa de origen porcina A(H1N1)pdm09 que contenía segmentos de virus humanos, aviares y porcinos, causó la última pandemia de gripe en humanos. Reforzándose la teoría de que los cerdos juegan un papel clave en la adaptación de IAVs aviares a humanos, ya que pueden ser infectados por ambos. Actualmente hay 3 subtipos dominantes del virus de la gripe porcina (SIV): H1N1, H3N2 y H1N2. La estrategia más usada para controlar el SIV en Europa es la aplicación de vacunas trivalentes, aunque la inmunidad generada no es completa. Esto provoca que la protección conferida no sea esterilizante, por lo que el virus puede replicar y por ende evolucionar generando variantes de escape vacunal Por lo tanto, el SIV supone una amenaza continua para la sanidad animal y humana, ya que su evolución puede afectar su antigenicidad, rango de huésped, virulencia, resistencia antiviral y patogénesis.

Debido a todos estos antecedentes, en la presente tesis doctoral se ha estudiado la dinámica evolutiva de las poblaciones víricas del SIV en modelo porcino con inmunidad preexistente contra el virus mediante tecnología de secuenciación masiva. El primer estudio evalúa la evolución del virus H1N1 Eurasian "avian-like" (EA) en animales vacunados y no vacunados, y se encontró que la selección positiva juega un papel importante en la evolución del virus en animales vacunados, detectando mutaciones importantes en la HA, la NS1 y la NP. En el segundo estudio, se analiza la evolución del virus H3N2 "human-like" en animales vacunados y no vacunados que previamente se habían recuperado de una infección natural inesperada con el virus A(H1N1)pdm09. En ambos escenarios la selección natural está influenciando la evolución del virus,

encontrando proporcionalmente más substituciones no sinónimas en la HA y la NA en virus recuperados de animales vacunados. En el último capítulo, se ha estudiado el papel que puede tener la vacunación en el reordenamiento y la deriva genética del virus durante una coinfección experimental con H1N1 EA y H3N2 "human-like". Los resultados muestran que la posibilidad de reordenamiento es mayor en animales que no han sido vacunados. Por otro lado, encontramos una mayor diversificación genética en el subtipo H1N1 en animales vacunados, reportando substituciones en los genes dela HA y la NA que podrían jugar un papel importante en la evasión de la respuesta inmune.

Los resultados obtenidos en la presente tesis doctoral corroboran la enorme capacidad de mutación y adaptación que tiene el SIV. Los diferentes patrones evolutivos encontrados en animales vacunados y no vacunados nos otorgan una visión más completa sobre las dinámicas evolutivas del mismo.

**Resumo**

O virus da influenza A (IAV) é un patóxeno mundialmente distribuído que pode infectar moitas especies de aves e mamíferos, incluídos porcos e humanos. Trátase dun virus de ARN cadea negativa cun xenoma de 8 segmentos: as polimerasas (PB2, PB1 y PA), a hemaglutinina (HA), a nucleoproteína (NP), a neuraminidasa (NA), a matriz (M) e o segmento das proteínas non estruturais (NS). As polimerasas da influenza, coma as doutros virus de ARN, posúen unha baixa tasa de fidelidade durante a replicación, o que fai que acumulen moitas mutacións no xenoma do IAV nunha escala temporal curta. Ademais, pódense producir intercambios de segmentos xenómicos entre diferentes subtipos cando coinfectan o mesmo hóspede. Estes mecanismos xenéticos son una fonte de diversidade xénica elevada, dándolle moita plasticidade ao virus en ambientes cambiantes. A evolución do IAV fai que os virus adquiran novos patróns antixénicos, evitando a inmunidade previa do hóspede, xerando gripes estacionais endémicas e pandémicas. No ano 2009, unha cepa de orixe porcina A(H1N1)pdm09 que contiña segmentos de influenzas humana, aviar e porcina, provocou a última pandemia de gripe no ser humano. Deste xeito, reforzouse a teoría de que os porcos xogan un papel importante na adaptación de virus aviares a humanos, xa que poden ser infectados por ambos os dous virus. Hoxe en día, hai 3 subtipos dominantes da gripe porcina (SIV) en porco: H1N1, H3N2 e H1N2. A estratexia máis empregada para o seu control en Europa é a aplicación de vacinas trivalentes, aínda que non xeran unha inmunidade completa fronte o virus. Deste xeito, a vacina non é esterilizante, polo que o virus pode replicarse e evolucionar, podendo xerar escapes vacinais. Polo tanto, o SIV supón unha ameaza constante para a sanidade tanto animal como do ser humano, xa que a súa evolución afecta á súa antixenicidade, rango do hóspede, virulencia, resistencia antiviral e patoxéneses.

Tendo en conta todos estes antecedentes, nesta tese doutoral estudáronse as dinámicas poboacionais víricas do SIV en modelo porcino con inmunidade preexistente contra o virus mediante tecnoloxía de secuenciación masiva. O primeiro estudo avalía a evolución do virus H1N1 Eurasian "avian-like" (EA) en animais vacinados e non vacinados, onde se atopou que a selección positiva xoga un papel importante na evolución do virus en animais vacinados, reportando mutacións importantes na HA, na NS1 e na NP. No segundo estudo, analízase a evolución do virus H3N2 "human-like" en animais vacinados e non vacinados que se recuperaran previamente dunha infección natural non esperada co virus A(H1N1)pdm09. En ambos os escenarios, a selección natural está a influenciar a evolución do virus, atopándose proporcionalmente máis substitucións non sinónimas na HA e na NA de virus recollidos de animais vacinados. No último

capítulo, estúdase o papel da vacina no reordenamento e deriva xenética do virus durante unha coinfección experimental con H1N1 EA e H3N2 "human-like". Os resultados amosan que a posibilidade de reordenamento xenético é maior en animais non vacinados. Pola contra, atopouse unha maior diversificación xenética no subtipo H1N1 en animais vacinados, con substitucións na HA e na NA que poden xogar un papel crucial na evasión do sistema inmune.

Os resultados da presente tese confirman a enorme capacidade de mutación e adaptación que ten o SIV. Os diferentes patróns evolutivos atopados en animais vacinados e non vacinados outorgan unha visión máis completa sobre as dinámicas evolutivas do SIV en diferentes escenarios

The results presented in this Thesis dissertation have been published or submitted for publication in international scientific peer-reviewed journals:

López-Valiñas Á, Sisteré-Oró M, López-Serrano S, Baioni L, Darji A, Chiapponi C, Segalés J, Ganges L, Núñez JI. Identification and Characterization of Swine Influenza Virus H1N1 Variants Generated in Vaccinated and Nonvaccinated, Challenged Pigs. Viruses. 2021 Oct 16;13(10):2087. doi: 10.3390/v13102087. PMID: 34696517; PMCID: PMC8539973.

López-Valiñas Á, Baioni L, Córdoba L, Darji A, Chiapponi C, Segalés J, Ganges L, Núñez JI. Evolution of Swine Influenza Virus H3N2 in Vaccinated and Nonvaccinated Pigs after Previous Natural H1N1 Infection. Viruses. 2022 Sep 10;14(9):2008. doi: 10.3390/v14092008. PMID: 36146814; PMCID: PMC9505157.

López-Valiñas Á, Valle M, Chiapponi C, Wang M, Cantero G, Ganges L, Segalés J, Núñez JI. Vaccination against swine influenza in pigs causes different drift evolutionary patterns upon swine influenza virus experimental infection and reduces the possibility of genomic reassortments. Submitted for publication.

# Part I

# General Introduction and objectives

# Chapter 1
# General introduction

## 1.1 Influenza Viruses (IVs)

*Orthomyxoviridae* is a family of enveloped negative-sense, single-stranded (ss) RNA viruses with spherical shape, which belongs to the group V according to the Baltimore virus classification. This family is divided into 7 genera: *Alphainfluenzavirus, Betainfluenzavirus, Gammainfluenzavirus, Deltainfluenzavirus, Isavirus, Thogotovirus,* and *Quaranjavirus*. The first four genera comprise the four types of influenza virus, A, B, C and D respectively, that infect many species of birds and mammals causing a zoonotic respiratory disease called influenza.

Influenza A viruses (IAVs) cause seasonal epidemics in humans that occasionally can spread worldwide leading to pandemics with high morbidity and mortality rates in humans [1]. IAVs have the greatest genetic variability among IVs, infecting a wide variety of birds and mammals, increasing it zoonotic potential. This type of influenza mainly infects birds from aquatic environments such as wild waterfowl, shorebirds, and poultry birds. Furthermore, mammal species like dogs, bats, horses, human and pigs can also be infected by IAVs [2].

On the other hand, influenza B viruses (IBVs), can also cause a respiratory infection that in some cases may lead to clinical complications resulting in hospitalisation or even death [1,3]. Nevertheless, IBV pandemic potential is low due to the lack of established animal reservoir [4]. Apart from humans, this type of influenza can also be found in seals [5]. Type C influenza viruses (ICVs) can lead to mild respiratory disease in children and adolescents, although so far it has not caused pandemics [6,7]. These viruses have been also detected in dogs, cattle, and swine [8–10]. Interspecific transmission between pigs and humans with ICV, although rarely, has been previously reported [11]. Lastly, influenza D viruses (IDVs), have been globally reported only in livestock, like cattle and swine [12–14].

## 1.2 Influenza A viruses (IAVs)

### 1.2.1 IAV genome

IAVs genome is composed of 8 single-stranded viral RNA (vRNA) segments of negative polarity, with a total length of 13,6 kilobases (kb). The segments have different genomic sizes, between 0.89 and 2.3 kb, and they are usually ordered according to its size, with the largest one being first. All vRNAs have conserved and complementary regions at their 3' and 5' ends, with 12 and 13 nucleotides respectively [15].

All segments code for eight structural proteins and several non-structural proteins (NSPs). The biggest segments, 1, 2 and 3 encode for the polymerase basic 2 (PB2), polymerase basic 1 (PB1) and polymerase acid (PA), which polymerase compose the heterotrimeric RNA dependent RNA polymerase (RdRp) complex.

Segment 4 and 6, encode for the surface glycoproteins hemagglutinin (HA) and neuraminidase (NA). The segment 5 contains the genetic information for the nucleoprotein (NP). The remaining segments, 7 and 8, encode for the matrix protein (M1) and for the non-structural protein (NS1), respectively [16]. Moreover, the ion channel (M2) and the nuclear export protein (NS2 / NEP) are also encoded by segment 7 and 8 by RNA alternative splicing [17,18] (Supplementary table S1.1).

Furthermore, there are mRNA with open reading frames (ORF), alternative splicing and coding region truncation that can encode for NSPs. These accessory viral proteins have been recently identified [19]. In segment 2, the PB1 mRNA starts its translation from the fourth and fifth AUG codon synthesizing the polymerase basic 1 frame 2 (PB1-F2) and the PB1-N40 respectively [20,21]. In the segment 3, alternate initiation codons code for PA-N115, PA-N182, PA-X proteins [22,23]. Finally, in segment 7 an ORF with an alternative splicing code for M42 protein while other splicing in segment 8 encodes for the NS3 one [24,25] (Supplementary table S1.1)

### 1.2.2 Virus particle

The virion particle of IAV possess a lipid envelope derived from the infected host cellular membrane. The virus particle has a spheric or elliptical morphology with a diameter between 80-120 nm, figure 1.1.a [26,27]. Eventually the virus could also achieve filamentous or irregular shape [28–30]. Filamentous virus particles have both higher infectivity and vRNA content [31,32].

Embedded in the envelope of the virion particle there are two spike surface glycoproteins HA, and NA. The quaternary structure of the HA is constituted by a homotrimer which binds with host cell sialic acid (SA) allowing virus attachment and cell entry [33]. On the other hand, the NA homotetramer also interacts with SA, in this case to grant virion progeny release [34]. Furthermore, the M2, formed by four monomers, also traverses the lipid bilayer and it serves as a conduit for the transport of protons into the virion [35,36]. In the surface of the virion, the proportion of HA is four times greater than NA, whereas for 10 HA there are between 1 and 2 M2 (Figure 1.1.a) [37,38].

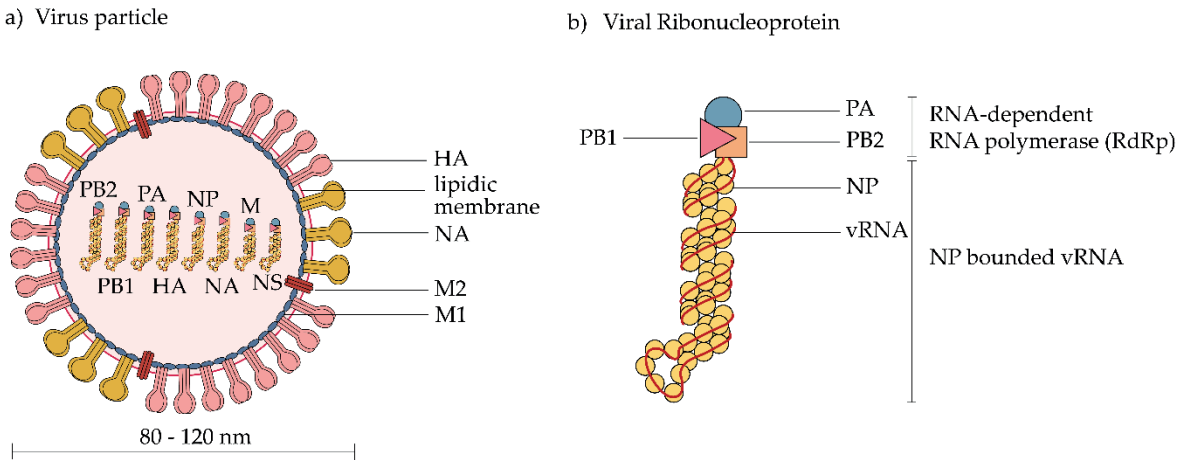


Figure 1.1. Structural representation of influenza A virus. A) IAV particle. B) Viral Ribonucleoprotein (vRNP) representation. *Figure designed by Lorena López Valiñas*.

Inside the virion particle, the vRNA are associated with the NP and the RdRp complex, forming together the 8 viral ribonucleoprotein (vRNP) complex [39]. The core of the RdRp is the PB1, which binds through the carboxyl terminus to PA and through the amino terminus to PB2[40,41]. The NPs interacts with another NP oligomers by two different sites, forming a single strand of NP monomers. When that strand folds back on itself, it forms a loop at the end, coiling on itself and forming a double strand of NPs. This structure forms a scaffold which gives to the vRNP its characteristics twisted rod-like structure [42]. The vRNA wraps around this scaffold structure, associating 25 vRNP nucleotides for each nucleoprotein by phosphate-sugar backbones [43,44]. Therefore, each vRNA segment is encapsidated in 8 scaffolds. Finally, the RdRp is associated with the doble-strand complementary terminus 5′ and 3′ vRNA at the opposite end of the loop (Figure 1.1 b) [45].

### 1.2.3 Replicative cycle of IAV

The IAV replication cycle occurs in epithelial cells of the respiratory tracts in the case of mammal species or in the epithelial cells of the intestinal tract in bird species [2]. The cycle starts with the attachment of the virions with the host cell, mediated by the attachment of the viral HA with the host cell surface oligosaccharides SA [2,46,47]. Consequently, the virus is internalized in the endosomes by endocytosis or micropinocytosis and will be trafficked on the host cell (Figure 1.2.) [48,49].

The acidic environment of the endosome causes irreversible conformational changes in the HA leaving the fusion peptide domain active. Hence, the fusion between the virion envelope and the endosomal membrane is carried out. Parallelly, another consequence of the acidic environment of the endosome is the flux of potassium ions and protons into the virion through the ion channel M2. This

passage causes the interior virion acidification and as consequence the dissociation of M1 from vRNP occurs. As a result, the vRNPs are released into the infected cell cytoplasm [50].

Once in the cytoplasm, the vRNPs are imported to the nucleus of the cell using nuclear localization signals through the nuclear pore complex [51]. In the nucleus, replication, and transcription of the IAV genome is taking place. The proteins of the RdRp carry out these procedures: PB2 regulates the mRNA cap recognition, the PB1 is the catalytic subunit with polymerase activity which carry out the RNA elongation and the PA has exonuclease activity, cleaving the cap of the RNA and promoting the initiation of mRNA translation [47,52] (Supplementary table S1.1). The replication of the vRNA occurs trough the complementary ribonucleoprotein (cRNP) complex which is a positive-sense intermediate that is used as template to synthesize the vRNA progeny. Regarding the transcription, the vRNAs are transcribed into positive-strand mRNAs with cap and poly-A tail. The mRNAs are later transported to the cell cytoplasm where will be translated to the viral proteins [53].

The HA, NA and M2 mRNA translation takes place in the ribosomes associated with the endoplasmic reticulum. These newly formed proteins are trafficked and inserted in the plasmatic membrane of the host cell. On the other hand, PB2, PB1, PA, NP, NS1 NEP and M1 mRNAs translation occurs in the ribosomes of the cytoplasm and newly synthesized proteins are transported again to the nucleus [54]. In this way the virus replication rate is increased since the amount of RdRp proteins are greater. The M1, NEP and NP proteins play an important role in the nuclear export of the new progeny of vRNPs trough the nuclear pore complex. Finally, the M1 helps in the cytoplasmatic transport of the vRNPs, avoiding its re-entry back in the nucleus and its cytoplasmatic migration to cell membrane.

Once the vRNPs are allocated in the membrane, the M1 and M2 protein interaction plays an important role in assembly and budding of the IAV virion progeny, whose membrane derives from the host with the viral transmembrane proteins[55]. The HA and NA glycoproteins expression promotes budding of the progeny in the membrane. Furthermore, the NA catalytic function prevents the attachment between HA and SA, and also hydrolyse glycosidic linkages between SA and cell membrane oligosaccharides. Consequently, the virion progeny is released, allowing its spread [56].

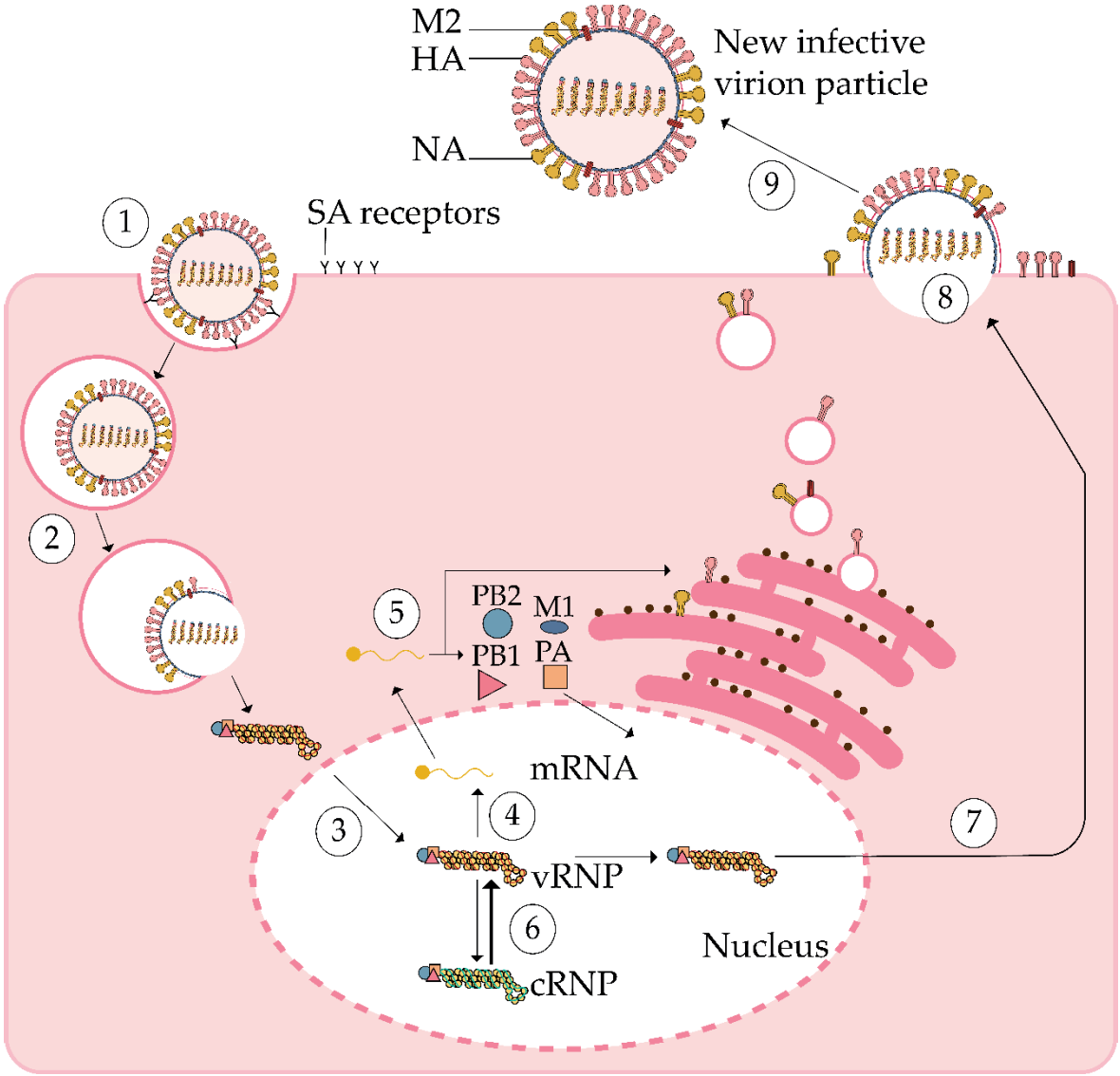


**Figure 1.2. Replicative cycle of IAV in host epithelial cell.** 1. Virus attachment. 2. Fusion of the virion and the endosome. 3. vRNP import to host cell nucleus. 4. Transcription. 5. Translation of PB2, PB1, PA, M1 in cytoplasm ribosomes and HA, NA, and M2 in the endoplasmatic reticulum. 6.Replication. 7 vRNP export. 8. IAV virion assembly and budding. 9.Virion progeny releasing. *Figure designed by Lorena López Valiñas.*

The virus replicative cycle causes the host cell death which is directly related to pathological damage. Besides, viral proteins activate the host's immune system causing the activation of both adaptive and innate immune cells that in excess, despite cleaning the virus, may cause immunopathology and pneumonia.

### 1.2.4 Other viral proteins involved on IAV replication

The non-structural proteins NS1, PB1-F2, and PA-X modulate viral replication and transcription, playing an important role during the IAV replicative cycle [19] (Supplementary table S1.1).

The NS1 protein has multiple functions that have an impact on viral mRNA translation, regulation of the viral replication and host immune modulation. Regarding the viral mRNA translation, NS1 recruits the host eukaryotic translation initiation factor 4G1 (eIF4G1), enhancing viral mRNA translation, causing host mRNA silencing [57]. NS1 regulates the viral replication by host cleavage and polyadenylation specificity factor (CPSF) interaction. This factor inhibits the 3'end cleaving and polyadenylation, avoiding correct host pre-mRNAs processing [58]. In relation to the modulation of the immune system, NS1 supress the host immune antiviral response by regulation of the interferon (IFN) [57]. Additionally, this protein increases the virulence of IAV trough phosphoinositide-3-kinase (PI3K) activation [59]. Furthermore, the linker region of the protein plays a role in the plasticity of the molecule, it provides different protein conformations changing the binding compatibility with different host cell substrates [60].

PB1-F2 protein interacts with the mitochondrial voltage-dependent anion channel 1 (VDAC1) and the adenine nucleotide translocator 3 (ANT3) host proteins causing pro-apoptotic activity, which is strain specific [61]. This protein also has pro-inflammatory activity, as causes an increment of cytokine levels which result in lung tissue damage [62]. Therefore, this protein contributes to the pathogenicity of the virus. Lastly, PA-X degrades the host RNA polymerase II and non-coding RNAs, this induces the silencing of host gene expression favouring viral growth and counteracting the antiviral response[63].

### 1.3 Subtype classification and nomenclature

The IAVs are serologically classified in different subtypes according to its surface glycoproteins HA and NA. To date, 18 different subtypes of HA (H1 to H18) and 11 of NA (N1 to N11) have been identified [1]. The multiple combination of both proteins is possible, although not all combinations have been found in the nature, having the possibility of many different subtypes of IAV found in many species of birds and mammals, for example H18N11 in bats [64,65]. Likewise, the different subtypes can be classified into different genetic clades and sub-clades, also called groups and sub-groups respectively. This division refers to the genetic differences between viruses of the same subtype, for instance a subtype that was in different geographical regions.

According to bulletin of the World Health Organization (WHO), published in 1980, an international nomenclature is established for the classification of IVs [66]. As published in the bullet, the name must contain the following ordered information separated by slashes. First, the type of IV (A, B, C or D) followed by the host of origin. Secondly, the geographical location where the strain was first isolated. After that, the strain number, and the year of isolation of the strain is also specified. Finally, the subtype of the strain noted in parentheses (Figure 1.3) [1].

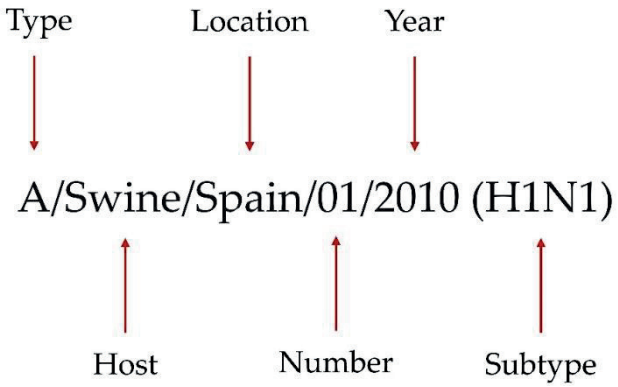


**Figure 1.3.** IVs nomenclature. The name of influenza type A, swine origin, isolated by the first time in Spain, and H1N1 subtype is shown in the figure.

## 1.4 Evolution

### 1.4.1 Quasispecies and population dynamics

The evolution of IAV is described under the quasispecies theory [67–70]. The concept of quasispecies was first stipulated by Eigen in 1971 [71,72]. Herein, quasispecies is defined as a cloud of macromolecular species, whose genetic sequences are highly interrelated generating the same consensus sequence. Those sequences better adapted to the environment are selected and spread, thereby known as the wild type.

According to the previous concept, in RNA viruses, the viral populations are composed of a spectrum or cloud of mutants (Figure 1.4). Hence, in a viral population we have a set of virions whose genomes are genetically very similar, although their RNA sequences are not strictly identical. This supposes an adaptive advantage for the virus, since there may be a reservoir of phenotypic variants in the mutation cloud that could be beneficial for the adaptability of the virus when it faces selection pressures, such as immune scape mutants, drug resistance or pathogenesis within the host [67,73]. Therefore, when pressure acts on virus evolution, those minor variants that possess a benefit on virus fitness become dominant along time [74].

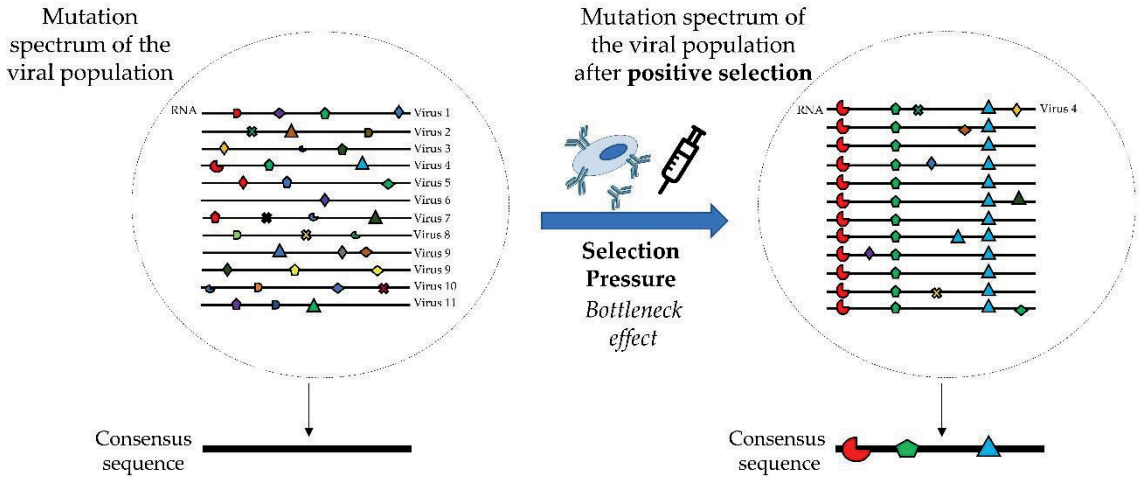


**Figure 1.4**. Quasispecies mutant spectrum and its evolution after host humoral immune pressure. Each black line within the circle represents the genome of each virion in the population, being at the bottom the consensus sequence of the viral population. Different shapes and colours on genomes shown nonsynonymous substitution in the mutation spectrum of the population. Initial viral population genetic diversity supposes an adaptive advantage for the virus, since beneficial mutations become dominant after a bottleneck effect, caused by the selection pressure.

The quasispecies are dynamic and are constantly evolving. There are three mechanisms that influence the evolution and so the dynamics of the quasispecies. The first mechanism, and the first source of genetic variation, is the incorporation of point mutations during the replication process. It is very common in RNA viruses, due to the low proofreading function of its polymerases[75]. Another important source of genetic variability in segmented RNA viruses are the genomic rearrangement events. Finally, recombination between different genomic regions of IVs is also a source of variability (See sections 3.4, 3.5 and 3.6).

All these mechanisms of genetic change cause the continuous evolution of IVs. This implies that the virus undergoes rapid antigenic evolution. Hence, IAVs control through vaccination campaigns is very difficult in both humans and domestic animals. On the other hand, continuous evolution also allows the virus to rapidly adapt to different environments, which contributes to a continuous circulation of the virus in avian and mammalian ecosystems.

Furthermore, the animal production industry, such as pigs and poultry, is ever-increasing, triggering a larger world population of these animals [76]. Considering animal population density, together with the fact that they usually live in small spaces having close contact among them, the low generation time of IAV and the high mutation rate of the virus, IAVs can rapidly evolve.

### 1.4.2 Natural, Neutral and Purifying selection

The number of nonsynonymous and synonymous variants accumulated in the virus genome along time could give us information about whether the virus is better or worse adapted to the host. Depending on the scenario the virus can be under natural or positive Darwinian, neutral, and negative or purifying selection [77].

When virus is poorly adapted to the host, selective bottleneck events will occur. In this event, a minimum proportion of the virions from the same viral population are selected, as its genomes contain variants that suppose an adaptive advantage. Once these virions are established in the population, the gained genetic richness suppose an improvement of virus fitness passing this variability to the progeny. Therefore, rapid viral genetic diversification occurs, gaining intrahost genetic diversity. Under this scenario, the virus is under natural or positive Darwinian selection, where the number of nonsynonymous mutations, which implies an increase in viral fitness, are greater than the synonymous ones[78] .

On the contrary, when virus is well adapted to the host, there are not natural selection events, so the virus remains genetically stable over time. In other words, genetic differences among different virions are low. Anyway, there are little increments of the intrahost diversity since neutral mutations, that do not imply a benefit or a loss on virus fitness, could occur. Moreover, under this scenario virus evolution is dominated by purifying selection, where deleterious mutations are removed. Likewise, the proportion of nonsynonymous new substitutions will be lower than synonymous ones.

Finally, neutral selection can also determine the evolution of the virus. In this case, bottleneck effect and intrahost purifying selection can occur simultaneously, leading to little genetic diversification since the new mutations that appear are deleterious or neutral, in the best of cases.

### 1.4.3 Point mutations

RNA viruses, including influenza, are characterized by the low rate of fidelity of their polymerases. Consequently, RNA viruses can add and accumulate a great deal of point mutations in their genomes during its replication. IAVs mutation rate is very high, on the order between $10^{-3}$ and $10^{-4}$ per gen per generation, allowing rapid viral evolution [75].

These point mutations can be accumulated over time in the viral genome, causing the progressive evolution of the virus. There are regions of the IAV genome that are under positive evolutionary pressure, such as the epitope regions of the HA and NA, which are the most immunogenic proteins. Along time, these regions can

evolve until they are no longer recognized by the previous immunity of the host population, in case of existing, therefore generating escape variants[79]. This phenomenon is known as antigenic drift, which can generate new viral subtypes and it is responsible for influenza seasonal epidemics outbreaks in humans (Figure 1.5.a) [80,81].

The accumulation of point mutations is not only associated with escaping previous immunity. There have been point mutations previously described that have an effect on the host range, virulence, and antiviral resistance of IAVs [73,79].

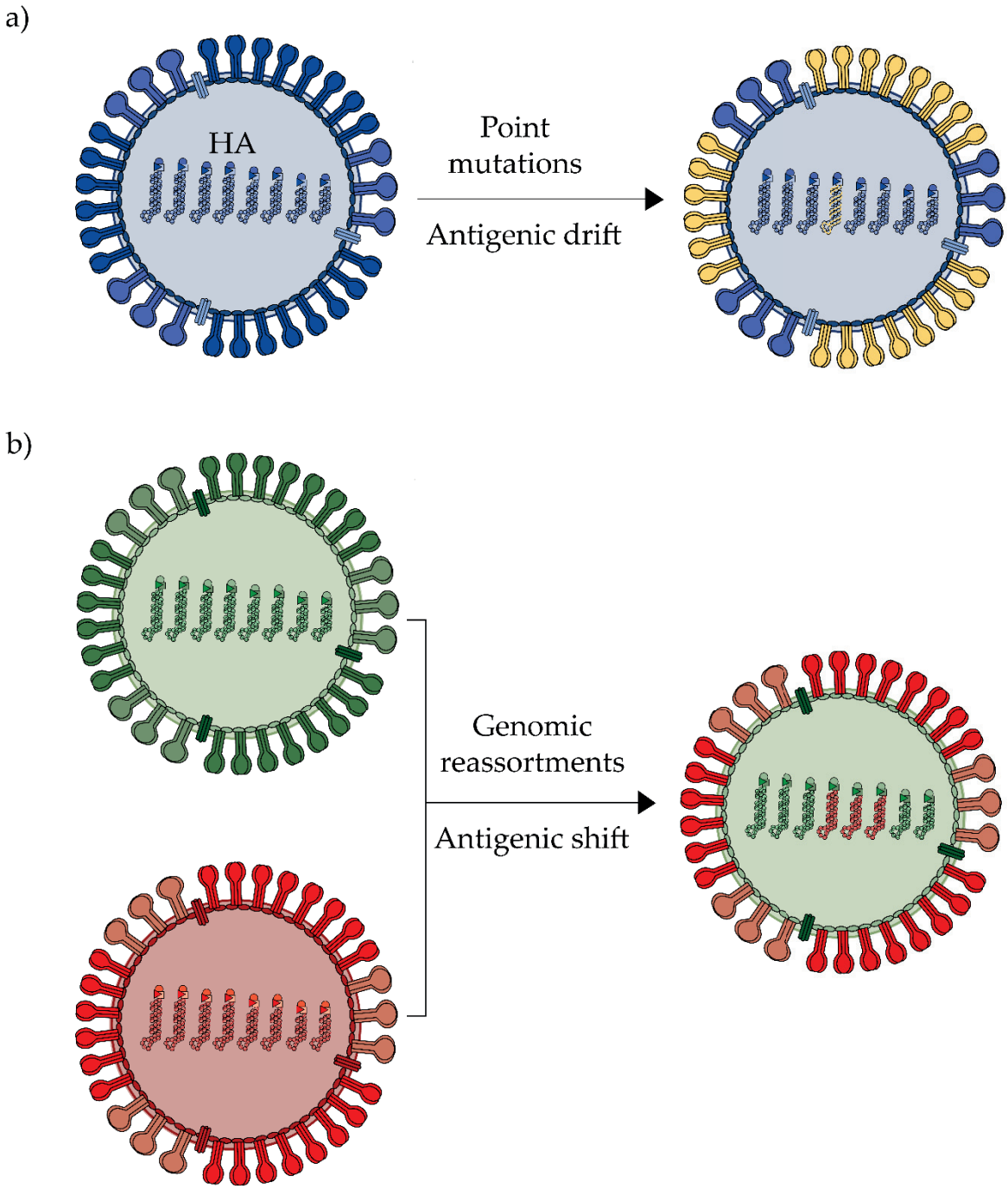


**Figure 1.5.** Main genetic mechanisms of IAV evolution. A) Accumulation of point mutations on surface glycoprotein can change the virus antigenic pattern, a phenomenon called antigenic shift. This evolutionary event is responsible for seasonal influenza flu. B) The reassortments events between two different subtypes during coinfection can also change the antigenic pattern of the virus, phenomenon called antigenic drift. This type of genomic event plays an important role in the generation of pandemic viruses, which pose a continuous threat to animal and human health. *Figure designed by Lorena López Valiñas.*

### 1.4.4 Reassortments

Another important genetic mechanism for IVs, due to its segmented genome, is the rearrangement of genomic segments between different IVs subtypes. This process occurs when two different subtypes simultaneously coinfect the same host cell. Consequently, a progeny of virions that contain segments from both subtypes could arise, posing a risk and a threat to human and animal health [79].

As in the previous section, IVs could achieve a new antigenic patterns trough genomic reassortments events, allowing for the escape from previous immunity. This phenomenon is known as antigenic shift and generates new strains and subtypes of IVs humans (Figure 1.5.b). Historically, these genomic events caused the emergence of major human influenza pandemics, such as the Asian flu in 1957 (H2N2), the Hong Kong flu in 1968 (H3N2) and the pandemic swine origin A(H1N1)pdm09 in 2009 [82–85].

### 1.4.5 Recombination

Influenza Viruses also have another mechanism to increase their genetic diversity called recombination. This phenomenon does not seem to play an important role during IVs evolution [86]. There are two possible types of recombination, non-homologous and controversial homologous recombination. The first type of recombination occurs between different segments of the same subtype. The controversial recombination occurs when the polymerase switch RNA template during virus replication in cells coinfected with more than one different subtype [87].

### 1.4.6 Next generation sequencing to study quasispecies and viral evolution

In the past, using Sanger sequencing, we could only obtain the consensus sequence of the virus, so the spectrum of mutants that make up the viral quasispecies could not be analysed. In 2005, with the incorporation of the next generation sequencing (NGS), the read depth of a sample was increased and as a result the viral quasispecies precision analysis improved. Nowadays, there are different sequencing platforms such as Illumina, Pacific BioSciences, and Ion torrent. Over time, sequencing technology becomes cheaper, so its use for the study of viral quasispecies is more common [74].

This sequencing technique is currently used to study viral population dynamics under different environmental pressures. These analyses give us very relevant information about the virus, pathogenesis, virulence, persistence, epidemiological evolution, genetic evolution, drug resistance, vaccine development and immune resistance [74,88,89].

One of the challenges that we face today in the scientific community is the enormous amount of sequence information that massive sequencing provides us. Therefore, it was necessary to develop a multitude of bioinformatic applications that, coupled in a workflow, allow us to align sequences and variant calling, essential for the analysis of viral quasispecies [77,90,91].

### 1.5 Ecology and host range

IAVs are a worldwide distributed pathogen with a very wide range of hosts, being able to infect a large number of birds and mammal species (Figure 1.6). The natural reservoir of IAV are the wild aquatic birds, being the main source of IAVs in other species [92]. In wild aquatic birds, such as wild ducks, shorebirds, waterfowl, gulls and passerine birds, subtypes harbouring the majority of HA identified (H1 to H16) have been isolated so far, except H17 and H18 subtypes that up to date have been only found in bats [65]. Bird migration around the world brings the different species into close contact, maintaining the virus globally, assuming an important reservoir for the IAVs [93,94]. The viral shedding in birds is maintained because the virus from contaminated animal faeces can be maintained in fresh water [95,96].

Wild birds are potential carriers of IAVs that could introduce virus to susceptible species of domestic birds such as chickens, turkeys, and quails. Avian influenza viruses can be typed as low and high pathogenic avian influenza virus (LPAIVs and HPAIVs, respectively), according to it level of pathogenicity. HPAIVs are considered those strains that cause mortality rates greater than 75% of infected birds in a period of 10 days [97]. These high pathogenic strains usually harbour H5, H7 and H9 subtypes, that occasionally infect humans although the transmission between them has not been reported [98]. In the last decade, H5 strains have been widely circulating in domestic and wild birds in Europe [99]. More specifically, an H5N1 strain that is spreading rapidly across Europe, has also been recently reported

in America. This poses a health risk, and is also causing significant economic losses in the poultry sector.

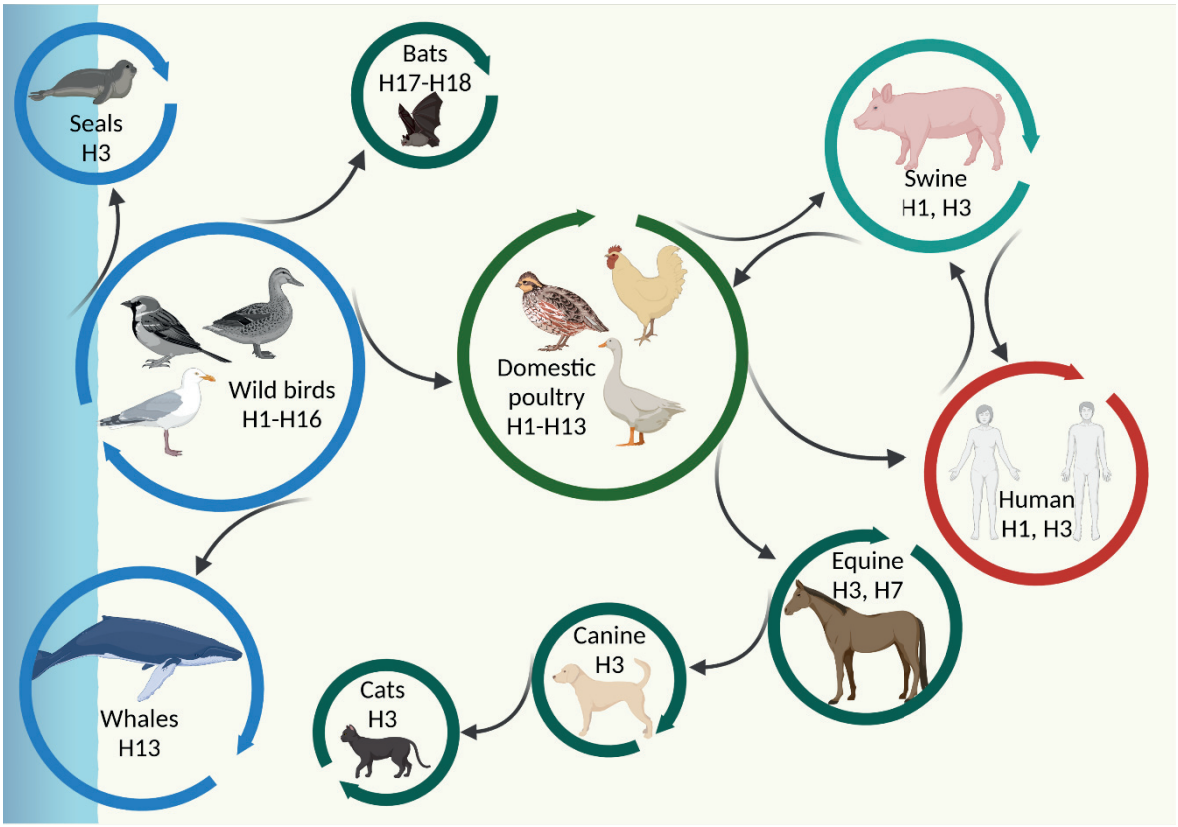


**Figure 1.6.** Ecology of influenza A virus. The arrows point the known interspecies transmission of the virus.

Birds can also be the IAVs reservoir for infecting other mammalian species such as horses, whales, seals, humans, and pigs [100–104]. Aquatic birds are the potential IAV carriers for seals, whales, and domestic poultry. IAV crosses species barriers from the domestic birds, to the infect the mammal species previously mentioned, especially humans and swine [64]. Currently, human and swine IAVs mostly harbour H1, H3, N1, and N2 subtypes [105,106].

## 1.6 History of IAV pandemics in humans

As previously mentioned, IAVs can evolve rapidly, changing its antigenic pattern and crossing species barriers. Consequently, new human IAVs strains arose causing important flu outbreaks that rapidly spread throughout the globe by human-to-human contact.

Historically, the first reported pandemic IAVs in humans was the Spanish flu, also known as Great influenza epidemic, in 1918. This pandemic strain was characterized as H1N1 subtype with avian origin[107]. To date, this influenza pandemic has been one of the deadliest infectious diseases in human history, only surpassed by the Black Death and smallpox, since it is estimated that it caused

between 50-100 million human losses[108]. This strain was very virulent, causing high mortality rates in healthy individuals, between 20 and 40 years old[109].

In 1957 a novel IAV emerged in Southern China, characterized as H2N2 subtype. This pandemic, denominated as Asian flu, caused over a million deaths. This strain arose from the genomic reassortment segments of the 1918 H1N1 strain with H2, N2 and PB1 segments with avian origin [82,83]. Eleven years later, in 1968, this strain reassorted with another avian strain that had emerged in Hong Kong [83]. As a result, the new pandemic Hong Kong flu, harbouring H3 instead of H1, emerged. It is estimated that this flu caused between 1 and 4 million deadly outcomes [110].

In 1977, an H1N1 strain that had already been circulating in Russia in the 1950s re-emerged in China, causing the Russian influenza (H1N1). It is estimated that 700,000 people globally died because of this pandemic, especially young people. The re-emergence of this virus could have been caused by a laboratory accident [111].

In 2009, the most recent IAV pandemic was reported first in Mexico. The new strain, A(H1N1)pdm09 swine origin, arose and rapidly circled the globe through human-to-human contact. According to CDC, during the first year of A(H1N1) pdm09 circulation, 151,700-574,400 deadly outcomes were estimated because of the infection. This strain was produced due to the genetic reassortment between two co-circulating strains in swine, harboring NA/M from the Eurasia "*avian-like*" (EA) swine (H1N1) strain and PB2/PB1/PA/HA/NP/NS from a previous swine triple reassortant (TR) (H1N2) strain (Figure 1.7). Likewise, this TR strain emerged in the 1990s and contained segments of human, avian, and porcine origin. First, the TR swine strain (H3N2) emerged, bearing H3/N2/PB1 from seasonal human H3N2, PB2/PA from North American avian (H1N1), and NP/M/NS from classical swine (H1N1). Years later, the TR swine origin (H3N2) was reassorted again with the Classical swine (H1N1), generating the TR swine origin (H1N2) strain [85].

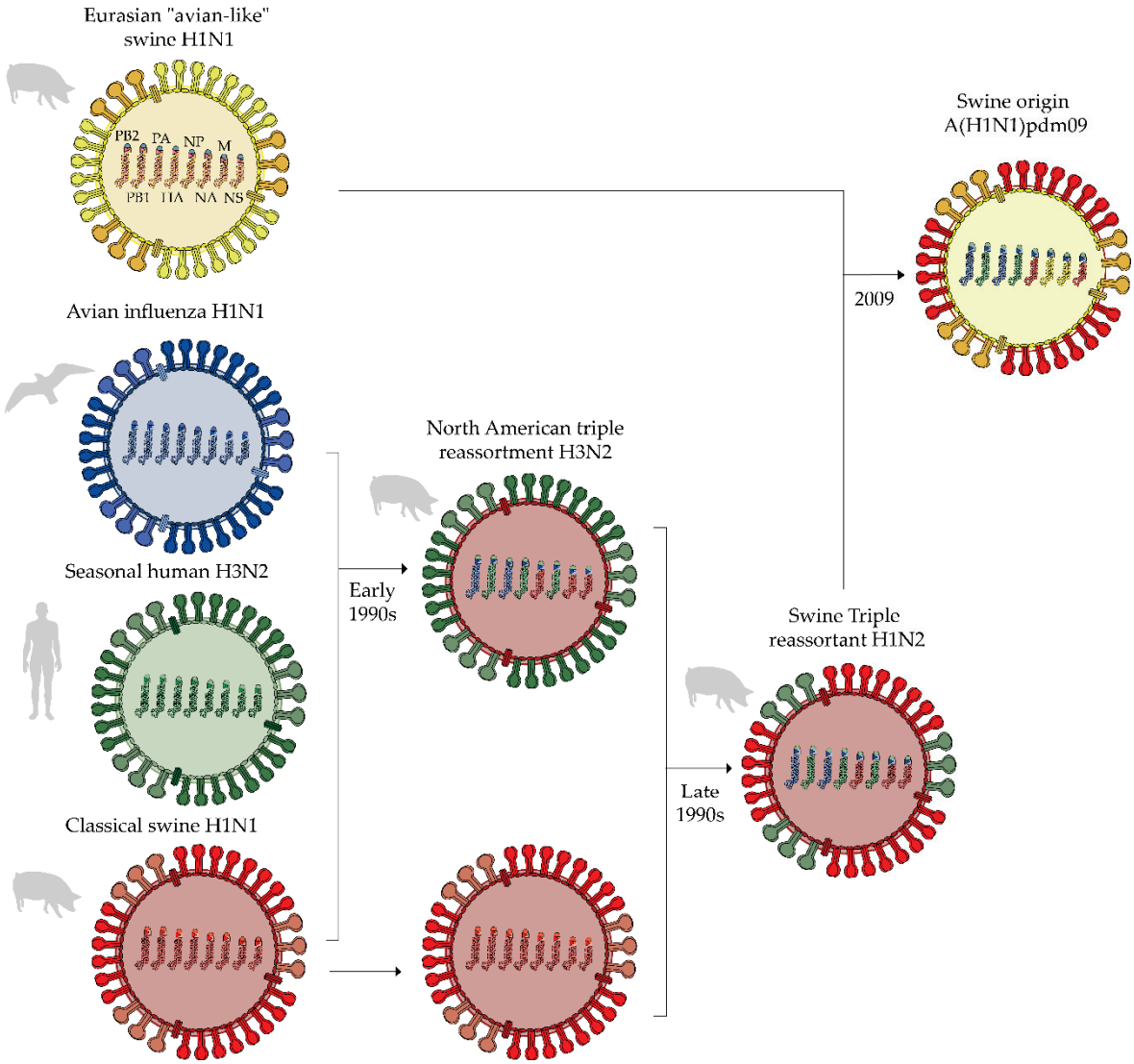


**Figure 1.7.** Origin of the pandemic H1N1 pdm09 strain. In the figure, segments from different Eurasian "avian-like" H1N1, Avian influenza H1N1, Seasonal human H3N2 and Classical swine H1N1 strains are represented in yellow, blue, green, and red colours, respectively. Swine, human and avian figures shown the animal origin of each strain. Lines followed by arrows encompass the strains from which the new strains are formed by genomic reassortments. The approximate date of emergence for new strains is indicated under the arrows. *Figure designed by Lorena López Valiñas*.

## 1.7 Swine host as IAV "mixing vessels" and pandemic risk

### 1.7.1 Mixing vessels hypothesis

As previously mentioned, surface glycoproteins HA and NA interact with host cell SAs to allow virus cell entry and release. IAVs from different animal origin interact with different host SA receptors. Therefore, depending on the SA present in the target epithelial cells, the virus tropism is defined. IAV with avian origin prefers SA $\alpha$2-3Gal type, while the human origin IAV prefers SA $\alpha$2-6Gal type. In the upper respiratory tract of pigs both SA receptors are present, being pigs susceptible to both, avian and human IAV. Hence, there is a possibility that IAVs from both origins may simultaneously co-infect a pig. Consequently, as happened

in 2009, new IAVs harbouring avian, human, and pig segments could arise by genetic reassortment, causing a continuous pandemic threat [112–115]. For all these reasons, according to a hypothesis described in 1990 by Dr. Scholtissek, pigs are considered as "mixing vessels", playing and important role in the adaptation of avian IAV to human and vice versa [116,117].

### 1.7.2 SIV Pandemic risk

Nowadays the pig industry is constantly growing, and the cross-border movement of animals is easier due to globalization [76]. Pigs to humans interspecies IAV transmission occurs occasionally in people who have close contact with animals, such as farm workers. Interspecies transmission requires prolonged virus exposure and a high viral load. On the contrary, SIV transmission through meat consumption is non-existent [118].

In recent years, several cases of SIV have been sporadically reported in humans. Most of the cases, the virus was reported individually due to the low spread efficacy of virus by human-to-human contact [119]. In 1976, the first outbreak of SIV H1N1 in humans was reported, in total 230 soldiers from Fort Dix military base got infected, with one casualty. Fortunately, the virus did not reach the civilian population of Fort Dix, spreading only among army recruits, none of whom had priorly been in close contact with pigsit [120]. According to a review published in 2007, since then, 50 cases of swine to human zoonotic events had been reported with a mortality rate of 14%. It affected civilians, most of whom had been in contact with pigs, and military personnel [121].

Therefore, before 2009 there were no major episodes of swine flu transmission from pigs to humans. However, A(H1N1) pdm09 swine origin, unlike previous swine flu reported, was able to quickly spread by human-to-human contact throughout the globe, posing a significant risk to human health. From this moment on, pigs were considered important reservoirs of IAV for the generation of new strains with pandemic capacity.

Since 2009, human infections with SIV have been periodically reported in America, Europe, Asia and Australia [119]. In 2013, a new genotype of EA H1N1 (G4) was first detected, harbouring fragments from A(H1N1)pdm09, TR, and EA. In 2016 this G4 strain became predominant in China, Being the only circulating strain in 2018. This virus shows heightened human infectivity, increasing its capability of generate a new swine origin pandemic strain [122].

Therefore, considering the growing swine industry, the number of strains currently co-circulating in the swine population (see section 7.4), and the rapid evolution of the virus, the possibility of another swine flu pandemic, as it happened

in 2009, is possible. For this reason, surveillance and virus evolution studies using next generation sequencing are important to control future influenza outbreaks in both, humans, and pigs.

## 1.8 SI: Pathogenesis, Clinical signs, Lesions and Diagnosis

### 1.8.1 Pathogenesis

Swine influenza viruses only replicate in the epithelial cells of the upper and lower swine respiratory tract, causing an acute infection. Hence, the affected organs are the nasal mucosa, ethmoid bone, trachea, and lungs. SIV excretion occurs through the respiratory route, being the route of transmission and contagion. After animal infection SIV could be detectable from 1 to 7 days post infection [123].

The strain and the initial viral infection dose play an important role in the kinetics of SIV replication. Based on this, the different levels of cytokines can be induced in the infected host during the acute phase of infection, causing different degrees of disease severity from subclinical infection to severe disease. Different cytokines such as alpha and gamma interferons, tumour necrosis factor-alpha, and interleukins 1, 6, and 12 are excreted during infection. The higher the viral load is during infection, the greater the excretion of these cytokines. Consequently, the induced acute-phase proteins cause lung inflammation and the characterized disease. On the other hand, the cytokines also have an important role in the virus clearance, with antiviral and immunostimulant functions [124].

### 1.8.2 Clinical signs

Swine influenza is an acute upper respiratory disease whose symptoms are characterized by pyrexia between 40.5 and 41.5 °C, anorexia, apathy, lethargy, excess of mucus secretion in nose and eyes, sneezing, shortness of breath, with tachypnoea, rapid abdominal breathing, dyspnoea, and coughing. All the current SIV subtypes circulating among swine population have similar clinical manifestation [123].

Clinical outcomes appear in a period of 1-3 days after the infection, and animal recovery starts between 5-7 days. The mortality rate caused by SIV on swine is low, usually less than 1%, although its morbidity rate is very high reaching up to the 100% [125,126]. The severity of influenza pathology may vary depending on the immune status of the infected animal, the existence of coinfection with other pathogen, the age of the pigs, and farm climatic conditions.

As previously mentioned, swine influenza disease can be enhanced by both secondary bacteria and other porcine respiratory viruses infection. Among the most frequent respiratory bacteria in pigs that can cause dual infection with SIV,

*Glaesserella (Haemophilus) parasuis*, *Mycoplasma hyopneumoniae*, *Streptococcus suis* and *Pasteurella multocida* are usually found. On the other hand, porcine respiratory coronavirus (PRCV), porcine circovirus type 2 (PCV2) and porcine reproductive and respiratory syndrome virus (PRRSV) are highly frequent viruses, allowing for higher possibility of concurrent infection with SIV [127].

These infectious agents, including SIV, are often simultaneously found in cases of porcine respiratory disease complex (PRDC). In this case, the respiratory disease and lesions are increased and prolonged along time because of the synergistic effect between these infectious agents[128].

### 1.8.3 Lesions

Lesions caused by swine influenza virus can be microscopically and macroscopically observed. In the first case, SIV causes lung cell epithelia necrosis and clustering of inflammatory cells, affecting airways obstruction. On the other hand, gross lesions produced by SIV are characterized by cranioventral bronchopneumonia that mainly affects apical and cardiac lobes of the lung, although multifocal consolidation on caudal lobe.

Furthermore, the vaccine-associated enhanced respiratory disease (VAERD) has been previously described in pigs. It consists in clinical manifestation increasement of the disease in vaccinated pigs. Although this phenomenon is not well understood, it seems that it is induced when a previous vaccinated animal, with a whole influenza inactivated vaccine, is infected by a strain with the same subtype as vaccine with heterologous antigenicity[129–131].

### 1.8.4 Diagnosis

Nowadays, there are two main methods for SI diagnosis, by detection of specific antibodies against SIV in sera samples by ELISA, and the detection of SIV genome by RT-qPCR.

In the first one, it can be detected if animals were previously infected by SIV and generated an immune response against it. There are subtype-specific serological tests, that indicate to which subtype the animal was exposed. Normally these ELISAS have as target the surface proteins. There are also generic ELISA tests, such as the multispecies one, which only indicates if animal developed antibodies against IAVs.

On the other hand, the RT-qPCR detection technique identifies whether the virus is present at a given time and the viral load at which it is found. Like ELISA tests, we can find subtypical RT-qPCR that indicate the subtype of the sample, and a universal RT-qPCR based on the amplification of M conserved segment [132].

## 1.9 SIV worldwide distribution

Nowadays H1N1, H1N2 and H3N2 are the most prevalent SIV subtypes circulating worldwide among swine population in farms[106,133].

In 1918 in Europe, after the H1N1 pandemic flu, the classic H1N1 (cH1N1) virus was introduced into swine population, and it became in the predominant subtype in pigs, being endemic (Figure 1.8) [133]. In 1979, cH1N1 was replaced by avian-like (EA) H1N1 which rapid spread in all Europe [134], and was later exported to Asia [135]. Years later, in 1982, a new human-like H3N2 virus arose and it established itself in swine by zoonotic reverse interspecies transmission. This new strain bore HA and NA segments from the epidemic 1968 Hong Kong flu H3N2 and the remaining segments from the previously established avian-like (EA) H1N1 [136]. In 1994, the human-like H1N2 subtype was introduced, with the same segments as the previous mentioned strain, but with H1 from 1980 human seasonal H1N1 and the N2 from another human-like H3N2 [137]. From that time, these three strains became established and predominant in the European swine population [133]. Since the 2009 swine origin pandemic, the human H1N1 pdm09 has also been introduced by reverse-zoonotic transmission into the pig population [138,139].

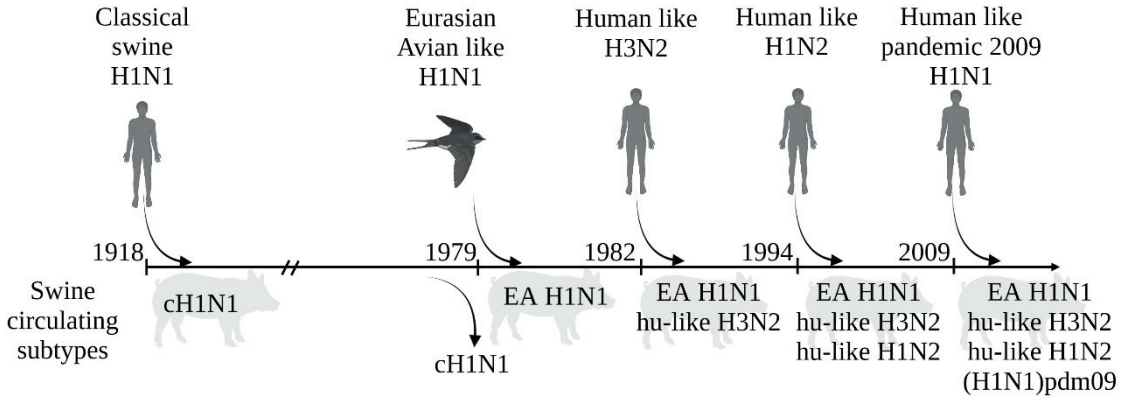


**Figure 1.8.** History of swine influenza virus in Europe during the last century.

Nowadays, different strains of H1N1, H3N2 and H1N2 are currently circulating in swine [140–145]. The wide variety of circulating strains increases the possibility of genomic reassortment events. Therefore, there are more variety of circulating genotypes, increasing concern about disease control. Lately, several reassortments of SIV have been reported worldwide, evidencing again the rapid evolution of this virus [122,146–148].

## 1.10 Control against SIV

Nowadays there are two main actions to control SIV, biosecurity measures and vaccine application. The first consists of applying biosafety protocols on farms to prevent the introduction and spread of the virus among animals, linked to

surveillance studies to control the status of presence or absence of SIV in the farm [149].

Currently, vaccination against SIV is the most effective and used strategy to control SIV in the swine population. Nowadays, the administration of the vaccine is limited in the pig population, only 10-20 % of the animals are vaccinated against SIV in Europe [150]. These vaccines, consist of the whole attenuated or inactivated virus together with an adjuvant. The administration of these vaccines is usually intramuscular, although there are also subcutaneous, intradermal, and even intranasal vaccines [151].

Three or four inactivated strains can be included in the vaccine formulation, to cover all circulating strains. In Europe, the most extended vaccines are trivalent, including inactivated EA H1N1, human-like swine H1N2, and human-like swine H3N2 strains [149]. These vaccines must be adapted to the geographical regions where they will be applied since there is a diversity of genotypes throughout the globe.

The objective of these vaccines is to stimulate Immunoglobulin G (IgG) production against HA and NA surface glycoproteins, which are the most immunogenic viral proteins [152]. Vaccines reduce both, clinical symptoms, and viral shedding. Despite the efficacy of vaccines, the protection afforded against SIV is not complete. The reason behind this effect is because of the HAs and NAs of the strains included in the vaccines, since the circulating strains are not genetically equal, producing partial immunity [153]. Therefore, the vaccine is not sterilizing given that it does not avoid viral replication. Over time, due to the rapid evolution of the influenza virus, the genetic distance between vaccine strains and circulating strains grows, which is why surveillance studies and vaccine reformulation are crucial for SIV control. Due to the limitations of current flu vaccines, novel generation vaccines are being investigated with the aim of develop a universal vaccine, simultaneously effective against different IAV subtypes and in different hosts. With the aim of novel vaccine development, different alternatives are being investigated such as recombinant protein vaccines, vector vaccines, DNA vaccines, and live attenuated vaccine with modifications in the NS1 protein [154–156].

# 2 Objectives

The high swine population due to the over increasing swine industry, the low generation time of the virus, and the high SIV mutation rate, causes that virus is constantly under rapid evolution. Understanding the main forces that shape SIV evolution is the cornerstone for virus control and prevention of new viral strains that may pose a threat to both, humans, and pigs health.

Trivalent vaccine against SIV, although limited, is the most common vaccine use in swine. It usually generates incomplete protection against SIV due to the genetic distance between vaccine and circulating strains. Consequently, vaccine is not sterilizing, allowing virus growth and evolving under immune pressure.

Considering this background, the present thesis aimed to study the evolutionary dynamics of SIV under immunity pressure and the identification of *de novo* nonsynonymous substitutions that may have an impact on viral fitness and host immune system evasion as well as the reassortment events. The specific objectives were as follow:

- To assess the evolutionary trends and the possible generation of escape mutants of EA "avian-like" H1N1 SIV subtype, in previously challenged vaccinated and nonvaccinated pigs, through whole-viral-genome deep sequencing (Study I).
- To determine the evolutionary dynamics of "human-like" H3N2 subtype in vaccinated and nonvaccinated pigs in previously naturally infected herds with A(H1N1)pdm09, through NGS (study II).
- To evaluate both, genetic drift, and shift in SIV, during a coinfection experiment with EA "avian-like" H1N1 and "human-like" H3N2 strains in vaccinated and nonvaccinated pigs (study III).

# Part II

# Studies

# Chapter 3

## Study I - Identification and Characterization of Swine Influenza Virus H1N1 Variants Generated in Vaccinated and Nonvaccinated, Challenged Pigs.

*Viruses* **2021** Oct 16;,*13*(10):2087

*Álvaro López-Valiñas[1,2], Marta Sisteré-Oró [1,2], Sergi López-Serrano [1,2], Laura Baioni [3], Ayub Darji [1,2], Chiara Chiapponi [3], Joaquim Segalés [1,2,4,5], Llilianne Ganges [1,2] and José I. Núñez [1,2*]*

[1] Institut de Recerca i Tecnologia Agroalimentàries, Centre de Recerca en Sanitat Animal IRTA-CReSA, 08193 Barcelona, Spain.
[2] OIE Collaborating Centre for the Research and Control of Emerging and Re-emerging Swine Diseases in Europe (IRTA-CReSA), Bellaterra, Barcelona, Spain
[3] OIE Reference Laboratory for Swine Influenza Virus, Istituto Zooprofilattico Sperimentale della Lombardia ed Emilia-Romagna, 25124 Brescia, Italy.
[4] Departament de Sanitat i Anatomia Animals, Universitat Autònoma de Barcelona, 08193 Bellaterra, Barcelona, Spain.
[5] UAB, Centre de Recerca en Sanitat Animal (CReSA, IRTA- UAB), Campus de la Universitat Autònoma de Barcelona, 08193 Bellaterra, Barcelona, Spain

## 3.1 Abstract

Influenza viruses represent a continuous threat to both animal and human health. The 2009 pandemic H1N1 A influenza highlighted the importance of swine host in adaptation of influenza viruses to human. Nowadays, one of the most extended strategies used to control Swine influenza viruses (SIVs) is the trivalent vaccine application, which formulation contains the most frequently circulating SIV subtypes H1N1, H1N2, and H3N2. These vaccines do not provide full protection against the virus, allowing its replication, evolution, and adaptation. To better understand the main mechanisms that shape viral evolution, here, the SIV intra-host diversity was analyzed in samples collected from both, vaccinated and nonvaccinated animals challenged with H1N1 influenza A virus. Twenty-eight whole SIV genomes were obtained by next generation sequencing and differences in nucleotide variants between groups were established. Substitutions were allocated along all influenza genetic segments, while the most relevant non-synonymous substitutions were allocated in the NS1 protein on samples collected from vaccinated animals, suggesting that SIV is continuously evolving despite vaccine application. Moreover, new viral variants were found in both vaccinated and nonvaccinated pigs, showing relevant substitutions in the HA, NA and NP proteins, which may increase viral fitness under field conditions.

**Keywords:** swine influenza virus (SIV); next generation sequencing; single nucleotide variants (SNV); non-structural protein (NS), hemagglutinin (HA); nucleoprotein (NP); neuraminidase (NA)

## 3.2 Introduction

Swine influenza is a widely distributed disease that generates important economic losses in the pig industry [157]. The aetiological agents, the swine influenza viruses (SIV) belong to the *Orthomyxoviridae* family and represent an important threat to public health due to the risk of potential zoonotic infections. The SIV genome is characterized by 8 genomic segments of negative sense, single-stranded RNA, each segment codes for at least one protein [158]. The proteins of the polymerase complex (formed by two polymerases basic (PB1, PB2) and one polymerase acidic (PA)), the hemagglutinin (HA) and neuraminidase (NA) surface glycoproteins and the nucleoprotein (NP) are coded by the RNA segment of the same name[159]. The matrix (M) and non-structural (NS) genome segments encode each one for two different proteins by splicing mRNA; matrix protein (M1), ion channel (M2) [17] and non-structural protein (NS1), and nuclear export protein (NEP) [18] respectively. Moreover, the PB1 segment has an alternative codon frame that codes for the accessory PB1-F2 protein [21].

In the spring of 2009, an outbreak of a new pandemic strain A(H1N1)pdm09 of swine origin was reported in the USA and it quickly spread to more than 30 countries by human to human contact [85]. Since then, according to the Centres for Disease Control and Prevention (CDC) between 151,700 and 575,400 fatal human cases have been recorded [160]. The A(H1N1)pdm09 strain arose from the genomic reassortment of an H1N1 Eurasian "avian-like" (EA) swine virus NA/M and triple reassortants of H1N2 and H3N2 harbouring the PB2/PA segments of a North-American avian influenza virus, the PB1 segment from a human H3N2 and the HA/NP/NS segments from a classical swine H1N1 [161].

In a recent published SIV surveillance study, performed on both pigs and farm workers in China, a new emerging genotype 4 (G4) reassortant EA H1N1 with some pdm09 genes (G4 EA H1N1 virus) was detected. The increasing capability to infect humans and the absence of pre-existing immunity against this strain concerns about the possibility of new pandemic virus generation [122].

The SIV evolution, explained under the quasispecies theory, plays an important role in adaptation, host range, virulence and emergence of new variants mainly due to both, point mutation and genomic reassortment [73]. Although recombination is a mechanism of change, it does not play an important role on influenza A virus (IAV) evolution [162]. The viral polymerase is characterized by the lack of proof-reading function during the replication process with a high mutation rate of $10^{-3}$ to $10^{-4}$ per gene per generation [79]. Taking that fact into account, the greater accumulation of point mutations on antigenic sites may drive a new antigenic pattern, phenomenon known as antigenic drift. Hence, in addition to the high prevalence of IAV, antigenic drift may trigger on the appearance of new influenza variants able to escape vaccination [163].

Vaccination against SIV is currently the main strategy in order to prevent and control the disease [164]. Nowadays, the most extended vaccines are based on inactivated or attenuated viruses [151] such as the trivalent vaccines that contain the most common circulating SIV subtypes in Europe, EA H1N1, human-like swine H1N2 and human like reassortant swine H3N2 [165,166]. These vaccines mainly stimulate the IgG production against HA viral protein and to NA and NP proteins to a lesser extent. These vaccines reduce both, clinical signs and viral shedding, although they do not prevent viral replication [167].With the aim to evaluate the viral evolution and the possible generation of escape mutants, the evolutionary trends of SIV under selection pressure due to vaccination were studied through whole viral genome deep sequencing in the present work. Two groups of piglets, vaccinated and nonvaccinated, were infected with SIV strain

of EA H1N1 subtype. In total, 27 whole viral genome sequences were obtained, and variants detected from both experimental groups were characterized.

## 3.3 Materials and Methods

### 3.3.1 Cells and virus

Madin-Darby Canine Kidney (MDCK, ATCC CCL-34) cells were used for both, viral titration and production. Dulbecco's Modified Eagle Medium DMEM (Lonza, Basel, Switzerland), supplemented with fetal bovine serum (Euroclone, Milan, Italy) (10%), L-glutamine (Gibco Life Technologies, Madrid, Spain) (1%), penicillin/streptomycin (1%) 100 U/mL (Gibco Life Technologies, Madrid, Spain) was used for the cell culture and cells were further kept at 37°C with 5% CO2 atmosphere.

The A/Swine/Spain/01/2010 H1N1 virus was propagated at a multiplicity of infection (MOI) of 0.01 in the MDCK monolayer cells in presence of 10 μg/mL porcine trypsin (Sigma-Aldrich, Madrid, Spain) and then harvested 48 hours later. Inoculum titration was performed by serial dilutions in MDCK cells culture. The 50% tissue culture infection dose ($TCID_{50}$) was calculated following the Reed and Muench method [168].

### 3.3.2 Experimental design

Fifteen 5 weeks-old domestic pigs free from SIV and its antibodies were distributed in two groups: group A (piglets from 1 to 8) and group B (piglets from 9 to 15). The number of animals used was considered taking into account similar animal experiments with swine pathogens [169–171]. One week after the acclimation period, pigs from group A were vaccinated with the first vaccine dose of an inactivated influenza vaccine (RESPIPORC FLU3, IDT®, Dessau-Rosslau, Germany). This vaccine includes the subtypes H1N1 (Haselünne/IDT2617/2003), H3N2 (Bakum/IDT1769/2003) and H1N2 (Bakum/1832/2000). According to manufacturer instructions, 2 mL of vaccine were intramuscularly administered per pig. After 21 days post-vaccination (dpv), a second immunization was carried out. In parallel, group B pigs were intramuscularly inoculated with the same volume of PBS (nonvaccinated group).

Three weeks after the second immunization (42 dpv), animals from both groups were challenged using two administration routes: intranasal (1 mL per nostril) with a diffuser device (MAD Nasal, Teleflex, Morrisville, USA) and endotracheal (5 mL), by intubation of the animal restrained with a pig lasso immobilizing, both with $10^6$ $TCID_{50}$ of the A/Swine/Spain/01/2010 (H1N1) [172]. After challenge, pigs were daily monitored for clinical signs and animal behaviour in a blind manner by trained veterinarians. Registered clinical signs

were scored from 0 to 3 as previously described [173]. After challenge, animals were euthanized at 2, 5 and 10 day post infection (dpi); 3 animals per group at 2 dpi, another 3 per group at 5 dpi and the remaining piglets at 10 dpi. Animal experiments were performed in AM Animalia facilities (La Vall de Bianya, Girona, Spain). All procedures were carried out according to the guidelines of the animal ethics committee from the *Generalitat de Catalunya*, preserving the Spanish and European regulation under the project number 9657.

### 3.3.3 Sample collection

Nasal swab samples were collected before the first and the second vaccination, at the viral challenge day and at 1, 2, 3, 5, 7 and 10 dpi. Blood samples were collected before each vaccination, at challenge and before necropsy.

Moreover, lung and nasal turbinate (NT) tissues were taken at necropsy, were homogenized in brain heart infusion medium (10% weight/volume). Broncho alveolar lavage fluid (BALF) was collected by filling the right lung of each piglet with 150 mL of PBS and after lung massage liquid were collected [174]. An extra lung tissue sample was also collected and stored in formalin.

### 3.3.4 Detection of antibodies against influenza nucleoprotein.

The presence of antibodies against influenza NP was assessed using the ID Screen ® -influenza A Antibody Competition ELISA kit (ID VET, Grabels, France). The ELISA and the inhibition percentage values calculations were performed following manufacturer instructions. Inhibition percentage values below 45% were considered positive, whereas values higher than 50% were negative. Values between 45-50% were considered doubtful.

### 3.3.5 Pathological analyses in lung and immunohistochemistry to detect SIV

Animal necropsies were performed, including a macroscopic examination of the lung parenchyma. The percentage of lung affected area was calculated by image analysis (IA) as previously described [175], using the software ImageJ® (https://imagej.nih.gov/ij/). T-test was applied to study statistical differences between both groups.

Lung from each individual was fixed by immersion in 10% buffered formalin, dehydrated and embedded in paraffin wax. For the examination under light microscopy, paraffin blocks were sectioned at 3-5 μm cuts and stained with hematoxylin-eosin (HE) [176,177].

Influenza virus detection by immunohistochemistry (IHC) in lung was based on two-step polymer method (Envision TM) [178]. For this purpose, the monoclonal antibody against influenza A virus (IgG2a, Hb65, ATCC) and system

+ HRP labelled polymer Anti-Mouse (K4001, Dako) were used as primary and secondary antibodies, respectively. To microscopically score lung lesions, a semi-quantitative method based on affected airways and amount of immunoreactivity were used, respectively [179].

### 3.3.6 Viral RNA detection

BALF, nasal swab, lung and NT supernatants collected throughout the study were further analyzed to isolate, detect, and quantify SIV. Therefore, viral RNA was extracted from samples using MagAttract 96 Cador Pathogen kit ® (Qiagen, Düsseldorf, Germany) according to the manufacturer's instructions. To quantify viral RNA of each sample, the quantitative reverse transcription-PCR (RT-qPCR) assay based on the amplification of the conserved segment of the matrix (M) gene was performed in the Fast7500 equipment (Applied Biosystem). The amplification reaction conditions were: 0.4 μM forward primer (M+25), 0.4 μM reverse primer (M-124), 0.3 μM probe (M+64 FAM-TAMRA), 3 μL of extracted RNA and 0.8 μL of one-step RT-PCR Master Mix Reagents (Applied Biosystems, Foster City, CA, USA) [132]. Threshold cycle (Ct) values equal to or lower than 40 were considered positive. Samples in which fluorescence was undetectable were considered negative.

### 3.3.7 Whole influenza genome sequence by NGS

The A/Swine/Spain/01/2010 (H1N1) inoculum and samples with RT-qPCR Ct value lower than 35 were used for whole genome sequencing, by simultaneously amplification of the eight influenza RNA segments [15]. In addition, to enhance the amplification of the longest segments (PB1, PB2 and PA), a second amplification reaction was performed, according to a previously described protocol [180]. The amplification reactions conditions were: 0.2 μM forward primer (MBTuni-12 or MBTuni12G), 0.2 μM reverse primer (MBTuni-13), 2.5 μL of extracted RNA and 0.5 μL SuperScript® III One-Step RT-PCR System with Platinum™ Taq High Fidelity DNA Polymerase (Thermo Fisher Scientific).

Samples with the eight influenza segments amplified [15] were sequenced by Illumina technology. Multiplexed sequencing libraries were created following Nextera-XT DNA Library Prep protocol (Illumina®, San Diego, CA). Libraries were sequenced using a Miseq Reagment Kit v2 in a 150 cycle paired-end run, on a Miseq Instrument (Illumina®, San Diego, CA). Finally, Illumina adapters were automatically removed from FASTQ files. Sequencing data were deposited at National Center for Biotechnology Information (NCBI, https://www.ncbi.nlm.nih.gov/), with the accession number (PRJNA763061).

### 3.3.8 Mapping and variant calling

Reads quality of raw data were verified by FastQC (v 0.11.8)[181]. Low quality reads (Phread < 30) were removed with Trimmomatic (v0.39) [182]. Subsequently, read alignment tool Bowtie2 (v2.3.5) [183], using the *very-sensitive* function, was used to align the A/swine/Spain/01/2010 (H1N1) inoculum reads against the reference SIV genome sequences (JX908038-45) [184]. Post-mapping, unmapped reads and reads with quality map lower than 30 were removed with Samtools (v.0.39) [185]. Moreover, PCR duplicates were removed with Picard "MArkDuplicatesSpark" command option and reads were recalibrated with "BaseRecalibrator", both included in GATK4 (v4.1). Finally, a consensus sequence was generated with Bcftools (v.1.9) using the *consensus* option [185].

To study possible single nucleotide polymorphisms, all sequenced samples were mapped against the previously generated consensus sequence. Subsequently, mapped read count per position and genomic segments, of each sample was calculated with "*-depth*" function included on Samtools (v1.9) and plotted with ggplot2 library [186] using RStudio software [187] .

The variant calling file (VCF) of each sample was generated with LoFreq software (v2.1.5) using default parameters [188]. To define a single nucleotide variant (SNV), the following requirements were considered: mapping quality > 30, minimum coverage depth of 50, alternative base supported by at least 10 reads and p value per change found < 0.01. The effect on variants was predicted by SnpEff software (v.4.3) [189], where H1N1 SIV database was previously built with "*build –gtf22*" function. Finally, SNV with an allele frequency lower than 1 % were excluded from the analysis. Moreover, Chi-squared test were performed to study statistical differences between the proportion of synonymous and non-synonymous SNV with an allele frequency greater than 1 and 5 % in both experimental groups. *P* values < 0.05 were considered significant.

### 3.3.9 Quasispecies analysis

The nucleotide diversity ($\pi$) of each sample population, including inoculum, were calculated with SNPGenie software as follow [190,191]:

$$\pi = \sum_{i<j} \frac{d_{ij}}{(n^2 - n)/2}$$

Where, $\pi$ of each segment is given by the mean number of changes per site (*dij*) divided by all pairs of sequences at that site, thus n is the coverage depth on site. In addition, analysis of variance (ANOVA) and subsequent Kruskal-Wallis post-hoc test by rank were performed to study statistical $\pi$ differences between

groups, segments, and collected samples per day. All these analyses were done using RStudio[187]. Kruskal-Wallis *P* values < 0.05 were considered significant. Samples with a mean depth per segment lower than 100 were excluded from this analysis.

## 3.4 Results

### 3.4.1 Kinetics of RNA viral detection and antibody induction after vaccination and SIV challenge

After the first vaccination, antibody response to the NP protein was found in seven out of eight vaccinated animals (group A), being all positive three weeks after the second immunization (day of viral challenge) (Figure 3.1). However, at viral challenge, lower antibody levels near to the cut-off were found in two vaccinated pigs (number 1 and 8). After challenge, similar values were maintained by most immunized pigs until the euthanasia day, except for pigs 1 and 8, which increased over time. Meanwhile, nonvaccinated pigs remained negative during the trial, except for pigs 14 and 15 which resulted positive at 5 and 10 dpi, respectively (Figure 3.1).

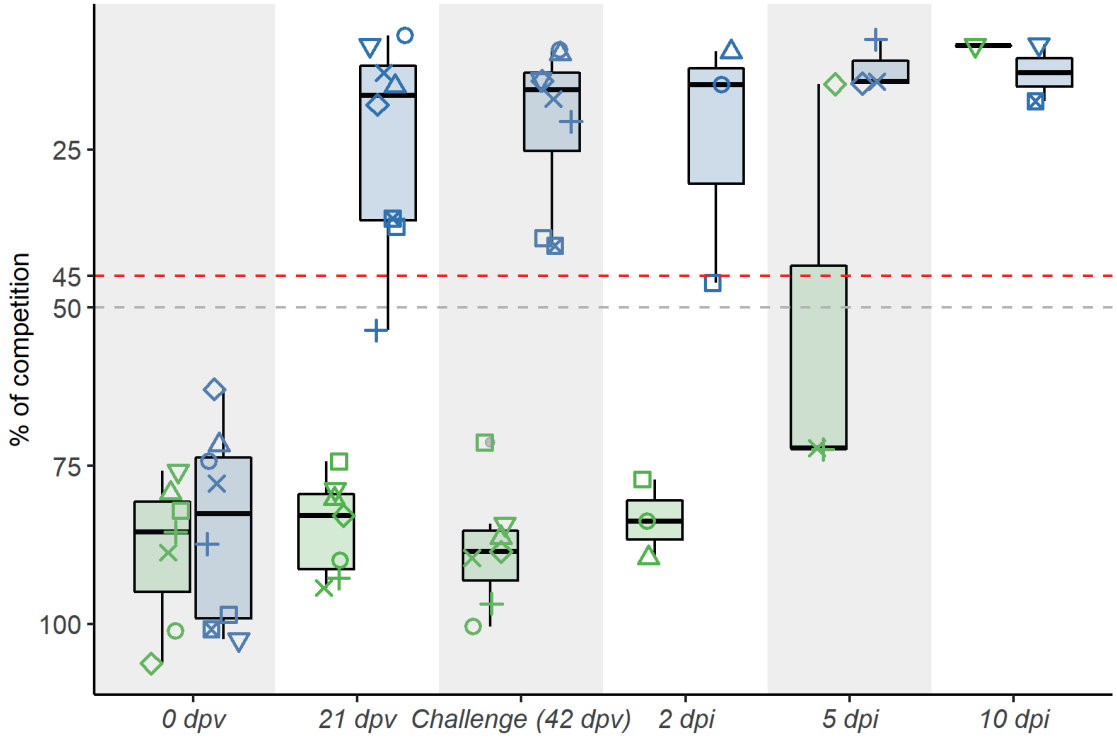


**Figure 3.1. Kinetics of the IgG antibody levels against the NP detected by ELISA in sera after vaccination and viral challenge**. IgG antibodies measured as percentage of competition at first vaccination (0 dpv), 21, 42 dpv (day of challenge) and at 2, 5 and 10 dpi are depicted. Points upper dashed red line (competition > 45%) are considered positive, whereas points under dashed grey line (competition < 50%) are considered negative. Values between two lines are considered doubtful. Group of vaccinated and nonvaccinated animals are shown in blue and green, respectively.

After SIV challenge, higher RNA viral loads were detected in the majority of nasal swab samples collected from nonvaccinated pigs as early as 1 and until 5 dpi. By contrast, lower RNA loads were detected in pigs from the vaccinated group (Table 3.1). Nonetheless, RNA viral shedding was found from day 2 until day 5 in all vaccinated-challenged pigs. Throughout days after challenge, a decrease in viral load was observed, until no SIV RNA detection at 10 dpi. Likewise, in the case of pulmonary tissue and BALF, higher RNA loads were found in all nonvaccinated pigs from 2 to 5 dpi. Although lower RNA loads were also found in lung and BALF from vaccinated-challenge pigs, the RNA levels were higher than those detected in nasal swabs (Table 3.1). Viral load was higher in lung at 2 dpi with values between 26 and 21, in animals from both groups. In NT, only three samples were positive, two from 2 dpi and one from 5 dpi (Table 3.1).

**Table 3.1. RT-qPCR Ct values results obtained from viral samples extracted from NS at different time points and from lung, BALF and NT.**

| | | Nasal swab | | | | | | | Tissues samples | | |
|---|---|---|---|---|---|---|---|---|---|---|---|
| **Group** | **Pig ID** | **1 dpi** | **2 dpi** | **3 dpi** | **5 dpi** | **7 dpi** | **10 dpi** | **Euthanized day** | **BALF** | **LUNG** | **NT** |
| *Vaccinated Group* | *1* | 35.8 | 38.7 | † | † | † | † | *2 dpi* | 30.2 | 25.7 * | 35.2 |
| | *2* | *Undet* | 39.4 | † | † | † | † | | **30.4** | 23.3 * | *Undet* |
| | *3* | *Undet* | 37 | † | † | † | † | | 33.9 | *Undet* | *Undet* |
| | *4* | *Undet* | *Undet* | 34.14 * | *Undet* | † | † | *5 dpi* | 36.7 | 35.1 | *Undet* |
| | *5* | *Undet* | *Undet* | **33.8** | *Undet* | † | † | | 35.4 | 32.31 * | *Undet* |
| | *6* | *Undet* | *Undet* | 37 | 36.5 | † | † | | *Undet* | *Undet* | *Undet* |
| | *7* | 38.4 | 30.7 | 34 | *Undet* | *Undet* | *Undet* | *10 dpi* | *Undet* | *Undet* | *Undet* |
| | *8* | *Undet* | 35.72 * | 33.2 | 34.11 * | *Undet* | *Undet* | | *Undet* | *Undet* | *Undet* |
| *Non vaccinated Group* | *9* | 34.8 | 31.3 | † | † | † | † | *2 dpi* | 28.4 | 21.4 | 28.8 |
| | *10* | 36.1 | 34.79 * | † | † | † | † | | 22.8 | 24.9 | *Undet* |
| | *11* | *Undet* | 33.42 * | † | † | † | † | | 29 | **21.8** | *Undet* |
| | *12* | 30.1 | 28.9 | 32.8 | **33.8** | † | † | *5 dpi* | 29.8 | **26.3** | 39.2 |
| | *13* | 26.9 | 28 | 29.3 | Undet | † | † | | 29.7 | **30.4** | *Undet* |
| | *14* | 32.9 | 29.9 | 32.8 | Undet | † | † | | 28.6 | **30.2** | *Undet* |
| | *15* | *39.67* | *36.7* | *35.25* | *35.28* | *33.18* | *33.72* | *10 dpi* | *Undet* | *Undet* | *Undet* |

*Neg.: negative; Highlighted in grey: sequenced samples; *: sequenced samples with low coverage; Bold: negative whole genome influenza amplification; † : euthanized animal. Cells shadowed in blue and green indicate vaccinated and nonvaccinated animals respectively.*

### 3.4.2 Lung lesions determined in vaccinated and nonvaccinated challenge pigs

Gross lung lesions were detected in both vaccinated (13.41±9.38 of affected lung) and nonvaccinated (33.03±15.7 of affected lung) pigs (Table 3.2), being these differences significant (T-test;*P*=0.0105). Similar microscopic lesion scorings were found in both experimental groups (Table 3.2), being the highest scores registered at 2 and 5 dpi. Remarkably, the viral labelling detected by immunohistochemistry in lung sections was higher in vaccinated animals at 2 dpi. At 5 dpi low viral immunodetection was found in nonvaccinated animals, whereas vaccinated ones remained negative.

**Table 3.2. Pathological results based on microscopic observation and quantitative scoring of HE and IHC staining lung samples, and percentage of lung affected area.**

| Group | Pig ID | Euthanasia day | Lung afected area (%) | Histopathological scoring | Immunohistochemistry for SIV |
|---|---|---|---|---|---|
| *Vaccinated Group* | *1* | *2 dpi* | 3.28 | *2* | ++ |
| | *2* | | 9.33 | *3* | +++ |
| | *3* | | 28.64 | *3* | ++ |
| | *4* | *5 dpi* | 13.22 | *2* | - |
| | *5* | | 27.23 | *3* | - |
| | *6* | | 7.23 | *0.5* | - |
| | *7* | *10 dpi* | 8.57 | *1.5* | - |
| | *8* | | 9.76 | *0.5* | - |
| | | *mean* | 13.41 | | |
| *Non vaccinated Group* | *9* | *2 dpi* | 29.52 | *3* | +++ |
| | *10* | | 33.65 | *1.5* | + |
| | *11* | | 65.72 | *3* | + |
| | *12* | *5 dpi* | 24.5 | *2* | + |
| | *13* | | 26.43 | *3* | + |
| | *14* | | 35.06 | *3* | + |
| | *15* | *10 dpi* | 16.36 | *1* | - |
| | | *mean* | 33.03 | | |

*Histopathology scoring: absence (0), few isolated (0.5), localized cluster (1), several (1.5-2), severely several (2.5) and many (3) airways affected. Moreover, minimal (1.5), mild (2) interstitial infiltrate and plus moderate interstitial and alveolar infiltrates (2.5-3). SIV immunohistochemical scoring: absence (-), low (+), scattered (++), moderate (+++) and abundant (++++) amount of immunoreactivity.*

### 3.4.3 Determination of whole genome sequences from vaccinated and nonvaccinated animals after A/Swine/Spain/01/2010 (H1N1) challenge

From a total of 37 samples, 28 influenza genomes were amplified and sequenced, 11 from vaccinated animals and 17 from nonvaccinated ones (Table 3.1 and Figure 3.2). In addition, the complete genome sequence from A/Swine/Spain/01/2010 (H1N1) strain used as inoculum was also obtained.

After quality control, as average, all processed reads had a length of 126.79 (± 4.3) nucleotides and 64,966 reads per sample, reaching a total of 1,948,362 reads for all samples. After mapping and duplicates removal, we obtained samples between 201,577 and 2,227 reads, both from nasal swabs samples collected in vaccinated pigs. The highest number of reads corresponded to animal 7 at 2 dpi and the lowest to pig 8 at 5 dpi. This last sample was removed for further analysis. Finally, we obtained 1,620,216 reads that were included in the genetic diversity analysis (Table S3.1).

The majority of SIV genomic segments were sequenced with a coverage greater than 50 reads per position in all samples, 309,214 out of 379,204 (81.54%) positions sequenced were represented with more than 50 reads, reaching 4,378 reads as maximum. In general, the short segments (NS, M, NA and NP) had better read depth per position than larger ones, being the segment of polymerase PA the segment with the lowest depth (Figure 3.2). In total, all the 8 genome segments sequenced, with mean depth value greater than 100 was obtained for 5 and 15 samples from vaccinated and nonvaccinated animals, respectively. By contrast, low coverage in all segments, except in NS and M, were found in the 8 remaining samples from pigs 1, 2 and 5 in lung, from pigs 8, 10 and 11 in nasal swabs at 2 dpi and from pig 4 at 3 dpi also in nasal swab (Figure 3.2a and Figure 3.2b).

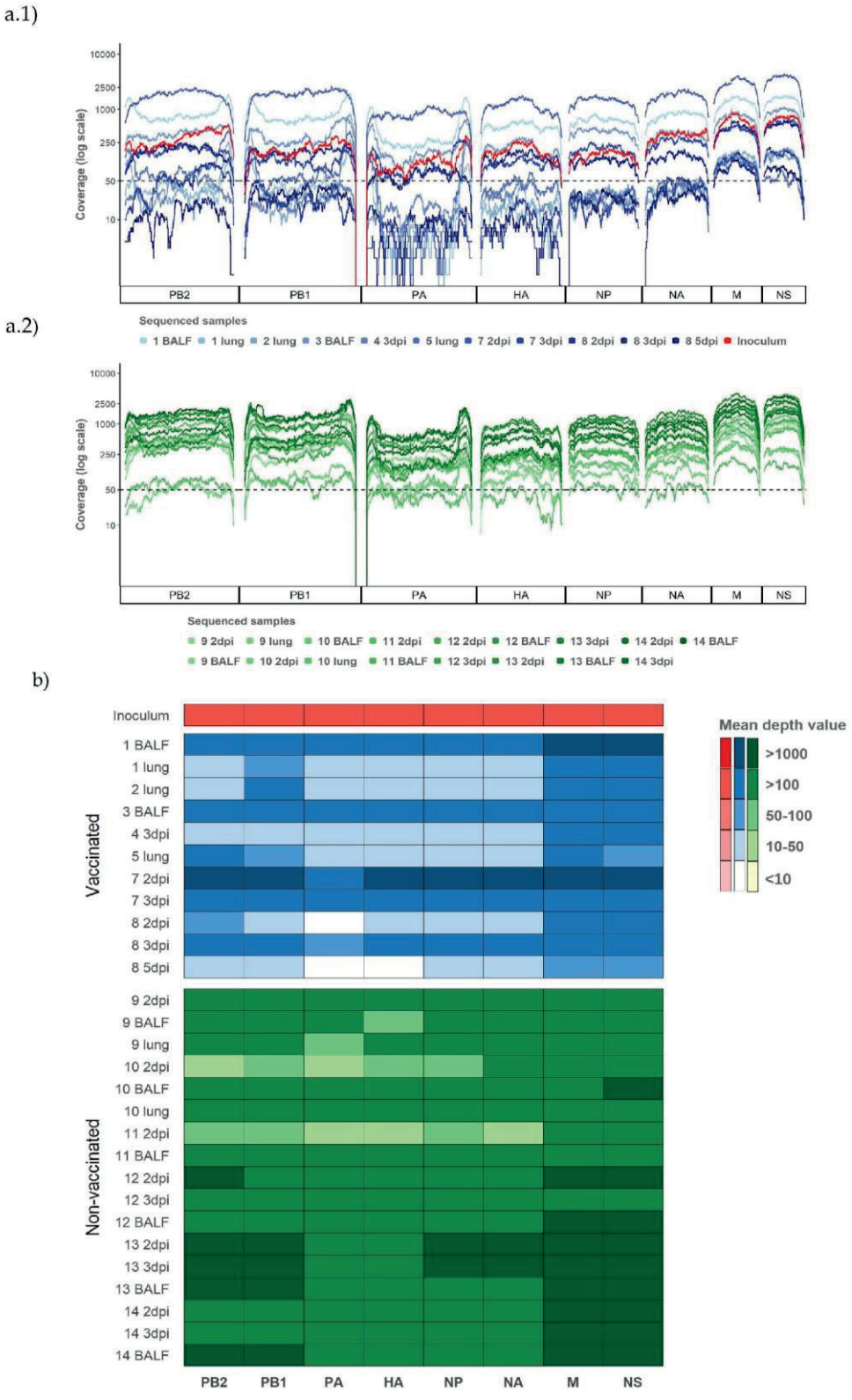


**Figure 3.2. Coverage per genomic segment and sample from both experimental groups and the challenge inoculum.** (a) Representation of the coverage of Illumina sequencing reads mapped against A/Swine/Spain/01/2010(H1N1) used for challenge. (a1) Sequencing profiles of sequenced samples from vaccinated animals and inoculum plotted in different tons of blues and red respectively. (a2) Sequencing profile of sequenced samples from nonvaccinated animals plotted in different tons of greens. (b) Representation of the mean read coverage heat map per segment.

The identification of the animal from which samples comes and the kind of collected sample, are specified on figures, being samples with dpi, nasal swab collected at indicated day.

### 3.4.4 Genetic variation between SIV samples collected from vaccinated and nonvaccinated pigs

The analysis of the mapped reads was performed to study the viral population dynamics in both vaccinated and nonvaccinated animals after viral challenge. A total of 276 SNV with allele frequency greater than 1% were identified from viral populations recovered from both experimental groups (Figure 3.3). Notably, in vaccinated animals, 40 synonymous and 56 non-synonymous variants were identified, representing 41.6 and 58.33 % of the total number of SNV found in this group. By contrast, the same number of synonymous and non-synonymous variants (90 SNV) was registered in the nonvaccinated group (Figure 3.3a).

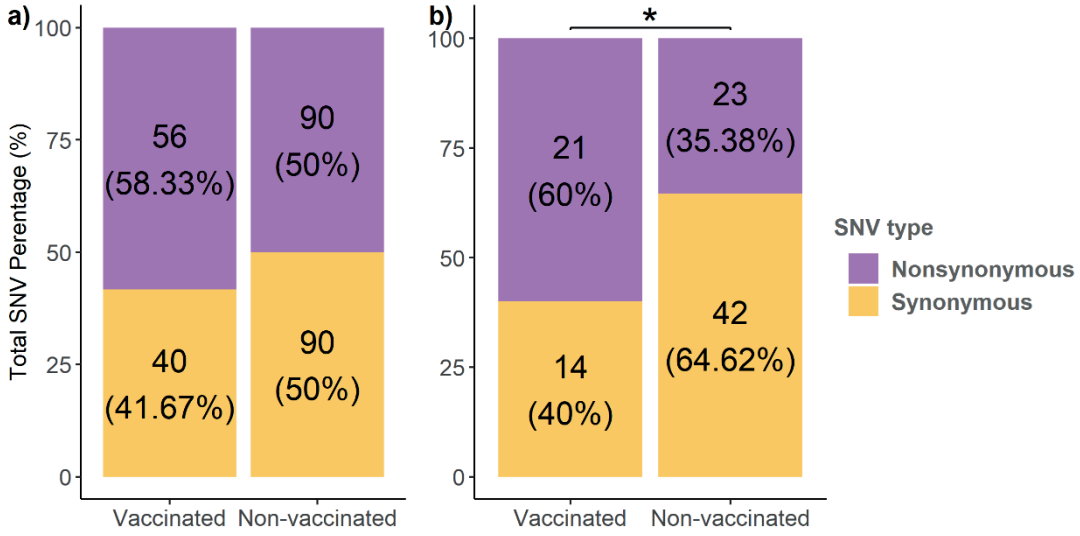


**Figure 3.3. Total number of synonymous and non-synonymous SNV found from vaccinated and nonvaccinated animals.** (a) Substitutions with an allele frequency greater than 1%. (b) Substitutions with an allele frequency greater than 5%. * $P < 0,05$.

In addition, 100 variants with an allele frequency higher than 5% were identified. The 60% of variants found in vaccinated pigs were non-synonymous, whereas this percentage decreased to 35.38% in nonvaccinated animals, being this difference in frequencies significant (Chi-squared; $P$=0.03123). Therefore, a total of 44 non-synonymous substitutions with allele frequency greater than 5% were detected (Figure 3.3b).

In general, amino acid substitutions were identified in all segments along the genome in both experimental groups (Figure 3.4). In vaccinated animals, 21 amino acid substitutions with an allele frequency greater than 5% were identified in PB2 (M567I, T98K, S506P, R310K and G586R), PA (Y130C), HA (V521M, V233I,

I513V), NP (D289E, A122E, A232T and G281V), NA (S354N), M1 (T113A), M2 (S73N) and NS1 (R81S, E179A, E65G, G161E, D67N). Whereas 23 were found in nonvaccinated animals, PB2 (E31G, P67L and H445Q), PB1 (N328S, I322V, M195I, G101R and T156I), PB1-F2 (E31G and P67L), PA (F646S, G81R and V618I), HA (I278V and D200N), NP (K97R and E243G), NA (V379I and S354N) and in M1 (T48N). For further variant details and variants noted with an allele frequency greater than 1% see the supplementary data (Table S3.2).

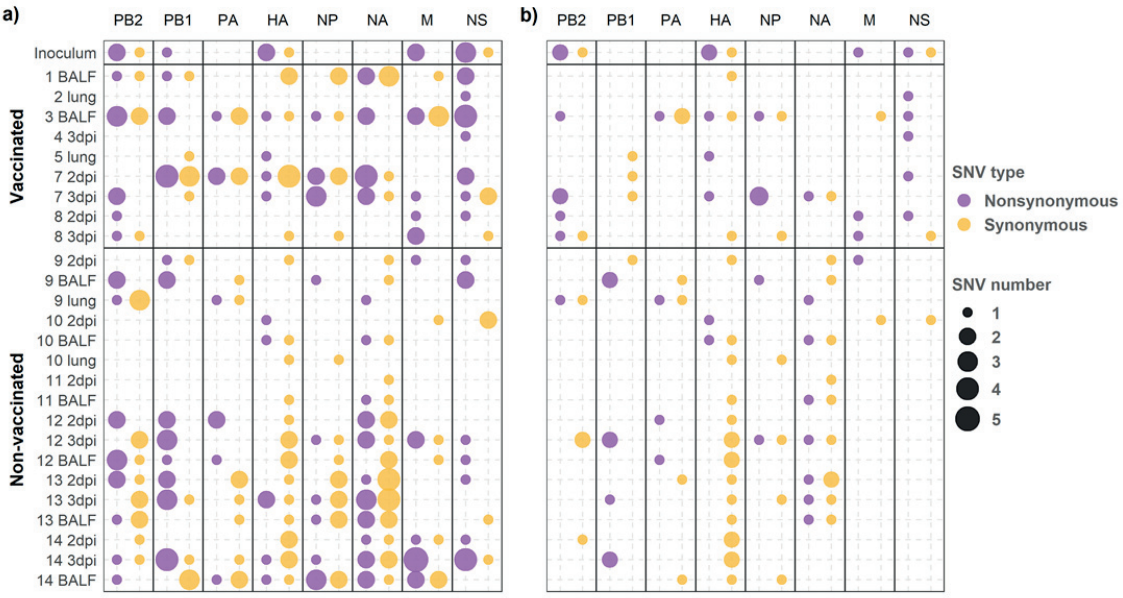


**Figure 3.4. Genome segment distribution and number of synonymous and nonsynonymous SNV found sequenced samples from vaccinated and nonvaccinated animals.** (a) Substitutions with an allele frequency greater than 1%. (b) Substitutions with an allele frequency greater than 5%.

### 3.4.5 Nucleotide diversity in the viral population at different time points

For the study of the nucleotide diversity on each genetic influenza segment, those samples with at least one segment with a mean depth value lower than 100 reads were excluded for the analysis (Figure 3.2 b). The nucleotide diversity was higher in the inoculum, then it decreased in samples collected at 2 dpi in both experimental groups (Figure 3.5). Besides, the $\pi$ was significantly higher at 2 dpi in vaccinated animals in comparison with that of the nonvaccinated group. However, at 3 dpi, the nucleotide diversity was higher in both groups in comparison with the previous day and significant differences were not found in any segment from the viruses recovered from both studied groups. In addition, at 5 dpi, the $\pi$ value decreased in nonvaccinated animals, while no sequences were determined in samples from vaccinated animals (Figure 3.5).

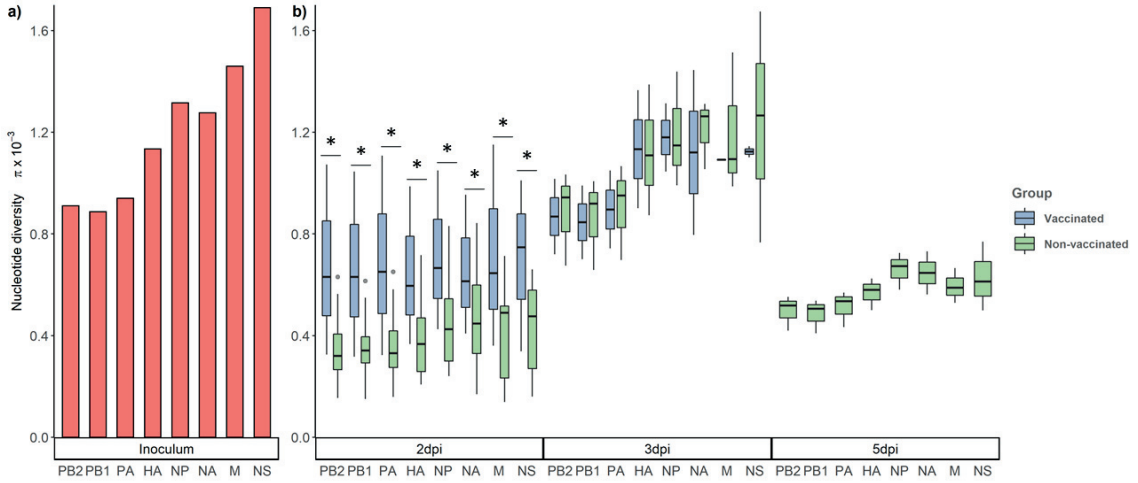


**Figure 3.5. Nucleotide diversity (π) in the viral population at different time points.** (a) Nucleotide diversity bars of inoculum sequence. (b) Box plot of viral population nucleotide diversity from all collected samples at 2, 3 and 5 dpi from vaccinated and nonvaccinated groups. Whiskers represent variability outside the lower and upper quartiles of each represented box. * $P < 0,05$.

## 3.5 Discussion

In the last decades, the increase in pork meat production has caused a significant global growth in the swine industry that contributes to the spread and maintenance of swine pathogens [192]. Swine influenza viruses are highly genetic diverse and worldwide distributed in pigs. These pathogens cause significant losses to the porcine industry and poses a continuous threat to both human and animal health due to the difficulty of formulating a universal effective vaccine to control disease [106]. Nowadays, the most extended vaccination strategies used against SIV are based on attenuated and inactivated vaccines that do not provide full protection against infection [167]. Vaccination can modify viral evolution trends, as the natural selection process could boost the accumulation of point mutations on antigenic sites, allowing the virus escape to pre-existing immunity as previously reported [193,194]. Knowing the biological mechanisms that shape SIV genetic diversity is crucial to understand the evolution of the virus and its implication in host-range, antigenicity, virulence, antiviral resistance, and pathogenesis [73,195]. Therefore, in the present study, differences in evolution trend and genetic diversity between virus collected from previously vaccinated with a trivalent vaccine and nonvaccinated animals were studied after an inoculation of a SIV H1N1 subtype by NGS.

In the present work, viral replication and pathological findings were observed in both vaccinated and nonvaccinated pigs, as already reported [195]. However, viral shedding was lower and pathological finding milder in vaccinated animals. Therefore, the vaccine used in the present study

demonstrated its efficacy by means of less severe lesions and lower viral load in vaccinated animals. This fact had a direct impact on sequencing results, as more samples could be sequenced from nonvaccinated animals and with greater coverage per genomic sample in comparison with samples obtained from vaccinated animals. Nevertheless, full SIV genome sequences from vaccinated animals could be also obtained and SNV were found in all sequenced samples from both experimental groups, evidencing intra-host variability.

Considering the total number of SNV found with an allele frequency greater than 1%, the same proportion of synonymous and non-synonymous variants were detected in samples from nonvaccinated animals, indicating that in this scenario neutral selection pressure may be involved in driving the SIV evolution. When considering variants with an allele frequency greater than 5%, non-synonymous variant proportion was greater than synonymous ones. This finding may indicate a purifying selection event where the deleterious mutations are being eliminated, as previously reported. [77,78]. Thus, no positive selection pressure was found in nonvaccinated animals. Meanwhile, in vaccinated animals, the proportion of non-synonymous variants found was greater than the synonymous ones, analyzed by both 1 and 5% of allele frequency. This analysis may support the viral evolution under positive selection pressure in vaccinated animals [196–198]. Based on obtained results, SIV could be increase its fitness in both, vaccinated and nonvaccinated animals, favoring viral maintenance in the field. Similar findings had been described for classical swine fever virus affecting pigs [199].

Synonymous and nonsynonymous variants were detected along all segments in sequenced samples from both experimental groups (Figure 3.4). Considering variants with an allele frequency greater than 5%, that could have a greater impact on virus fitness, non-synonymous substitutions were mainly found in the PB2, HA, NP and NS1 SIV proteins in samples collected from vaccinated animals. On the contrary, in samples from nonvaccinated animals, most viral changes were found in PB1.

Five non-synonymous substitutions were detected within the viral NS1 protein recovered only in samples from vaccinated animals (Figure 3.6a). The role of NS1 protein in the translation of viral mRNAs and interferon regulation has been previously described. This protein has been associated with the regulation of viral replication and host immunity, including the interferon mechanism regulation [200–203]. NS1 has two structural domains linked by a flexible linker region (LR); the RNA binding domain (RNA BD) formed by the 73 first residues and the effector domain (ED) from residue 85 until the end of the molecule [204–

206] (Figure 3.6a). Considering that, the substitution E65G located in the RBD, D67N in the LR and the R81S, G161E and E179A, located in the ED from the NS1 protein may regulate the SIV replication capacity, the pathogenicity, and the immune response.

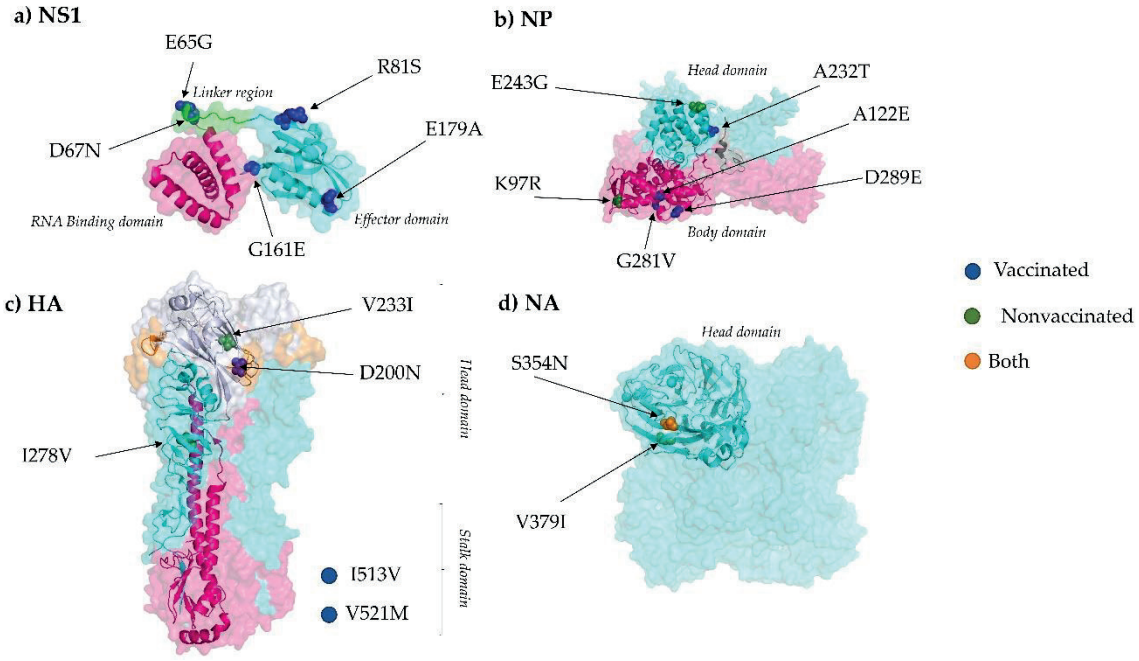


**Figure 3.6. Location of all substitutions (allele frequency > 5%) described in this study in NS1, NP, HA and NA proteins.** (a) NS1 protein (PDB accession no. 4OPH) [204] RNA Binding (RBD), Linker region and effector domain (ED), are highlighted in pink, green and cyan respectively. (b) NP trimer protein (PDB accession no.2IQH), head domain is indicated in cyan colour whereas body domain in pink [207]. (c) HA trimer is also represented (PDB accession no. 3LZG); cyan, pink and blue domains represent HA1, HA2 and Receptor binding domains respectively. In orange the CA antigenic site is highlighted [208]. I513V and V521M substitutions are not in the limit of crystallographed structure. (d) NA tetramer (PDB accession no. 4B7Q) protein [209]. By last, highlighted substitutions in blue were found in vaccinated animals, highlighted green ones in nonvaccinated and orange one in both. The PyMOL Molecular Graphics System, Version 4.3 was used to visualize the protein structures.

Substitutions E65G and D67N could play a role in the plasticity of the molecule, resulting in a different conformation of the NS1 protein and allowing it to bind to different host substrates affecting it activity [60]. Likewise, the R81S substitution, allocated in a domain that interacts with the host eukaryotic translation initiation factor 4G1 (eIF4G1). The recruitment of this factor by NS1 promotes viral mRNA translation instead of host mRNA [57,210]. A previous study has demonstrated the relation between this region and pathogenesis in birds with H5N1 [211]. This substitution was detected with an allele frequency of 18% in a viral sample collected in lung of animal 2, which had the maximum histopathological score. Therefore, variation on NS1 protein could be contributing to both, mRNA viral translation and pathogenesis. Another

substitution found inside the NS1 protein was the G161E. As previously reported, this position was allocated in the human leukocyte antigen B7 (HLA-B7) [212] binding motif that could be equivalent of the swine leukocyte antigen B7 (SLA-B7). Thus, this substitution may affect the antigen presentation capability by the host. Last substitution found in the NS1 was the E179A. Notably, a mutation in this position was previously described in the host cleavage and polyadenylation specificity factor (CPSF) binding domain [213]. The interaction with CPSF subunit avoids correct host pre-mRNAs processing, inhibiting the 3'end cleavage and the polyadenylation [58]. Substitutions in the same position had been found also in equine and canine influenza virus H3N8 subtype. Mutation in this position may have a great impact on the adaptation ability of avian influenza virus to the horses [214]. In addition, this substitution on canine influenza virus is related with the ability of the virus to inhibit the host gene expression [72]. Interestingly, this substitution was found in a viral sample recovered from animal 3, which develop a severe lung lesion despite being vaccinated. Therefore, this substitution may play a role in disease pathogenesis. The changes reported in the present study support the high relevance of one or few substitutions in the NS1 protein on viral replication and host adaptation, as previously reported [214–217].

In the case of the NP, it has been associated with RNA synthesis and trafficking, and also interacts with viral polymerases and host polypeptides [218,219]. Three substitutions were simultaneously noted in a viral sample sequenced from the vaccinated animal number 7 at 3 dpi; A122E and G281V in polymerase interaction sites of the body domain and A232T in the head domain [207,220] (Figure 3.6b). Besides, substitution D289E in the body domain of the protein was also detected in the vaccinated animal 3. On the other hand, two substitutions were allocated in the head and body domains, E243G and K97R respectively (Figure 3.6b). It should be highlighted that in the inoculum consensus sequence, other arginine residues were allocated in R292, R421 and R445. Four arginines inside NP were previously described as interferon (IFN)-inducible tripartite motif 22 (TRIM22) protein resistance [221]. This resistance avoided the interaction between NP and TRIM22, preventing viral polyubiquitination and subsequent degradation by proteasome [222]. This arginine signature was reported in A(H1N1)pdm09; however, the lysine (K) signature at the four residues was being kept in seasonal influenza until 2009. Besides, the arginine signature was also described in the IAV derived from the 1918 pandemic flu [221]. Therefore, fixation of the K97R substitution in nature, found in nonvaccinated animal 9, could pose a risk for both animal and human health due to it similarity to previous pandemics flu.

The HA protein has been associated with the binding to host acid sialic receptor causing membrane fusion within the endosome, allowing virus cell entry [102]. This protein is an important target to generate neutralizing antibodies during IAV infection,[223]. Notably, in this study, five substitutions were found in the HA protein, three in vaccinated animals, whereas 2 in nonvaccinated animals (Figure 3.6c-d). Two substitutions were found in the receptor binding domain (RBD) of the HA protein, the D200N, and V233I, both allocated close to the Ca antigenic site according to the antigenic structure of CA04 HA from the 2009 H1N1 pandemic virus [208,224]. Substitutions in the RBD were also found in vaccinated and nonvaccinated pigs in a previous study [225] (highlighting the relevance of this region that could affect the host-range. The substitution V233I was recovered with high allele frequency (30.4 %) from a vaccinated animal (number 5) that, after viral challenge, showed moderate clinical signs and severe lung lesions. This substitution may be involved in evading the pre-existing immunity in this animal after vaccination. The other two substitutions, I513V and V521M, both from vaccinated animal samples, are allocated in the transmembrane region of the stalk domain of the protein. Substitutions in this domain could change its interaction with surrounded lipids and its structural properties, changing the antigenic exposure of the HA allowing the virus avoiding the immune response [226]. Finally, the I278V substitution was allocated in the esterase subdomain [224].

The NA protein plays an important role at the final stage of IAV infection by interacting with host sialic acid, releasing virion progeny [34]. This protein has been also described as one of the main targets to generate neutralizing antibodies during IAV infection [223]. Two non-synonymous substitutions were found in the head domain of the NA, the S354N, located in the second sialic acid binding site [227] and the V379I (Figure 3.6d). The substitution S354N originated a new N-glycosylation site (NSSS), fulfilling the requesting motif N-X-S/T-X, where X is any amino acid except proline. Changes in N-glycosylation sites can affect properties of viral surface antigens and virions by acting in viral incorporation and replication [228]. This substitution was found in both experimental groups; this could be indicating two different scenarios: a selective advantage independently of the vaccination or virus readaptation from MDCK cells to porcine host.

Our findings suggest, once again, the broad range of adaptation and evolution capacity of SIV. Herein the impact of each substitution found is hypothesized according to previous literature. Further analysis, including viral transmission assays, should be performed to study deeply the impact of each substitution on viral fitness. Overall, the increasing pig population in Europe and

the continuous persistence of SIV in farms, make that SIV is continuously evolving, affecting it in host-range, antigenicity, virulence, antiviral resistance and pathogenesis. Therefore, the generation of a new pandemic SIV is feasible as happened in the 2009 H1N1 IAV pandemic. Stricter vaccination schedules should be carried out on farms to avoid SIV circulation as maximum, increasing the current percentage of swine population vaccinated against SIV in Europe (10-20%) [150].

**Supplementary Materials:** The following are available online at https://www.mdpi.com/article/10 .3390/v13102087/s1, Supplementary table S3.1. Total number of reads obtained in each sequenced sample. Total number of reads and total number of reads mapped against reference genome after PCR duplicate removal in each influenza genome segment. Supplementary table S3.2. SNV and its effect on variant found in viral inoculum and samples collected from previously challenged vaccinated and non-vaccinated piglets with A/Swine/Spain/01/2010 (H1N1).

**Author Contributions:** Conceptualization, J.I.N.; Methodology, A.L., M.S., J.S. and S.L.; HTS Libraries Preparation L.B. and C.C.; Bioinformatic Analysis, A.L.; Formal Analysis, A.L., L.G and J.I.N.; Resources, A.D. and J.I.N; Writing—Original Draft Preparation, A.L., L.G. and J.I.N.; Writing—Review & Editing, A.L., S.L., J.S., L.G. and J.I.N.; Supervision, J.I.N.; Project Administration, J.I.N.; Funding Acquisition, A.D. and J.I.N.

**Funding:** This research was funded by grants AGL2016–75280-R from Ministerio de Ciencia, Innovación y Universidades from the Spanish government. A.L has a pre-doctoral fellowship FPI 2017, Ministerio de Ciencia, Innovación y Universidades from Spanish government.

**Conflicts of Interest:** The authors declare no conflict of interest.

**Acknowledgments:** IRTA is supported by CERCA Programme/Generalitat de Catalunya. The authors thank Lorena López Valiñas for the graphic technical support in the figures. Besides, Dr. Miguel Berduñez for the initial advice on big data management and statistical application guidance.

# Chapter 4

## Study II - Evolution of Swine Influenza Virus H3N2 in Vaccinated and Nonvaccinated Pigs After Previous Natural H1N1 Infection.

*Viruses* **2022** Sep 10;14(9), 2008

*Álvaro López-Valiñas[1,2,3], Laura Baioni[4], Lorena Córdoba[1,2,3], Ayub Darji[1,2,3], Chiara Chiapponi4, Joaquim Segalés[1,3,5], Llilianne Ganges[1,2,3,6] and José I. Núñez[1,2,3]**

1 IRTA. Programa de Sanitat Animal. Centre de Recerca en Sanitat Animal (CReSA). Campus de la Universitat Autònoma de Barcelona (UAB), Bellaterra, Barcelona, Spain.
2 Unitat mixta d'Investigació IRTA-UAB en Sanitat Animal. Centre de Recerca en Sanitat Animal (CReSA). Campus de la Universitat Autònoma de Barcelona (UAB), Bellaterra, Barcelona, Spain
3 WOAH Collaborating Centre for the Research and Control of Emerging and Re-Emerging Swine Diseases in Europe (IRTA-CReSA), 08193 Barcelona, Spain.
4 WOAH Reference Laboratory for Swine Influenza, Istituto Zooprofilattico Sperimentale della Lombardia ed Emilia-Romagna, 25124 Brescia, Italy.
5 Departament de Sanitat i Anatomia Animals, Universitat Autònoma de Barcelona, Bellaterra, 08193 Barcelona, Spain.
6 WOAH Reference Laboratory for Classical Swine Fever, IRTA-CReSA, 08193 Barcelona, Spain.

## 4.1 Abstract

Swine influenza viruses (SIV) produce a highly contagious and worldwide distributed disease that can cause important economic losses to the pig industry. Currently, this virus is endemic in farms and, although used limitedly, trivalent vaccine application is the most extended strategy to control SIV. The presence of pre-existing immunity against SIV may modulate the evolutionary dynamic of this virus. To better understand these dynamics, the viral variants generated in vaccinated and nonvaccinated H3N2 challenged pigs after recovery from a natural A(H1N1) pdm09 infection were determined and analyzed. In total, seventeen whole SIV genomes were determined, 6 from vaccinated, and 10 from nonvaccinated animals and their inoculum, by NGS. Herein, 214 de novo substitutions were found along all SIV segments, 44 of them being nonsynonymous ones with an allele frequency greater than 5%. Nonsynonymous substitutions were not found in NP; meanwhile, many of these were allocated in PB2, PB1, and NS1 proteins. Regarding HA and NA proteins, higher nucleotide diversity, proportionally more nonsynonymous substitutions with an allele frequency greater than 5%, and different domain allocations of mutants, were observed in vaccinated animals, indicating different evolutionary dynamics. This study highlights the rapid adaptability of SIV in different environments.

**Keywords:** swine influenza virus; viral evolution; next-generation sequencing (NGS); vaccine; hemagglutinin (HA); neuraminidase (NA)

## 4.2 Introduction

Swine influenza viruses (SIVs) are the etiological agents of a pig respiratory disease that causes important economic loses in the pig industry. Although the mortality rate associated with SIV infection is usually low, it is a highly contagious disease with morbidities that can reach almost 100% of exposed animals [229,230]. SIVs belong to the *Orthomyxoviridae* family type A. The SIV genome, with approximately 13.6 kb size, is characterized by having 8 RNA negative polarity strain segments: the polymerases (polymerase basic 2 and 1 (PB2 and PB1) and acidic polymerase (PA)), the hemagglutinin (HA), nucleoprotein (NP), neuraminidase (NA), matrix (M), and the nonstructural (NS)[231].

The surface glycoproteins HA and NA are responsible for interacting with host cells through sialic acid, allowing the entry of viral particles and the exit of virions after the influenza A virus (IAV) infection cycle [158,232,233]. Both proteins generate different antigenic patterns used to classify IAVs. Nowadays, H1N1, H1N2, and H3N2 are the most prevalent circulating enzootic subtypes in the swine population worldwide [234]. Moreover, those proteins play an

important role in generating protective immunity against SIV, more specifically against HA protein [152]. Currently, though its utilization is still limited, the trivalent vaccine, which contains the three previously mentioned SIV inactivated subtypes, is the most widely used to prevent and control the disease [151,152,164]. Although the vaccine can reduce disease and virus spread, the host immune system does not generate sterilizing immunity, so viral replication can occur despite vaccination [167,235].

Influenza viruses have a high evolutionary capacity to evade pre-existing immunity [236,237]. This ability is related to the low proof-reading fidelity of IAVs' polymerase, which can lead to the accumulation of point mutations in the IAV RNA segments, achieving new antigenic patterns in a short time, a phenomenon known as antigenic drift [73,79]. HA and NA have a great relevance in the humoral response against IAVs. Punctual nonsynonymous substitutions in both the HA globular and NA head domains can interfere with host capacity to generate an effective antibody response to the virus [238–240]. Previous studies have shown that the lack of effectiveness of pre-existing immunity against IAVs may favor the virus's evolution due to a strong antigenic selection driving the rapid generation of new epitopes [223,241].

During the 1990s, SIV H3N2 subtype arose from the triple-reassortment of HA, NA, and PB1 segments from seasonal human H3N2 and PB2, and PA from avian IAV, and NP, M, and NS from the classical H1N1 SIV [242]. This subtype was first identified in swine, and it has been circulating since then all over the world [242–244]. In 2009, A(H1N1) pdm09 triple-reassortment virus arose from the Eurasian "avian-like" swine H1N1 and swine triple-reassortments H1N2 and H3N2 [161]. Thereby, pigs play an important role in the IAVs' adaptation to different hosts, avian to human and vice versa [113]. The current dominating IAV strains in the European swine population are "avian-like" swine H1N1, "human-like" reassortment swine H1N2, "human-like" reassortment swine H3N2, and A(H1N1) pdm09 virus [230].

Considering the enormous genetic variability and evolutionary capacity of IAVs, their endemic character, the continuous increase in the pig population around the world and the close contact among pigs, birds, and humans, IAV poses a constant threat to human and animal health. Thus, SIV evolution studies including determination of new viral variants emergency are fundamental to improve surveillance and disease control.

Against this background, the aim of the present study was to determine the evolutionary trends of SIV H3N2 subtype in vaccinated and nonvaccinated pigs in previously naturally H1N1 infected herds. To this end, 14 whole SIV genome

samples were sequenced by next generation sequencing, and new viral variants were determined.

## 4.3 Materials and Methods

### 4.3.1 Cell and Viruses

Madin-Darby Canine Kidney (MDCK, ATCC CCL-34) cells were used for both viral titration and production. Dulbecco's Modified Eagle Medium (DMEM), supplemented with fetal bovine serum (FBS) (10%), L-glutamine (1%) and penicillin/streptomycin (1%), was used for cell culture kept at 37 °C with 5% $CO_2$ atmosphere in an incubator.

The A/Swine/Spain/SF32071/2007 H3N2 virus was propagated via infection of a MDCK monolayer cell culture, with addition of 10 μg/mL of porcine trypsin (Sigma-Aldrich, Madrid, Spain), at a multiplicity of infection (MOI) of 0.01. Forty-eight hours later, virus was harvested, and titration was performed by serial dilutions in a MDCK cell culture to calculate the 50% tissue culture infection dose ($TCID_{50}$) according to the Reed and Muench method [168].

### 4.3.2 Experimental Design

Sixteen 5-week-old domestic pigs were selected from a Spanish commercial farm where the flu vaccine was not applied. Animals were distributed into two groups, Group A (animals from 1 to 8) and Group B (animals 9 to 16). After one week of acclimation period, animals from Group A were immunized with the first dose of the commercial inactivated influenza vaccine (RESPIPORC FLU3, IDT®, Dessau-Rosslau, Germany), according to the manufacturer's instructions. In the vaccine formulation, the following strains are included H3N2 (Bakum/IDT1769/2003), H1N1 (Haselünne/IDT2617/2003), and H1N2 (Bakum/1832/2000). The vaccine was administered by the intramuscular route using a 2 mL dose injected in the neck muscle. Twenty-one days post-vaccination (dpv), Group A received the second vaccine dose, using the same protocol. In parallel, pigs from Group B were intramuscularly inoculated at 0 and 21 dpv with 2 mL of phosphate buffered saline (PBS).

Three weeks after the second vaccination dose (42 dpv), pigs from both experimental groups were challenged with A/Swine/Spain/SF32071/2007 (H3N2) by two administration routes, intranasal and endotracheal, with a viral concentration of $10^7$ $TCID_{50}$ in a final volume of 2 and 5 mL per route, respectively [176]. For the viral challenge, animals were restrained with a pig lasso, and a diffuser device (MAD Nasal, Teleflex, Morrisville, NC, USA) was used to administrate intranasally 1 mL of inoculum per nostril; animals were intubated for the endotracheal administration[172].

Clinical signs, including rectal temperature and animal behavior, were daily measured by a trained veterinarian after challenge. The registration of clinical signs was scored as previously described [173]. The same number of animals per group was serially euthanized, three animals each at 2 and 5 days post-inoculation (dpi), and the remaining two at 9 dpi.

Nasal swabs and sera were collected before vaccination, viral challenge, and on day of euthanasia. In addition, nasal swabs were daily collected from 1 dpi until the euthanasia day. Lung, nasal turbinate (NT) and broncho-alveolar lavage fluid (BALF) were collected and stored at −80 °C. The BALF was collected by filling the right lung of each pig with 150 mL of PBS. An extra lung tissue was collected and fixed by immersion in 10% buffered formalin.

Animal experiments were performed in AM Animalia facilities (La Vall de Bianya, Girona, Spain). All procedures were approved by the animal ethics committee from the Generalitat de Catalunya, under project number 10442, following the Spanish and European regulations.

### 4.3.3 Humoral Response against SIV

The detection of antibodies against influenza NP was performed using the ID Screen® Influenza A Antibody Competition ELISA kit (ID VET, Grabels, France). The inhibition percentage value was calculated, with values higher than 50% considered negative, those below 45% positive, and those between both values doubtful, according to manufacturer's instructions.

Hemagglutination inhibition (HI) assay was performed at 42 dpv (challenge) and on euthanasia day as previously described [172]. Briefly, collected sera from pigs were treated 18 h at 37 °C with RDE II Seiken (Denka Chemicals, Tokyo, Japan) and inactivated for one hour at 56 °C. A volume of 50% chicken red blood cells (RBCs) was added to remove unspecific inhibitors by hemadsorption and subsequently diluted in PBS (1:10). Then, pig sera were twofold diluted in PBS until 1:1024 in v-bottomed 96-well plates. Twenty-five microliters of viral antigen were used on challenge (A/Swine/Spain/SF32071/2007 (H3N2)), diluted to 4 hemagglutination units (HAU) was dispensed. After 1 h of incubation at room temperature, 25 µL of 0.5% of chicken RBC was also added. Finally, after another hour of incubation, hemagglutination was evaluated by tilting the plate. The antibody titers were established as the reciprocal dilution where inhibition was complete, considering seroprotective titers ≥1/40.

### 4.3.4 Pathological Analyses in Lung and Immunohistochemistry to Detect SIV

Macroscopic examination of the lung parenchyma was performed during the necropsies of animals. Moreover, an image analysis was performed to calculate the percentage of lung-affected area, as previously described [175], with ImageJ® software (v 1.8) [245].

A sample of each collected lung was fixed in 10% buffered formalin, dehydrated, and embedded in paraffin wax. Two sections of 3–5 μm thick were cut and stained with hematoxylin-eosin (HE) for the examination under light microscopy [30,35] to detect SIV antigen by immunohistochemistry (IHC). For the latter, a two-step polymer method (Envision TM) was performed using a monoclonal antibody against influenza A virus (IAV) (Hb65 from the ATCC) and system + HRP-labeled polymer anti-mouse (K4001, Dako, Santa Clara, CA, USA) as primary and secondary antibodies, respectively [178]. To determine the degree of lung lesions, a semiquantitative method was used based on affected airways on HE examination; the amount of immunoreactivity on IHC examination was also assessed [246].

### 4.3.5 SIV RNA Detection

Lung and NT were homogenized in brain heart infusion medium (10% weight/volume). RNA was extracted from nasal swab, BALF, lung, and NT using the MagAttract 96 Cador Pathogen kit ® (Qiagen, Düsseldorf, Germany) following the manufacturer's instructions. Subsequently, the SIV RNA of each sample was quantified by RT-qPCR assay based on the amplification of the conserved segment of the matrix (M) gene [132]. The amplification was performed in the Fast7500 equipment (Applied Biosystem, Foster City, CA, USA). Samples where fluorescence was not detected were considered negative whereas threshold cycle (Ct) values under 40 were considered positive [132,235].

### 4.3.6 Whole Influenza Genome Sequence by NGS

The RNA extracted from samples of vaccinated and nonvaccinated animals with a RT-qPCR Ct value lower than 37 were used for whole genome amplification [12,39]. The PCR conditions were: 0.2 μM of forward and reverse primers MBTuni-12 and MBTuni-13, respectively, 2.5 μL of extracted RNA and 0.5 μL of SuperScript® III One-Step RT-PCR System with Platinum™ Taq High Fidelity DNA Polymerase (Thermo Fisher Scientific, Waltham, MA, USA). Moreover, for the biggest segments (PB2, PB1 and PA), amplification was enhanced by a second amplification with the same conditions but adding a modification of forward primer (MBTuni12G) [180].

Those samples with the eight segments amplified were selected for sequencing [15] by Illumina technology. The Nextera-XT DNA Library Prep protocol (Illumina®, San Diego, CA, USA) was followed for multiplexed sequencing libraries and sequencing was performed by Miseq Reagment Kit v2 in a 150-cycle paired-end run, on a Miseq Instrument (Illumina®, San Diego, CA, USA).

Sequencing data were deposited at the National Center for Biotechnology Information (NCBI, https://www.ncbi.nlm.nih.gov/ (accessed on 10 May 2022)) with the accession number (PRJNA853173).

### 4.3.7 De Novo Assambly, Mapping, and Variant Calling

After the Miseq run, adapters were automatically removed and reads quality were analyzed by FastQC (v 0.11.8) [181]. All reads with a low quality (Phread < 30) were trimmed using Trimmomatic (v0.39) [182]. De novo assembly was performed using the SPAdes algorithm with the very sensitive option [247]. The assemblies generated were screened using NCBI BLAST (https://blast.ncbi.nlm.nih.gov/Blast.cgi (accessed on 10 May 2022)) to determine the strain. To obtain inoculum consensus sequence, inoculum sequencing reads were mapped against A/Swine/Spain/SF32071/2007 (H3N2) reference SIV genome sequences (HE774666-73) [248], using the very sensitive function of the read alignment tool Bowtie2 (v2.3.5) [183]. The consensus sequence was generated using the consensus option from Bcftools (v.1.9) [185]. To detect single nucleotide polymorphisms, reads obtained from each sequenced sample were mapped against it. Post-mapping, all reads with a mapping quality lower than 30 were removed from the analysis using Samtools (v.0.39) [185]. The Picard "MArkDuplicatesSpark" option and the "BaseRecalibrator" options, both included in GATK4 (v4.1), were used for removing PCR duplicates and reads recalibration, respectively. For each sample, the number of mapped reads against SIV whole genome and its depth were calculated with the "-depth" function included in Samtools (v1.9) and represented with RStudio using ggplot2 library [186,187].

All variants found in each sample were noted using the default parameters of LoFreq software [188]. A single nucleotide variant was considered if at least 50 reads of depth, 10 reads of the alternative base count, and $p$ value < 0.01 requirements were obtained. The effect of each variant was predicted with SnpEff software (v.4.3) [189]. A previous database from the H3N2 subtype was built with "build–gtf22" function, using the previous annotated genome [248].

#### 4.3.8 Nucleotide Diversity ($\pi$)

The genetic diversity of all sequenced samples per genomic segment was calculated with SNPGenie software (v 1.2) [190]. The nucleotide diversity ($\pi$) was calculated as the mean number of pairwise difference per site across each genomic segment. Moreover, the nonsynonymous and synonymous nucleotide diversity ($\pi_N$ and $\pi_S$) was calculated as the mean number of nonsynonymous and synonymous differences per nonsynonymous and synonymous sites in each genomic segment, respectively.

#### 4.3.9 Lolliplot and 3D Structural Representation of SIV Proteins

The trackViewer package from Bioconductor was used to visualize the lolliplot proteins representation of PB2, PB1, PA, HA, NA, matrix (M1), and nonstructural 1 (NS1) [249]. Moreover, the PyMOL Molecular Graphics System Version 4.6 was used to perform the structural representation of HA and NA proteins. Indeed, all nonsynonymous variants with an allele frequency greater than 5% were pointed in all protein representations.

#### 4.3.10 Satatistical Analysis

Statistical differences in rectal temperatures per day between both groups were studied by T-test application. Pearson's chi-squared and Kruskal–Wallis tests were also applied to study significant differences between groups in the proportion of synonymous and nonsynonymous substitutions and nucleotide diversity, respectively.

### 4.4 Results

#### 4.4.1 Detection of Natural SIV Circulation in Both Experimental Groups at Vaccination Day

At first vaccination day (0 dpv), an antibody response against NP was already detected by ELISA test in pigs from both experimental groups (7 in vaccinated and 4 in nonvaccinated groups) (Figure 1a). Due to such unexpected antibody detection, SIV RNA detection was attempted and confirmed by RT-qPCR in 6 and 7 nasal swab samples from vaccinated and nonvaccinated animals, respectively. High Ct values between 36.3 and 39.14 were found (Figure 4.1b). Three weeks later (21 dpv), all animals were RNA SIV negative except one animal from each experimental group, being all animals RT-qPCR negative on the day of challenge (42 dpv) (Figure 4.1b).

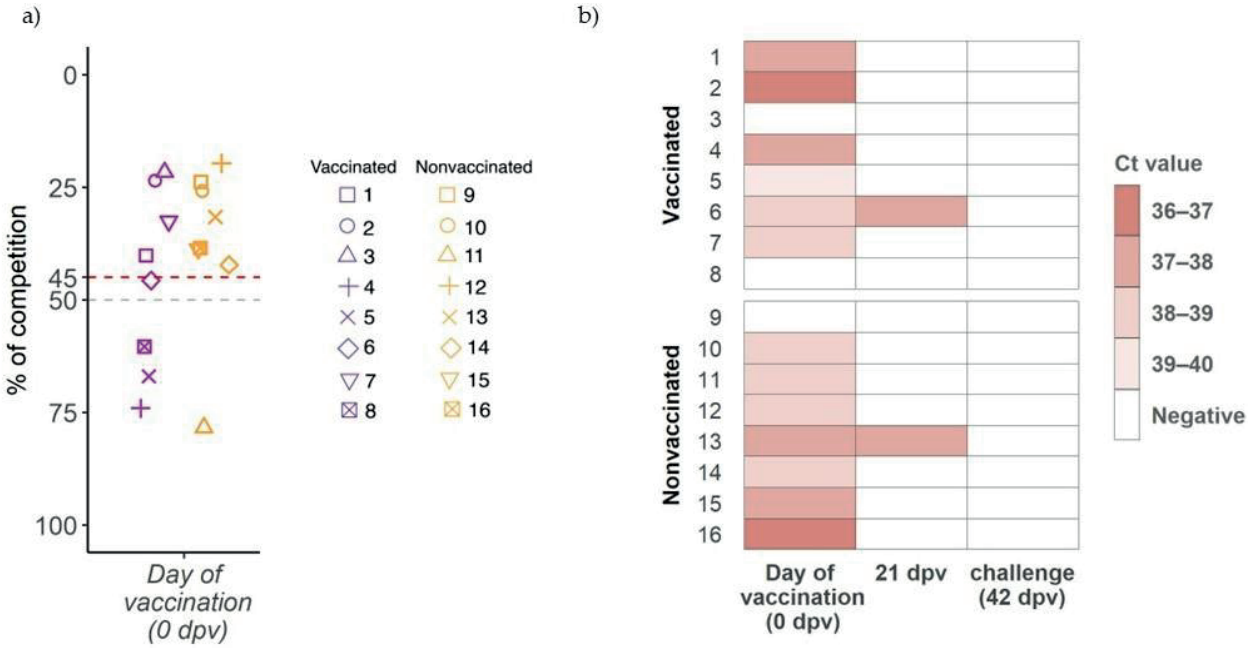


**Figure4.1. Detection of antibodies against influenza NP at day of first vaccination and SIV detection before challenge.** (**a**) IgG antibody levels against NP detected by ELISA, where levels are shown on ordinate axis expressed as percentage of competition. Samples with a value greater than 45 (red line) are considered positive, below 50 (gray line) negative, and between both doubtful. Violet and orange boxplots and dots indicate samples from vaccinated and nonvaccinated groups. Each animal is represented by one sot shape. (**b**) SIV detection by RT-qPCR heatmap. Animal IDs are indicated in ordinate axis.

### 4.4.2 Identification of H1N1 Subtype as Natural Circulating Virus before Challenge

After detection of the unexpected SIV infection, the characterization of the circulating virus was performed by NGS. The NCBI BLAST screening of de novo assembly indicated that the circulating strain detected was H1N1, more specifically a strain derived from A(H1N1) pdm09.

### 4.4.3 Humoral Response againts SIV after Vaccination and H3N2 Challenge

At three weeks after the first immunization (21 dpv) as well as on day of challenge (42 dpv), high levels of antibodies against NP were developed in all vaccinated animals, reaching values of 13.97% of competition detected by ELISA test. After the H3N2 SIV challenge, high antibody titers were detected, being similar at all time points until the end of the study (Figure 4.2). Meanwhile, 6 out 8 nonvaccinated animals were NP antibody positive with lower antibody values and heterogeneous response at 21 and 42 dpv. After challenge, from 5 dpi until

the end of the study, the levels of antibodies from the nonvaccinated group reached the same values as those of vaccinated ones (Figure 2).

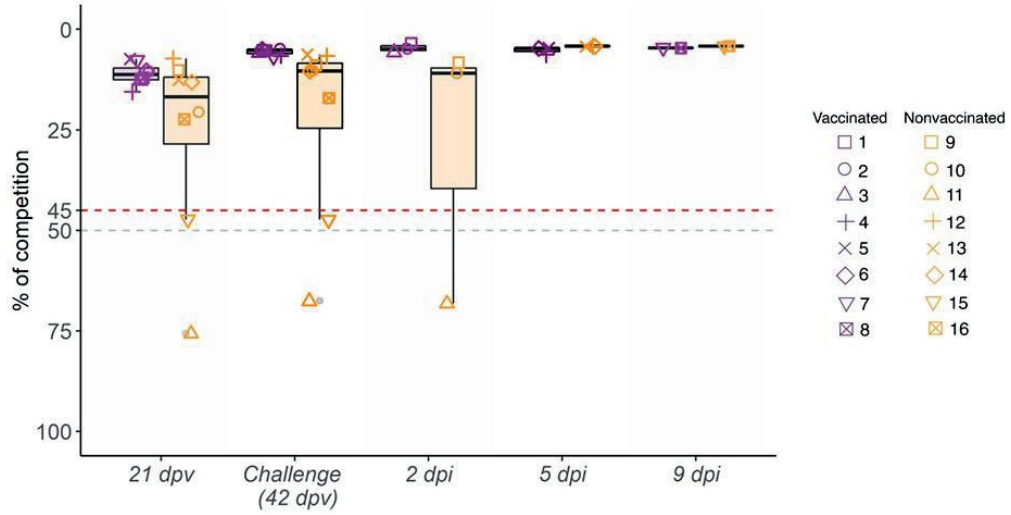


**Figure 4.2. Kinetics of antibody levels against SIV NP in serum samples collected from 21 dpv to 9 dpi.** Percentage of competition (%) and the day of sampling are represented in ordinate and abscissa axes, respectively. Violet indicates vaccinated animals, whereas the nonvaccinated group is indicated in orange box plots, where whiskers indicate quartiles' variability. Each animal ID is represented by different shapes. Values plotted as the upper red line (<45%) are considered positive, whereas values of the lower gray line (>50%) are considered negative. Values between both lines (45% and 50%) are considered doubtful.

HI titers against H3N2 subtype were detected in all vaccinated pigs at 42 dpv, showing values greater than 40 in 5 out of 8 sera. After challenge, titers rapidly increased from 2 dpi to the end of the trial in all vaccinated animals with values from 40 to 320. By contrast, in nonvaccinated animals, HI titers were not detected until 5 dpi, with low values. However, at 9 dpi titers increased (Table 4.1).

**Table 4.1. HI activity of sera against challenge strain A/Swine/Spain/SF32071/2007 (H3N2).**

| Group | Pig ID | HI Antibody Titer Against Challenge Strain in Sera | | | |
|---|---|---|---|---|---|
| | | 42 dpv | Euthanasia Day | | |
| | | | 2 dpi | 5 dpi | 9 dpi |
| Vaccinated animals | *1* | 10 | 40 | | |
| | *2* | 40 | 320 | | |
| | *3* | 20 | 160 | | |
| | *4* | 80 | | 80 | |
| | *5* | 80 | | 160 | |
| | *6* | 20 | | 80 | |
| | *7* | 40 | | | 160 |
| | *8* | 40 | | | 80 |
| | mean | 41.3 | 173.3 | 106.7 | 120 |
| Nonvaccinated animals | *9* | 0 | 0 | | |
| | *10* | 0 | 0 | | |
| | *11* | 0 | 0 | | |
| | *12* | 0 | | 10 | |
| | *13* | 0 | | 20 | |
| | *14* | 0 | | 0 | |
| | *15* | 0 | | | 640 |
| | *16* | 0 | | | 320 |
| | mean | 0 | 0 | 10 | 480 |

### 4.4.4 Kinetics of Rectal Temperature after SIV Challenge

After H3N2 SIV challenge, most nonvaccinated animals had fever at 1 and 2 dpi. Afterwards, all animals displayed normal rectal temperature until the end of the study, except pig 14, which showed a fever peak at 5 dpi (Figure 4.3). By contrast, none of the vaccinated pigs developed fever during the trial (Figure 4.3). The rectal temperature recorded in nonvaccinated animals was statistically significant with respect to vaccinated ones at 1, 2, and 3 dpi (t-test; $p = 0.002833$, $p = 0.02164$, $p = 0.03623$, respectively).

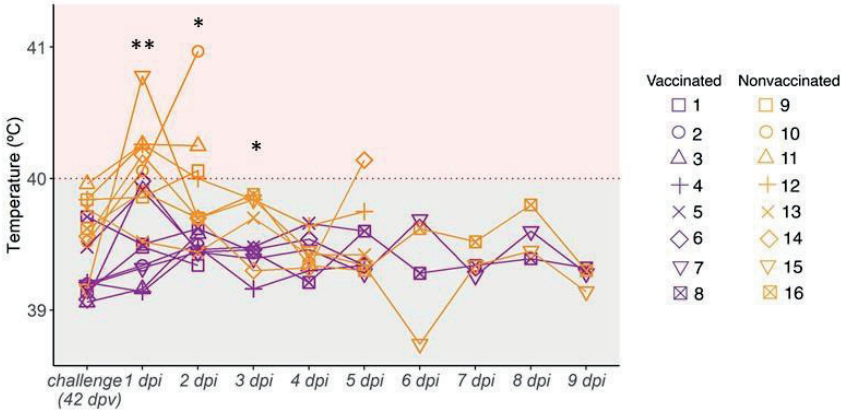


**Figure 4.3. Kinetics of rectal temperature after H3N2 SIV challenge.** Pigs are considered to have fever with temperatures greater than 40 °C (red dashed line). Vaccinated animals are represented in violet whereas nonvaccinated ones are represented in orange. Each line represents the rectal temperature measured in each pig over time; (*) $p \leq 0.05$ and (**) $p \leq 0.01$.

### 4.4.5 SIV Genome Detection after Challenge

All vaccinated pigs were negative for SIV RNA detection in nasal swabs at 2 dpi. Later, only animal 4 tested positive at 3, 4, and 5 dpi (time of euthanasia). Meanwhile, pigs 5, 7, and 8 were positive at 5, 3, and 9 dpi, respectively. By contrast, all nonvaccinated pigs tested positive from 2 to 4 dpi, most showing Ct values below 33 (Table 4.2). From 5 to 9 dpi, all nasal swabs analyzed were RT-qPCR negative, except for those of animals 13 and 16 at 5 and 6 dpi, respectively.

**Table 4.2. SIV detection in nasal swab samples collected at different time points and from BALF, lung, and nasal turbinate.** RT-qPCR Ct values results are shown in the table. Neg.: negative. Highlighted cells represent sequenced samples. Violet and orange cells indicate the group of each animal, vaccinated and nonvaccinated, respectively.

| | | Nasal swab samples | | | | | | | | | | Tissues samples | | |
|---|---|---|---|---|---|---|---|---|---|---|---|---|---|---|
| Group | Pig ID | 1 dpi | 2 dpi | 3 dpi | 4dpi | 5 dpi | 6dpi | 7 dpi | 8 dpi | 9 dpi | Euthanized day | LUNG | NT | BALF |
| Vaccinated animals | 1 | Neg. | Neg. | | | | | | | | | 32.96 | Neg. | 34.45 |
| | 2 | Neg. | Neg. | | | | | | | | 2 dpi | 34.48 | Neg. | Neg. |
| | 3 | Neg. | Neg. | | | | | | | | | 39.36 | Neg. | Neg. |
| | 4 | Neg. | Neg. | 33.45 | 32.56 | 37 | | | | | | Neg. | Neg. | 39.58 |
| | 5 | Neg. | Neg. | Neg. | Neg. | 37.42 | | | | | 5 dpi | Neg. | Neg. | Neg. |
| | 6 | Neg. | Neg. | Neg. | Neg. | Neg. | | | | | | Neg. | Neg. | Neg. |
| | 7 | Neg. | Neg. | 38,56 | Neg. | Neg. | Neg. | Neg. | Neg. | Neg. | 9 dpi | Neg. | Neg. | 38.09 |
| | 8 | Neg. | Neg. | Neg. | Neg. | Neg, | Neg, | Neg. | Neg. | 37.23 | | Neg. | Neg. | Neg. |
| Nonvaccinated animals | 9 | Neg. | 31.21 | | | | | | | | | 26.49 | Neg. | 35.98 |
| | 10 | Neg. | 33.42 | | | | | | | | 2 dpi | 25.27 | 31.68 | 34.88 |
| | 11 | 39.48 | 33.39 | | | | | | | | | 33.34 | Neg. | 34.14 |
| | 12 | Neg. | 38.28 | 30.98 | Neg. | Neg. | | | | | | 34.41 | Neg. | Neg. |
| | 13 | 37.28 | 35 | 30.02 | 33.6 | 39.48 | | | | | 5 dpi | 34.36 | 39.5 | 37.14 |
| | 14 | Neg. | 38.75 | 36.96 | Neg. | Neg. | | | | | | 35.38 | Neg. | Neg. |
| | 15 | Neg. | 37.13 | 32.45 | 34.93 | Neg. | Neg. | Neg. | Neg. | Neg. | | 39.78 | Neg. | Neg. |
| | 16 | Neg. | Neg. | 32.8 | 30.17 | Neg. | 34.64 | Neg. | Neg. | Neg. | 9 dpi | 39.54 | Neg. | Neg. |

In the case of BALF samples, SIV genome was detected in those collected from 3 vaccinated pigs at 2, 5, and 9 dpi. Likewise, RT-qPCR positive BALF samples were found in 4 nonvaccinated pigs, three at 2 dpi and the other at 5 dpi. In relation to lung samples, SIV was found only in the three vaccinated animals euthanized at 2 dpi, whereas all nonvaccinated animals were positive in all collected samples in the trial. Finally, all nasal turbinate samples from vaccinated animals were negative, while two samples from the nonvaccinated group were positive (Table 4.2).

From all the RT-qPCR positive samples, 16 SIV whole genomes were amplified and sequenced. From vaccinated animals, complete SIV sequences were obtained from 3 nasal swab samples (pig 5 from 3 to 5 dpi), two lung samples (pigs 2 and 3), and one BALF sample (pig 1). From nonvaccinated pigs, complete SIV genomes were obtained from seven nasal swab samples (pigs 9, 10, and 11 at 2 dpi, pigs 12, 13, and 15 at 3 dpi and pig 16 at 4 dpi), two lung samples (pigs 9 and 10) and one nasal turbinate sample (pig 10) (Table 4.2).

### 4.4.6 Lung Gross Lesions, Histopathological Assessment, and Immunohistochemistry to Detect SIV Antigen

On average, more extensive gross lung lesions were detected in nonvaccinated animals compared to vaccinated ones (Table 4.3). The highest percentages of lung affected area were recorded in animals 9 and 10 from the nonvaccinated group euthanized at 2 dpi, reaching values of 21.4%.

**Table 4.3. Pathological results based on gross (percentage of lung-affected area) and histopathological observations, including the semi-quantitative scorings for HE and IHC in lung samples.**

| Group | Pig ID | Euthanasia day | Lung affected area (%) | Histopathological scoring | Immunohistochemistry for SIV |
|---|---|---|---|---|---|
| Vaccinated animals | 1 | 2 dpi | 1.44 | 2.5 | - |
| | 2 | | 0.32 | 2 | - |
| | 3 | | 0.32 | 2 | - |
| | 4 | 5 dpi | 0.18 | 1.5 | - |
| | 5 | | 0 | 0.5 | - |
| | 6 | | 10 | 2.5 | - |
| | 7 | 9 dpi | 1.25 | 0.5 | - |
| | 8 | | 0 | 0 | - |
| | | mean | 1.69 | 1.44 | |
| Nonvaccinated animals | 9 | 2 dpi | 21.4 | 3 | ++ |
| | 10 | | 20.38 | 3 | +++ |
| | 11 | | 1.54 | 3 | - |
| | 12 | 5 dpi | 7.3 | 2.5 | - |
| | 13 | | 2.07 | 2 | + |
| | 14 | | 4.98 | 3 | - |
| | 15 | 9 dpi | 1.11 | 1 | - |
| | 16 | | 0.69 | 1.5 | - |
| | | mean | 7.43 | 2.38 | |

*Histopathology scoring: absence (0), few inflammatory cells isolated (0.5), localized cluster of inflammatory cells (1), several clusters of inflammatory cells (1.5–2), severely several (2.5), and many (3) airways affected. Moreover, minimal (1.5), mild (2) interstitial infiltrate, and plus moderate interstitial and alveolar infiltrates (2.5–3). SIV immunohistochemical scoring: absence (-), low (+), scattered (++), moderate (+++), and abundant (++++) amount of immunoreactivity.*

Microscopic lesions were detected in both groups, with a lower scoring in vaccinated animals at all sampling days. Remarkably, the highest scoring values were detected in all lung sections from nonvaccinated animals at 2 dpi, still being high at 5 dpi. No viral labeling by immunohistochemistry in lung sections was detected in vaccinated animals. In contrast, low to moderate immunoreactivity was found in three nonvaccinated animals (Table 4.3).

### 4.4.7 Whole SIV Genome Sequences Obtained from Vaccinated and Nonvaccinated Challenged Animals

The complete inoculum sequence (A/Swine/Spain/SF32071/2007 H3N2 strain) used in the viral challenge was determined (Figure 4.4). In addition, 16

SIV whole genomes were retrieved from samples collected from challenged pigs (Table 4.1 and Figure 4.4). Notably, six sequences were recovered from vaccinated pigs and 10 from nonvaccinated ones. From all sequenced samples, a total of 1,198,942 reads were obtained after quality control and 84.36% of them (1,011,412) matched the SIV genome. The maximum number of mapped reads was obtained in the nasal swab collected from nonvaccinated animal 11 at 2 dpi (135,062). By contrast, the minimum number of reads was obtained in the nasal swab of the nonvaccinated animal 12 at 3 dpi (20,581) (Table S4.1).

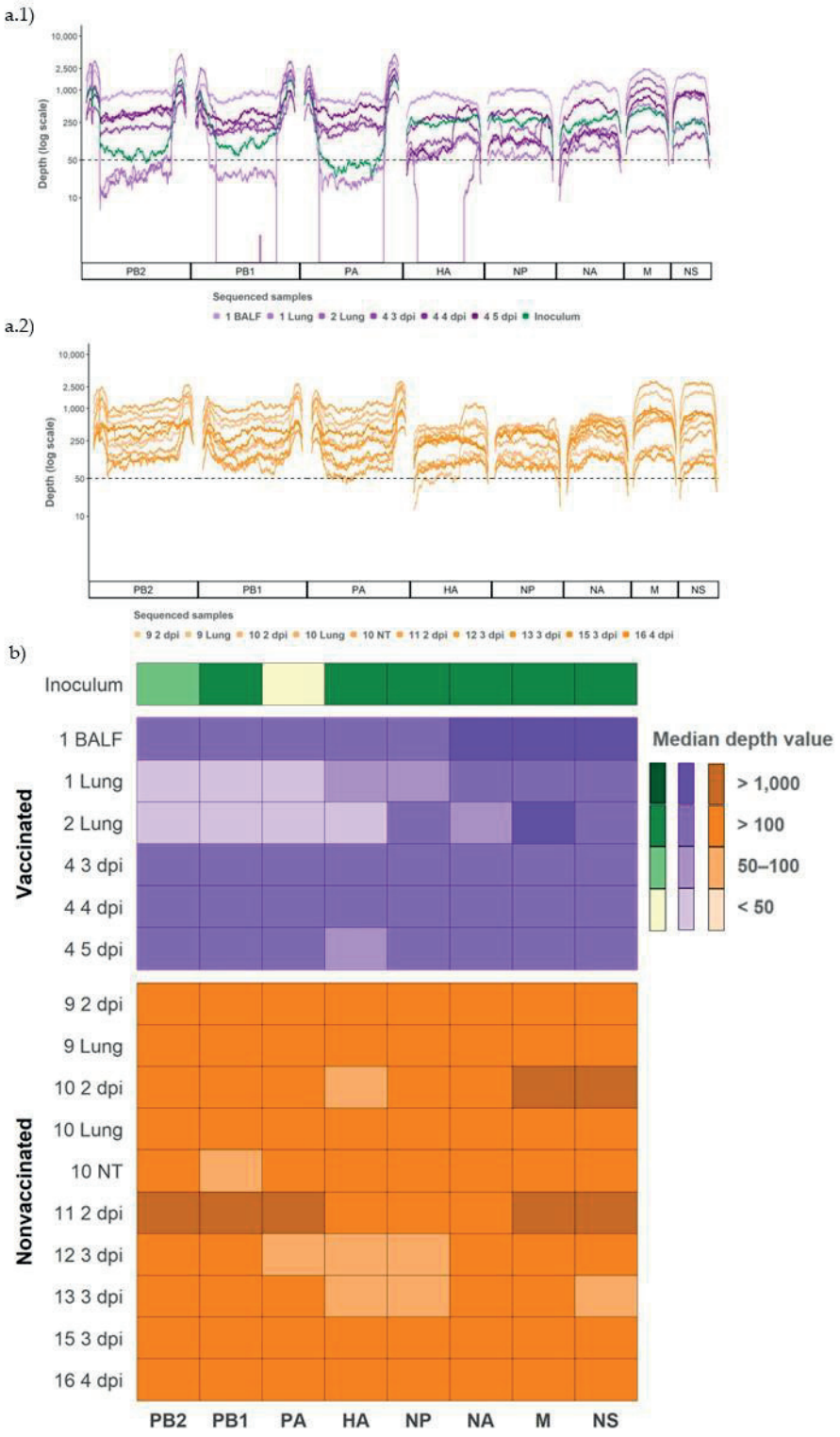


**Figure 4.4. Coverage and depth obtained per genomic segment of SIV H3N2 in inoculum and vaccinated and nonvaccinated pig samples.** (a1) Illumina sequencing profile reads coverage against H3N2 SIV and its depth in inoculum (plotted in green) and samples from vaccinated animals (plotted in different tones of violet). (a2) Illumina profile of samples collected from nonvaccinated animals plotted in different orange tones. (b) Heat map of the median depth value per genomic segment in all sequenced samples. The origin and the collection day of each sample are specified in the figure. Virus samples from BALF, lung, and NT were collected on indicated euthanasia day.

Regarding coverage per position, 93.91% from all determined SIV genomes was represented with more than 50 reads and selected for further analysis (Figure 4.4a1,a2). Specifically, most genome segments were obtained from samples of vaccinated and nonvaccinated pigs, with a depth median greater than 50. Only the segments PB2, PB1, and PA from lung samples collected from vaccinated pigs 1 and 2, and the HA from lung collected also from vaccinated pig 2, had a depth median lower than 50 (Figure 4.4b).

### 4.4.8 Evolution of Variants Found in Inoculum

From the viral inoculum, five nonsynonymous variants were detected, all of them in the polymerase segments: D55N (2.98% allele frequency), E617A (19.05%), V618I (17.5%) and L683I (5.09%) in PA, and Q73K (2.32%) in PB2 (Table 4.4).

**Table 4.4. SNV detected in the inoculum.**

| | Gene | Depth of read | Nucleotide change | | Alt. Base count | Allele frequency | Aminoacidic change | |
|---|---|---|---|---|---|---|---|---|
| | | | position | ref. → alt. | | | ref. → alt. | position |
| **Inoculum** | PA | 503 | G → A | 163 | 15 | 2.99 | D → N | 55 |
| | | 147 | A → C | 1850 | 28 | 19.05 | E → A | 617 |
| | | 160 | G → A | 1852 | 28 | 17.5 | V → I | 618 |
| | | 1375 | C → A | 2047 | 70 | 5.09 | L → I | 683 |
| | PB2 | 863 | C → A | 217 | 20 | 2.32 | Q → K | 73 |

Abbreviations: alt. (alternative) and ref. (reference).

Those variants were later detected in sequenced samples from both experimental groups (Figure 4.5). For most samples collected during the trial, these substitutions were maintained at the same frequency, or they were lost over time, with a few exceptions. In vaccinated pigs, PA substitutions D55N, E617A, and V618I showed a rapid allele frequency increase in the lung sample from animal 1. The allele frequency of detection of the L683I substitution in PA also increased over time in nasal swabs collected from pig 4 (Figure 4.5a). On the other hand, in nonvaccinated animals, PB2 Q73K substitution considerably increased its frequency in the nasal swab sample from animal 15 at 3 dpi (Figure 4.5b).

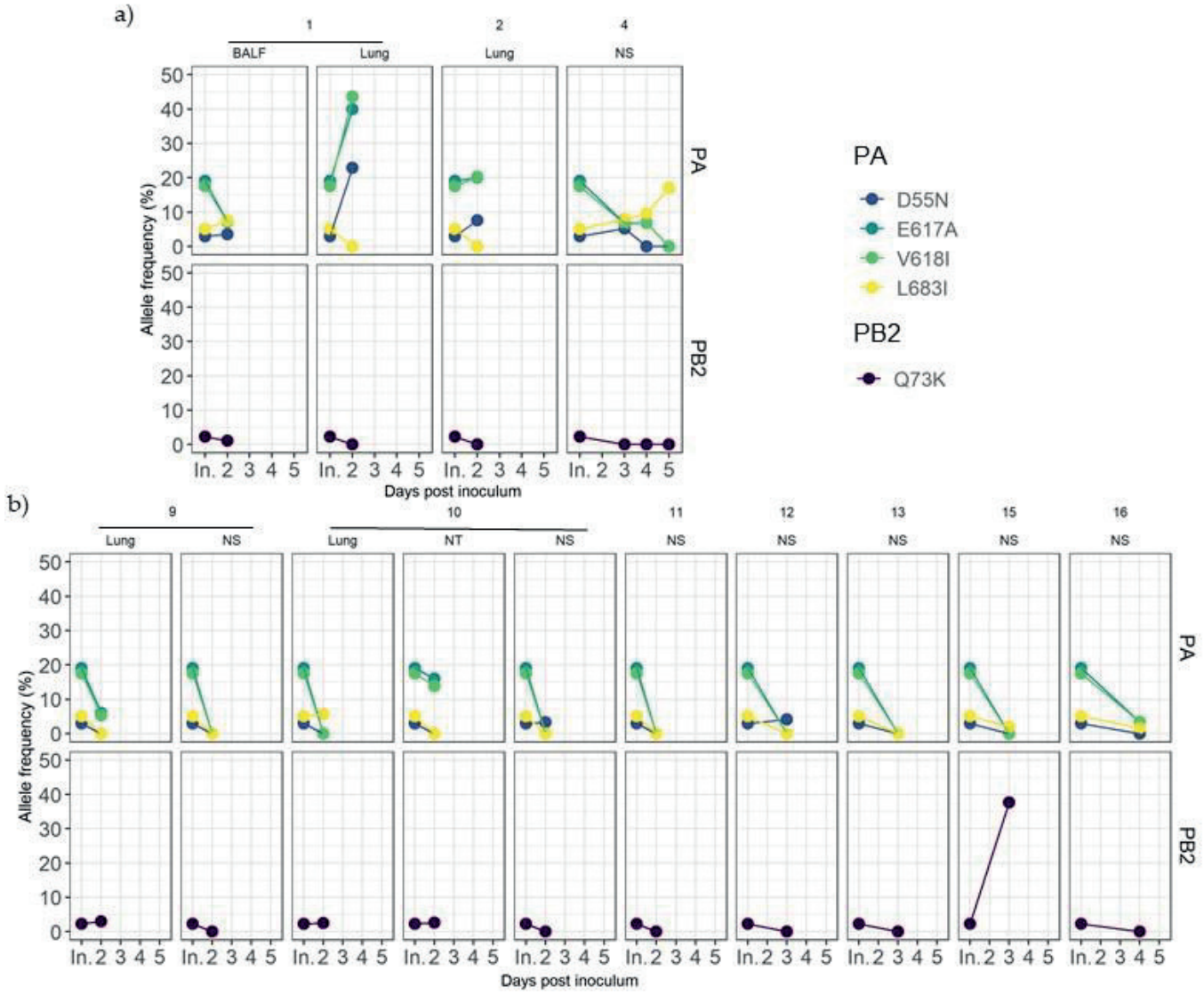


**Figure 4.5. Dynamics of inoculum variant frequencies over time. (a) Samples from vaccinated animals.** (**b**) Samples from nonvaccinated animals. Rows indicate genomic segments PA and PB2. Columns correspond to each animal and sample origin. X axes correspond to post-inoculation time in which each sample was recovered, where "In." indicates the inoculum. Y axes show the allele frequency. Each substitution is plotted in a different color.

### 4.4.9 Detection of De Novo SIV Variants in Sequenced Samples Collected from Vaccinated and Nonvaccinated Animals

From samples collected during the trial, single nucleotide variants (SNV) were noted for an allele frequency of 1, 2.5, 5, 7.5, and 10% (Figure 4.6). The proportion of nonsynonymous variants was higher than that of the synonymous ones for the 5 allele frequencies analyzed (Figure 4.6). No significant differences between groups were found applying Pearson's chi-squared test.

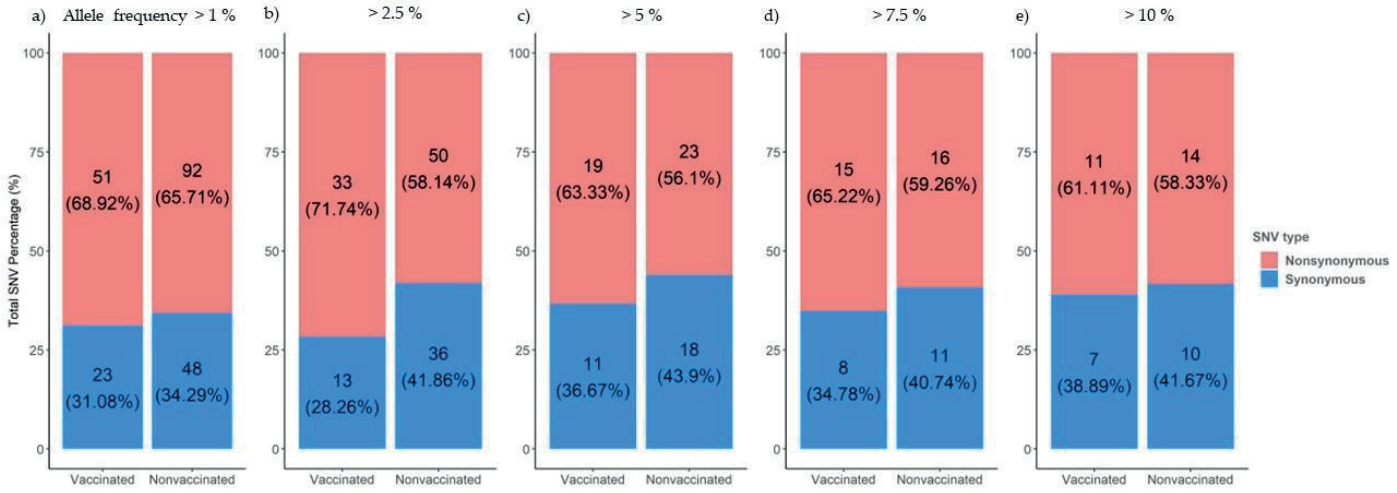


**Figure 4.6. Proportion of synonymous and nonsynonymous de novo SNVs generated in sequences collected from vaccinated and nonvaccinated pigs.** Substitutions with an allele frequency greater than 1% (**a**), 2.5% (**b**), 5%(**c**), 7.5% (**d**), and 10% (**e**) are represented.

The synonymous and nonsynonymous variants were allocated in all genomic segments recovered from both experimental groups (Figure 6). Regarding SNV with an allele frequency greater than 1%, 56, 33, and 49 were detected in polymerase segments PB2, PB1, and PA, respectively. Notably, most of them were nonsynonymous substitutions (Figure 4.7a). By contrast, the most of these variations did not exceed an allele frequency of 5% (Figure 4.7b); we detected only 16 in PB2, 6 in PB1, and 14 in PA(Figure 4.7b).

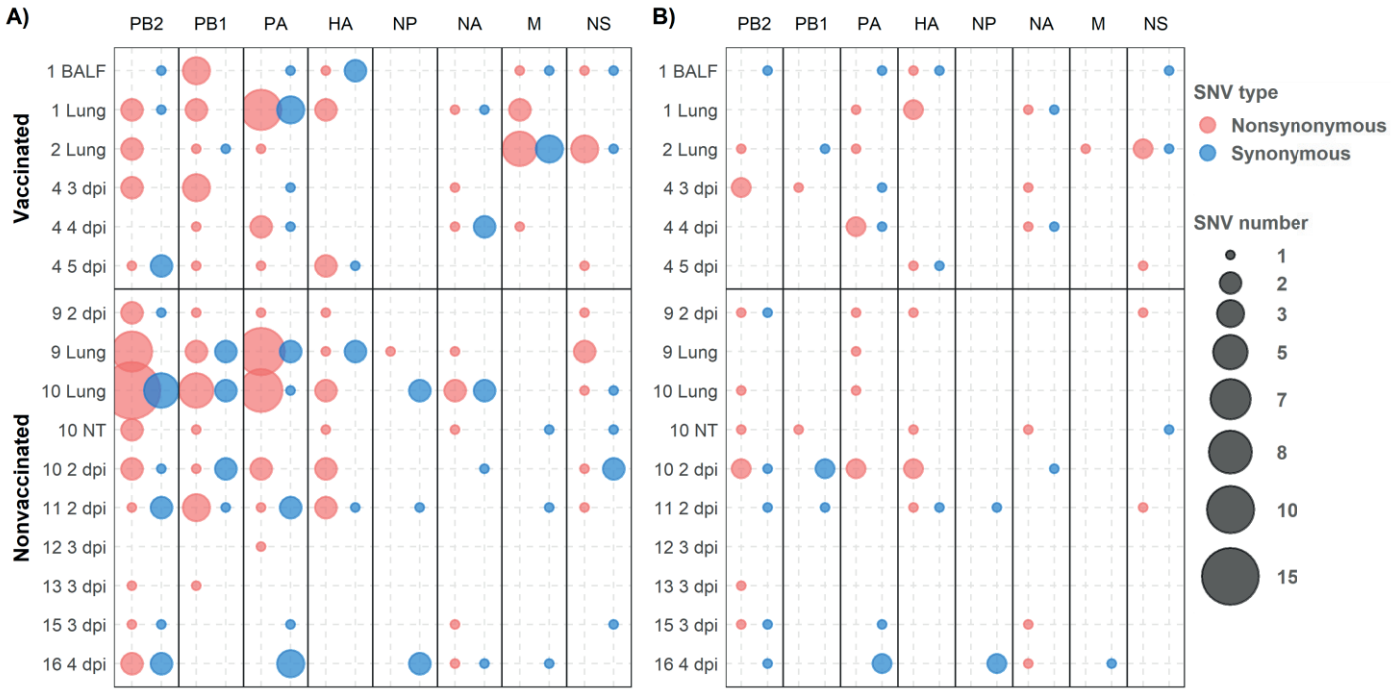


**Figure 7. De novo synonymous and nonsynonymous SNV allocation.** Nonsynonymous and synonymous variants are represented in red and blue, respectively. Circle size indicates the total number of substitutions found per genomic segment (abscissa axis) and sample (ordinate axis). (**A**) SNVs with an allele frequency greater than 1%. (**B**) SNVs with an allele frequency greater than 5%.



In relation to HA and NA segments, 20 and 16 SNVs were detected, respectively, of which nine and six were nonsynonymous variants with an allele frequency greater than 5% (Figure 4.7). In the NP gene, no nonsynonymous variants were found with an allele frequency greater than 5% (Figure 4.7a). Notably, in the M segment, 16 SNVs were detected with an allele frequency greater than 1%, nine of which were nonsynonymous substitutions found only in samples from vaccinated animals. Only one nonsynonymous and one synonymous substitution in the M segment gene were detected with an allele frequency greater than 5% (Figure 4.7). Lastly, in the NS segment, 19 SNVs were detected, with eight variants exceeding 5% of allele frequency, five of them being nonsynonymous ones (Figure 4.7).

In vaccinated animals, 16 amino acid substitutions with an allele frequency greater than 5% were identified in PB2 (M51I and L697R), PB1 (P64S), PA (E56K, N331S, and E677K), HA (I339V, T467I, and N505S), NA (F167L, V303I, and G313S), M2 (E70K), and NS1 (S99P, S135I, and S135C). By contrast, 14 nonsynonymous substitutions were detected in nonvaccinated animals: PB2 (T81K, R340K, E472K, and Q591K), PB1(A139D), PA (M211V and R256K), HA (V239I, V283A, and N364D), NA (P45L, N329S, and T434A), and NS1 (G72R)

(Figures 4.8 and 4.9). Further information about all substitutions with an allele frequency greater than 1% is noted in the Supplementary data (Table S.4.3).

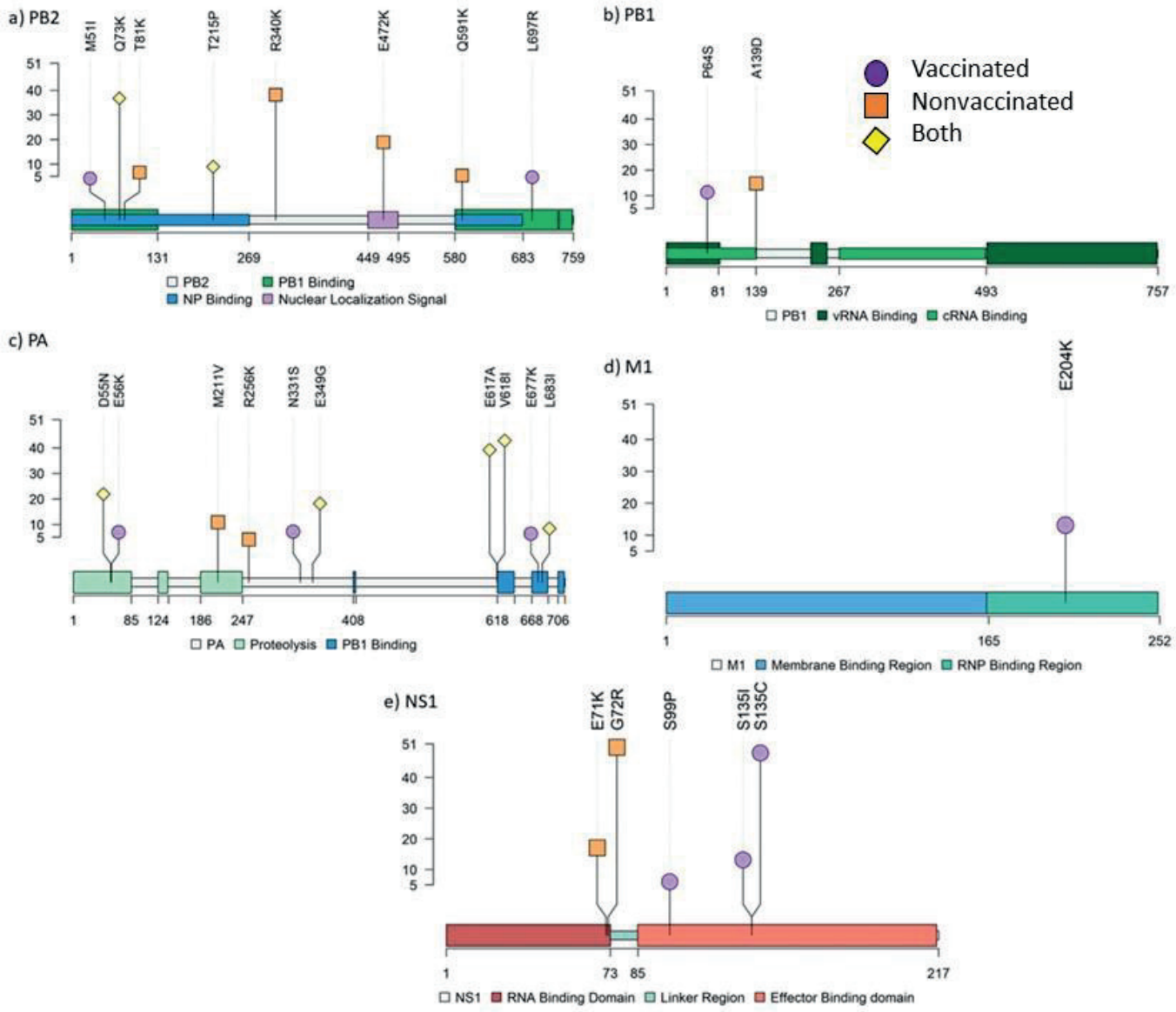


**Figure 4.8. Lolliplot representing the allocation of all amino acid substitutions with an allele frequency greater than 5% found in PB2 (a), PB1 (b), PA (c), M1 (d), and NS1 (e) SIV proteins.** Allele frequency of each variant is indicated on ordinate axis. If one substitution was found in more than one sample, only the highest allele frequency is indicated. Amino acid substitutions from vaccinated, nonvaccinated, and both groups are represented in purple circles, orange squares, and yellow diamonds, respectively.

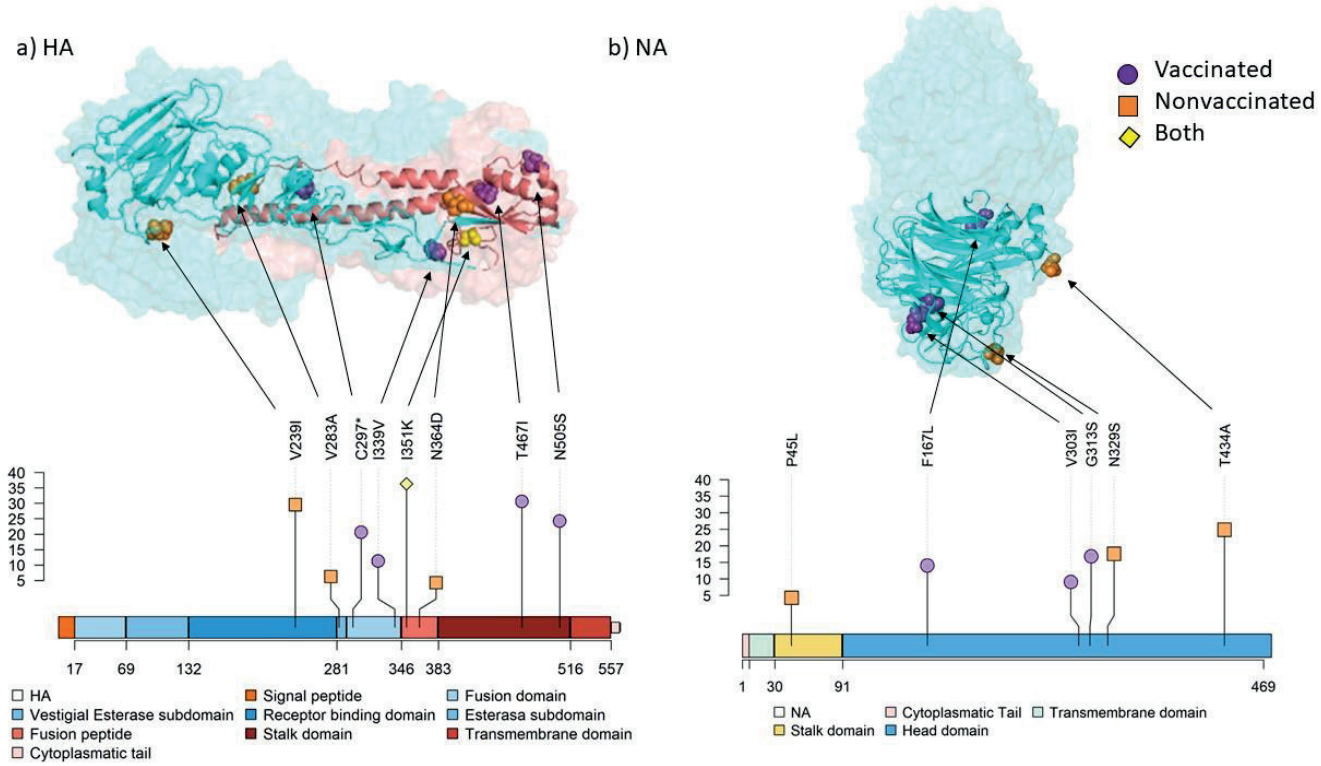


**Figure 4.9. Location of substitutions with an allele frequency greater than 5% found in surface glycoproteins by both protein structure and lolliplot representation.** The allele frequency is indicated on ordinate axis. (**a**) HA 3D trimer (PDB accession no. 7VDF) [250] and lolliplot domain representation. HA1 domains are represented in different tones of blues and HA2 domains in different tones of reds. (**b**) NA 3D tetramer head domain (PDB accession no. 4GZO) [251] and lolliplot domains representation. Substitution P45L from the stalk domain is not included in the limits of the crystallography structure used.

In samples sequenced in animal 4 at different time points, nonsynonymous substitutions PA L697R and NS1 S135I, and synonymous substitutions PA G1485A, HA A1500G, and NA A405G were detected in several samples. Indeed, in lung and NT samples collected in nonvaccinated animal 10, the nonsynonymous variant L655V was found (Table S4.2).

Nonsynonymous substitutions PB2 T2090G (L697R) and NS1 A403T (S135I), and synonymous substitutions PA G1485A, HA A1500G, and NA A405G were found in animal 4 at different time points. Indeed, nonsynonymous variant PA T1993G (L655V) was noted in lung and NT from animal 10 (Table S4.2).

Regarding stop-gained mutations, 11 different mutations were recorded only in lung samples from vaccinated animal 1 and nonvaccinated animals 9 and 10. Mutation S86* in PB2 was found in nonvaccinated animals 9 and 10, whereas E739* in PB1 was found in animals 1 and 10 (Table S4.3). Notably, all these substitutions were noted with an allele frequency lower than 5%, except C289* in

HA from animal 1, which was represented with an allele frequency of 21.43% (Figure 49, Table S4.3).

### 4.4.10 Genetic Diversity in Viral Populations

Nucleotide diversity ($\pi$) increased in both experimental groups at similar levels at 2 dpi with respect to inoculum (Figure 4.10a.1). At 3 dpi, $\pi$ decreased in viral samples from nonvaccinated animals and then increased at 4 dpi. In contrast, in vaccinated animals, $\pi$ decreased slightly at 3 dpi and remained constant the rest of the days.

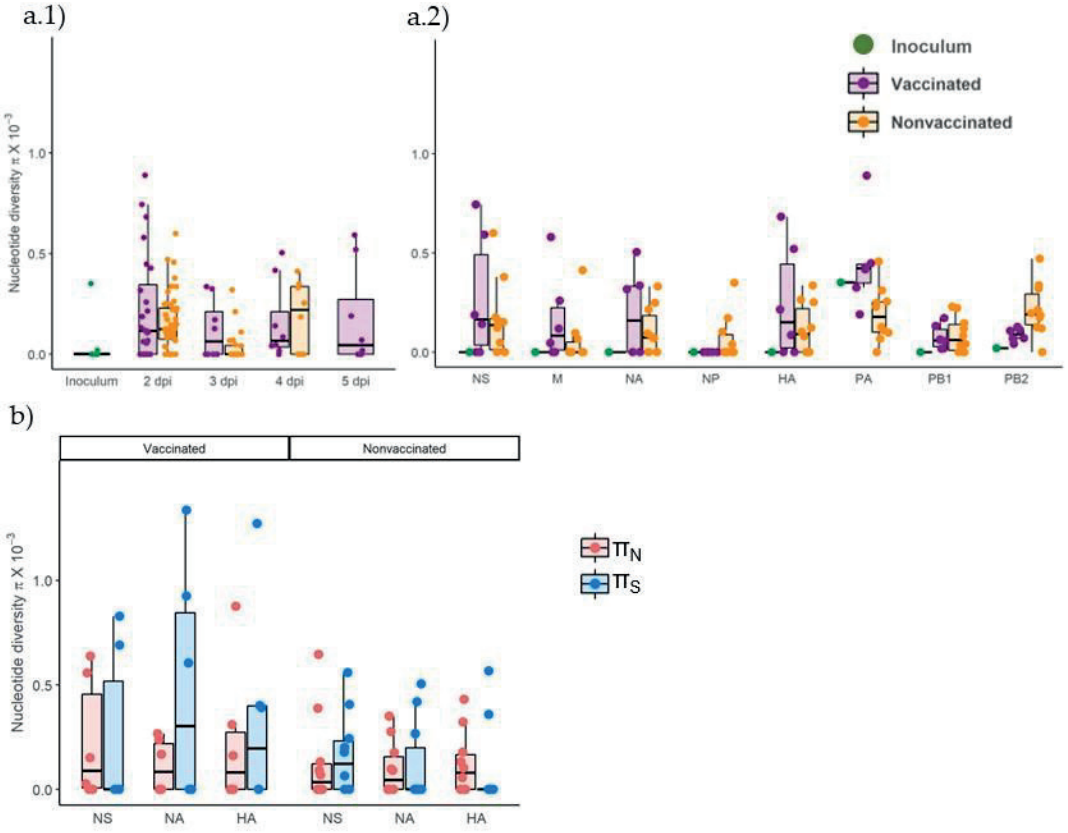


**Figure 4.10. Genetic diversity in viral populations collected from vaccinated and nonvaccinated animals.** (**a**) Nucleotide diversity ($\pi$) box plot representation of total viral population collected from inoculum, vaccinated, and nonvaccinated animals, plotted in green, violet, and orange, respectively. (**a.1**) Whole genome $\pi$ per collection day (**a.2**) Total $\pi$ per genomic segment. (**b**) Nonsynonymous and synonymous nucleotide diversity ($\pi$N and $\pi$S) box plot representation of all sequenced samples for NA, HA, and PA segments. The $\pi$N is represented in blue whereas $\pi$S is represented in red. Mean, lower, and upper quartiles are represented in each box plot, where whiskers indicate the variability outside quartiles. Points represent each analyzed sample.

Regarding $\pi$ by genomic segments, it increased in most samples in both experimental groups compared with the inoculum, in which only diversity was

found in PA and PB2 segments (Figure 4.10a.2, Table 4.4). The π only decreased in comparison with inoculum in the segment PA in virus collected from nonvaccinated animals.

According to the nonsynonymous and synonymous nucleotide diversity (πN and πS, respectively), on average, the πS was greater than πN in NA and HA segments in viral samples collected from vaccinated animals, whereas it was lower in NS. Meanwhile, in samples from nonvaccinated pigs, πS was greater than πN in the NS segment but lower in NA and HA segments (Figure 4.10b). No significant differences between groups were found applying the Kruskal–Wallis test.

## 4.5 . Discussion

Swine influenza viruses are pathogens distributed worldwide in pigs that cause an important economic loss in the ever-growing pork production industry [76,234]. According to the Food and Agriculture Organization (FAO), Spain is the fourth country in the world in terms of the largest pig production, behind China, USA, and Brazil [76]. There are several SIV subtypes worldwide co-circulating in the field, namely H1N1, H3N2, and H1N2 [252,253], with high seroprevalence levels in farms, including in Spain [254]. Nowadays, together with biosecurity measures, vaccination, although limited, is one of the most used strategies to avoid the disease although it does not prevent virus replication [149,152,235]. The latter, together with the current increase in pig population and the capacity of SIV evolution, could change viral host range, antigenicity, and virulence. A previous study showed different evolutionary trends according to pig vaccination status, showing positive selection pressure in trivalent vaccinated animals, whereas purifying selection pressure was noticed in nonvaccinated ones [235]. Considering the capability of IAVs to escape pre-existing immunity acquired by natural infections and vaccine application [14], both scenarios were studied herein. Hence, for a better understanding of the mechanisms that shape the evolution trends of SIVs, a differential whole SIV genomic analysis was performed by deep sequencing after an experimental H3N2 inoculation in vaccinated and nonvaccinated pigs that had suffered a previous natural infection by A(H1N1)pdm09.

In the present study, antibodies against NP and SIV RNA were unexpectedly detected in pigs the day of the first vaccination (0 dpv). Viral and antibody detection methods evidenced that virtually all animals had a previous contact with an IAV before challenge. After genome detection and sequencing, the SIV A(H1N1)pdm09 genome was determined in one of these positive samples. Consequently, this virus was circulating in the farm, probably unnoticed, which

highlights the high prevalence of this virus in the field, as previously reported [254]. Animals showed levels of antibodies against NP until the end of the experiment, these values being more heterogeneous in nonvaccinated animals. On the day of challenge, only sera from vaccinated pigs showed HI activity against the SIV H3N2 strain. Consequently, the viral replication was lower, and the pathological findings were milder in vaccinated animals, proving again the efficacy of the vaccine [235]. Furthermore, the clinical manifestation of the disease in nonvaccinated animals previously naturally infected with the A(H1N1)pdm09 pandemic virus does not provide apparent cross-protection against the H3N2 SIV subtype [255]. However, as the vaccine does not confer sterilizing protection, viral shedding and clinical–pathological features were also observed in vaccinated animals, as previously described [195,235]. The vaccine effect had a direct impact on sequencing results as viral shedding is lower in vaccinated animals, thus NGS coverage and depth were less favored in collected samples from vaccinated animals. Nonetheless, whole SIV genome sequences could be obtained from six samples recovered from vaccinated animals, allowing the possibility to compare the genetic variability in the viral population collected from both experimental groups. The percentage identity among challenge, vaccine, and pandemic strains HA and NA proteins are available in the supplementary Table S4.4.

The virus used for pig inoculation was generated after three passages on MDCK cells. This virus, A/Swine/Spain/SF32071/2007 (H3N2), was isolated from a Spanish porcine influenza outbreak [248]. Regarding the genetic diversity found in the inoculum, only five nonsynonymous substitutions were found in PA and PB2 segments. According to the literature, PA D55N substitution was identified as a possible adaptation of IAV H3N2 subtype virus to mammals [256]. Furthermore, the substitution V618I was already noted in a previous similar study, where it was found at 5 dpi in one nonvaccinated animal challenged with H1N1 subtype [235]. In relation to the Q73K substitution found in PB2, it was already detected in the human influenza isolate A/Anhui/1/2013 (H7N9)[257]. Most of the substitutions found in the inoculum were later lost in the sequenced samples from animals after challenge; this result could indicate that these substitutions are implied in the adaptation of field virus in MDCK cells, and they are lost with the readaptation to the natural host. However, the allele frequencies of some substitutions tended to increase over time in some analyzed samples; thus, the presence of these substitutions does not seem to affect the virus fitness when it is readapted to pig.

Regarding de novo nonsynonymous and synonymous SNV proportions, they were greater in both experimental groups at all analyzed frequencies,

although always slightly higher in samples of vaccinated pigs. Globally, the de novo analysis may support that under both scenarios (vaccination or not), the viral evolution of SIV H3N2 was under positive selection pressure, suggesting that virions are poorly adapted to swine hosts [77]. This positive evolutionary pressure could be influenced by the readaptation of virions from cell culture to their natural host or by host immune pressures.

From all sequenced samples collected from vaccinated and nonvaccinated animals, a total of 214 de novo SNVs were detected, proving once again the high mutation rate of RNA viruses such as IAVs [79,235,258]. The appearance of new variants with increased fitness could help virus adaptation to a novel host environment, those variants being naturally selected and therefore perpetuated in viral populations. However, many of these mutations may have a negative effect on the fitness of the virus. For instance, in the polymerase segments (PB2, PB1, and PA), 99 nonsynonymous variants were detected but only 21 exceed 5% of the allele frequency, showing that most mutations that are generated in these segments do not represent a benefit in viral fitness, probably affecting their replicative capacity.

In relation to the polymerase segments, in the PB2 protein responsible for host pre-mRNA cap binding [52], M51I and L697R, both retrieved in samples from vaccinated animals, were allocated in the PB1 binding domain of the protein [259]. Notably, substitution R340K was found in the nonvaccinated animal 13 with an allele frequency of 39.13%. According to previous studies, this substitution contributes increasing the activity of the polymerase, mammal adaptation, and virulence of H10N8, H7N9, and H9N2 avian IAV [260,261]. Therefore, this substitution may affect viral replication since it was found in the unique lung sample where immunoreactivity was detected at 5 dpi. The Q591K substitution was observed in the nonvaccinated animal 10, which showed one of the highest pathological scores and the highest rectal temperature registered in the study. This substitution was previously related to mammal adaptation and increased virulence of H5N1, H7M9, and H9N2 IAVs [262]. In the protein with polymerase activity, PB1, the substitution P64S was found in the vaccinated animal 4; this mutation has been previously found circulating in the swine population from Guangdong (China) in an SIV H1N1 virus [263]. With reference to the PA protein, whose key role is cleavage host pre-mRNA and transcription initiation [52], the substitution R256K noted in nonvaccinated animal 10 was found predominant in IAVs H1N1, H2N2, H3N2, and H5N1 [264]. Furthermore, the substitution E349G was found in samples collected from the vaccinated animal 4 and nonvaccinated animals 9 and 10. In previous works, this substitution has been shown to increase the virulence of IAV [265,266].

NS1 protein is implied in viral replication and host immunity regulation. In the present study, five nonsynonymous substitutions with an allele frequency greater than 5% were found in this protein: two in the RNA binding domain in samples from nonvaccinated animals and three in the effector binding domain from vaccinated ones. The two substitutions found in nonvaccinated animals, E71K and G72R, were located close to the linker region of the protein, which play an important role in its plasticity. Hence, these substitutions could be involved in different protein conformations, affecting their interaction with other molecules and therefore functions [60]. Moreover, the E71K substitution was previously studied by reverse genetics in avian IAV, and it reduced IFN-β expression [267]. This substitution was found in the viral population collected from the nasal swab of the nonvaccinated animal 10. Thus, the E71K substitution may limit IFN-β expression by increasing virus replication and virulence [268]. By contrast, in the vaccinated animal 2, substitutions S99P and S135I were simultaneously found. The first one interacts with the cellular polypeptide tripartite motif-containing protein 25 (Trim25), which regulates the host innate immune response to infection by ubiquitin ligases [269,270]. The second one is implied in host p85β binding, which interacts with phosphoinositide 3-kinase (PI3K), activating a cellular pathway resulting in inhibition of apoptosis by phosphorylation of caspases, contributing to virus replication and virulence [271,272]. Another substitution at position 135 (S135C) was found in the nasal swab from animal 4 at 4 and 5 dpi. It should be highlighted that allele frequency of this substitution increased from one day to the other from 6.35 up to 48.85%. Therefore, this substitution may benefit the viral fitness because of the rapid allelic increase and the viral shedding recorded during 3 consecutive days from this animal. In a previous study, nonsynonymous substitutions in this protein were only found in vaccinated animals, showing that this protein could rapidly change, facilitating the adaptability of the virus under immune pressure [235].

In relation to the M segment, nonsynonymous substitutions were only found in viral populations collected from vaccinated animals. From the seven substitutions identified, only M1 E204K found in the animal 2 exceeded 5% of allelic frequency (14.28%). The role of this protein is virion assembly by interaction with proteins and lipids [273]. A previous study revealed that at this position, it induces filamentous changes in infected cells, affecting virus growth [29]. Notably, only one nonsynonymous substitution was found in the NP protein with an allele frequency of 2.9%. This protein interacts with polymerases and has an important role in the synthesis of RNA and its traffic [219,220]. Nonsynonymous substitutions in this protein could impair viral fitness, as it is a highly conserved protein among IAVs [274]. Therefore, our findings could

support NP as a good therapeutic target for antiviral and universal vaccine development [155,156,275]. However, in a previous study from our group, in which the evolutionary capacity of the H1N1 virus was evaluated, six nonsynonymous substitutions were described in this protein [235].

The surface glycoproteins HA and NA are the main targets to generate antibodies against IAV after natural infection and/or vaccination [223]. Therefore, substitutions in these proteins may play an important role in the generation of mutants that may allow viruses to escape pre-existing immunity. The $\pi N$ and $\pi S$ proportion was lower in vaccinated animals, whereas the opposite was found in nonvaccinated ones, pointing to different evolutionary patterns depending on immunological pressure. Thus, under both scenarios, these segments showed different evolutionary tendency, acting to purify and enable natural selection in viruses collected from vaccinated and nonvaccinated animals, respectively. Notably, on average the $\pi$ was greater in vaccinated animals, and this could indicate that HA and NA are evolving faster in these animals, regardless of whether those substitutions were synonymous or not. Regarding substitutions found with an allele frequency greater than 5%, more changes were found, proportional to the number of obtained sequences per group, in samples from vaccinated animals.

In nonvaccinated animals, three substitutions were identified in the HA segment. Substitution V239I was the only one found in the receptor binding domain and it is allocated in one epitope region. This substitution was previously identified in epidemic H3N2 SIV subtype isolated in Southern China in 2012 [276]. Furthermore, V283A and N364D substitutions were found in the vestigial esterase domain and in the fusion peptide. In contrast, four substitutions were found in the fusion (C297* and I339V) and the stalk domains (T467I and N505S) in vaccinated animals. The stop codon mutation, originated by C297* mutation, generates a truncated protein with 296 amino acids. In a previous study, stop codon substitutions were found in HA and those substitutions were transmitted among pigs [225]. Furthermore, avian IAV HA truncated proteins have been previously found in environmental reservoirs [277]. The I339V substitution, close to the cleavage domain, has been previously reported in H3N2 canine IAV in China [278]. Regarding the stalk domain, substitutions T467I and N505S were simultaneously found in the lung sample of the vaccinated animal 2, with allele frequencies of 31.25 and 25%, respectively. According to a previous study, evolution of this domain is slower and independent from immune pressure [279]. Interestingly, our findings suggest that pre-existing immunity may have an implication in the positive evolution of substitutions in this domain, as no

substitutions were found in the head domain. Finally, the substitution I351K in the fusion peptide was found in three samples from both experimental groups.

Regarding the NA segment, substitutions N329S and T434A, located in the head domain, were recovered from nonvaccinated animals 10 and 16, respectively. In a previous study, substitution N329S was associated with losing one glycosylation site, although it did not alter the activity of the protein [280]. According to a previous study, this substitution is allocated in the antigenic epitope F′ 329–339 [281]. In vaccinated animals, substitution F167L was recovered in animal 2, whereas V303I and G313S ones were detected in nasal swab samples from animal 4 at 3 and 4 dpi, respectively. Substitution V303I was previously reported circulating in Bulgaria during the 2019–2020 winter season in H3N2 human IAV [282]. This substitution is allocated in the epitope region E'302-308 of the N2 protein [281]. Considering that this substitution, like the previously mentioned S135C in NS1 protein, was found in nasal swab samples collected in the only vaccinated animal which showed SIV detection during three consecutive days, this substitution may favor at 3 dpi some adaptative advantage to viral replication.

In the present study, the high mutability rate of SIV has been further demonstrated [235], showing that IAVs' genomes is constantly changing. The high population of pigs and the high persistence of the virus make IAVs a continuous threat to both animal and human health, as virus evolution could affect viral host range, antigenicity, and virulence. Hence, rapid virus evolution contributes to the fact that the virus remains in the field continuously, which simultaneously implies that the virus is constantly evolving. Herein, the impact of each de novo substitution found on virus fitness is hypothesized according to previous literature. Therefore, future research will be necessary to deeply understand the role of these substitutions, either alone or together, through reverse genetic technology studies [283]. Altogether, the risk of future pandemic IAVs, as happened in 2009, is not negligible. To avoid or minimize the damage it could cause, the reduction of SIV circulation as much as possible by applying stricter vaccination schedules and a more rational swine production are highly advisable. Furthermore, SIV surveillance studies in farms and more effective or universal vaccine development are also crucial to prevent future flu pandemics.

**Supplementary Materials:** The following are available at https://www.mdpi.com/article/ 10.3390/v14092008/s1, Supplementary Table S4.1. Sequenced reads obtained per sample. The total number of reads and reads mapped against reference genome after post-mapping filter application. Supplementary Table 4.S2. SNV and its allele frequency reported in several

samples. Supplementary Table S4.3. SIV H3N2 single nucleotide variants detected in all samples collected from vaccinated and nonvaccinated pigs. Table S4.4. HA and NA amino acid percentage identity among challenge, vaccine, and pandemic strains.

**Author Contributions:** Conceptualization, J.I.N.; methodology, Á.L.-V., L.C., J.I.N., and J.S.; HTS libraries preparation, L.B. and C.C.; bioinformatic analysis, Á.L.-V.; formal analysis, Á.L.-V., L.G. and J.I.N.; resources, A.D. and J.I.N.; writing—original draft preparation, Á.L.-V., L.G. and J.I.N.; writing—review and editing, Á.L.-V., J.S., L.G., and J.I.N.; supervision, J.I.N.; project administration, J.I.N.; funding acquisition, A.D. and J.I.N. All authors have read and agreed to the published version of the manuscript.

**Funding:** This research was funded by grants AGL2016–75280-R from Ministerio de Ciencia, Innovación y Universidades from the Spanish government. Á.L.-V. has a pre-doctoral fellowship FPI 2017, Ministerio de Ciencia, Innovación y Universidades from the Spanish government.

**Institutional Review Board Statement:** The experiment was carried out in accordance with the Spanish and European regulations and was approved by the animal ethics committee from the Generalitat de Catalunya, Spain, under approval code 9657.

**Informed Consent Statement:** Not applicable.

**Data Availability Statement:** Sequencing data were deposited at NCBI, with the accession number (PRJNA853173).

**Acknowledgments:** The authors thank Diego Pérez and Gemma Guevara for their contribution in the field studies. Authors also thank Carlos Neila, Miguel Blanco, and Lola Pailler for their support and advice in bioinformatics biostatistics and figure layout.

**Conflicts of Interest:** The authors declare no conflict of interest.

# Chapter 5

## Study III - Vaccination against swine influenza in pigs causes different drift evolutionary patterns upon swine influenza virus experimental infection and reduces the possibility of genomic reassortments.

*Álvaro López-Valiñas [1,2,3], Marta Valle [1,2,3], Miaomiao Wang [1,2,3], Guillermo Cantero [1,2,3], Ayub Darji [1,2,3], Chiara Chiapponi [4], Joaquim Segalés [1,3,5], Llilianne Ganges [1,2,3,6] and José I. Núñez [1,2,3]*

1 IRTA. Programa de Sanitat Animal. Centre de Recerca en Sanitat Animal (CReSA). Campus de la Universitat Autònoma de Barcelona (UAB), Bellaterra, Barcelona, Spain.Unitat mixta d'Investigació IRTA-UAB en Sanitat Animal.

2 Centre de Recerca en Sanitat Animal (CReSA). Campus de la Universitat Autònoma de Barcelona (UAB), Bellaterra, Barcelona, Spain.

3 WOAH Collaborating Centre for the Research and Control of Emerging and Re-Emerging Swine Diseases in Europe (IRTA-CReSA), 08193 Barcelona, Spain.

4 WOAH Reference Laboratory for Swine Influenza, Istituto Zooprofilattico Sperimentale della Lombardia ed Emilia-Romagna, 25124 Brescia, Italy.

5 Departament de Sanitat i Anatomia Animals, Universitat Autònoma de Barcelona, Bellaterra, 08193 Barcelona, Spain.

6 WOAH Reference Laboratory for Classical Swine Fever, IRTA-CReSA, 08193 Barcelona, Spain.

## 5.1 Abstract

Influenza viruses (IVs) can infect wide variety of bird and mammal species. Its genome is characterized by having 8 RNA single stranded segments. The low proofreading activity of its polymerases and the genomic reassortment between different IVs subtypes allow virus to be continuously evolving, constituting a constant threat to human and animal health. In 2009, a pandemic of an influenza A virus highlighted the importance of the swine host in IVs adaptation between humans and birds. The swine population and the incidence of swine influenza (SI) is constantly growing. In previous studies, despite vaccination, SI virus (SIV) growth and evolution was proven in vaccinated and challenged animals. However, how vaccination can drive the evolutionary dynamics of SIV after coinfection with two subtypes is poorly studied. In the present study, vaccinated and nonvaccinated pigs were challenged by direct contact with H1N1 and H3N2 independent SIVs seeders. Nasal swab samples were daily recovered and BALF was also collected at necropsy day from each pig for SIV detection and whole genome sequencing. In total, 39 SIV whole genome sequences were obtained by NGS from samples collected from both experimental groups. Subsequently, genomic and evolutionary analyses were carried out to detect both, genomic reassortments and single nucleotide variants (SNV). Regarding the segments found per sample, we observed that the simultaneous presence of segments from both subtypes was much lower in vaccinated animals, indicating that the vaccine reduced the possibility of genomic reassortment events. In relation to SIV intra-host diversity, a total of 239 and 74 SNV were detected in the H1N1 and the H3N2 subtypes, respectively. Different proportion of synonymous and nonsynonymous substitutions was found, indicating that vaccine may be influencing the mechanism of natural, neutral, and purifying selection that play the main role in SIV evolution. SNV were detected along the whole SIV genome with important nonsynonymous substitutions on polymerases, surface glycoproteins and nonstructural protein, which may have an impact on virus replication, immune system escaping and virulence of virus, respectively. The present study further emphasized the vast evolutionary capacity of SIV, under natural infection and vaccination pressure scenarios.

## 5.2 Introduction

Influenza A viruses (IAVs) are worldwide distributed pathogens whose natural hosts are lots of birds and mammals species including humans and pigs. IAVs genome is composed of 8 RNA negative sense strand segments: two polymerases basic (PB1 and PB2), polymerase acidic (PA), the hemagglutinin (HA), the nucleoprotein (NP), the neuraminidase (NA), the matrix proteins (M) and the non-structural proteins (NS1)[284]. The evolution of IAVs, like other RNA viruses, is described under the quasispecies theory [73,285]. On one hand, IAVs genome can rapidly accumulate point mutations along the whole genome, because of the low proofreading activity of their polymerases [79,286], which

could confer to progeny adaptative advantages. The evolution of the surface glycoproteins, HA and NA, are constantly under immune pressure if the host has pre-existing immunity against SIV. Therefore, both segments, after genetic diversification, could achieve a new antigenic pattern, avoiding pre-existing immunity [163]. On the other hand, genomic segment reassortments, between different IAVs subtypes, generate higher levels of variability. This genetic mechanism can occur when a host is simultaneously coinfected by different IAVs, and as a result, new viruses could arise with different host range, antigenicity, and virulence. Historically, these reassortment events were responsible for the emergence of important pandemic flu such as the Asian flu in 1957 (H2N2) and the Hong Kong flu of 1968 (H3N2) [82–84].

In 2009, a new pandemic swine origin influenza strain A(H1N1)pdm09 quickly spread, human to human contact, to more than 30 countries and it causes between 151,700 and 574,400 human deaths associated with the infection [85,118]. This new strain arose from the reassortment of two circulating swine influenza viruses (SIVs), the H1N1 Eurasian "avian-like" (EA) swine and a previous circulating triple reassortant of H3N2 and H1N2 harbouring avian, human and swine IAVs segments [85,287]. Lately, in China, a new strain H1N1 G4 EA, with pandemic and triple reassortant segments, became predominant in the swine population. This strain is capable of infecting humans and therefore could pose an imminent pandemic risk [122]. Hence, pigs play an important role in the generation of new IAVs strains with pandemic potential as they are considered "mixing vessels" being susceptible to avian, human, and swine IAVs [112–114]. Accordingly, pigs serve as intermediaries in the adaptation of avian IAVs to humans and vice versa [117].

Therefore, to prevent future influenza pandemics, it is important to conduct ongoing swine influenza viruses (SIVs) evolution studies on the porcine population. In the last decade, the most circulating subtypes among pig population on farms are "avian-like" swine H1N1, "human-like" swine H1N2, "human-like" reassortment swine H3N2 and A(H1N1) pdm09 virus [125,166,252–254]. The mortality rate caused by SIV in swine is low, but it is a highly contagious disease whose morbidity rate could reach 100 % in exposed animals [125,126]. Both, the high seroprevalence and the ever-increasing pig population make greater reassortment events possibilities. Nowadays, biosecurity measures and trivalent vaccine application are the main strategies to avoid disease and reduce SIV prevalence [149,167], although its use is limited in Europe reaching only 10-20% of the pig population [150]. Trivalent vaccine against SIV includes H1N1, H3N2, and H1N2 subtypes in their formulation in the EU. It reduces virus spread and disease, although it does not generate

sterilizing immunity in the host allowing viral replication [151,167]. Previous studies suggest that the application of the trivalent vaccine can influence on the evolutionary dynamics of SIV viral populations, being different in vaccinated and nonvaccinated animals [235,288]. However, the impact that vaccine application could have on SIV evolution in coinfected animals needs more study. Thus, the aim of the present study was to evaluate the evolutionary dynamics of SIV during a coinfection trial in pigs with EA "avian-like" swine H1N1 and "human-like" swine H3N2 strains in vaccinated and nonvaccinated pigs. In total, after pig infection, 39 viral quasispecies collected from vaccinated and nonvaccinated pigs were analyzed by NGS, finding different evolutionary patterns, and nonsynonymous substitutions that could be playing an important role in the evasion of the swine immune system and virulence.

## 5.3 Material and Methods

### 5.3.1 Cells, viruses, and vaccine

Viral titration and production were performed using Madin-Darby Canine Kidney (MDCK, ATCC CCL-34). For cell culture, Dulbecco's Modified Eagle Medium (DMEM) was used supplemented with fetal bovine serum (FBS) (10%), L-glutamine (1%) and penicillin/streptomycin (1%). The cell culture conditions were 37 °C with 5% $CO_2$ atmosphere in an incubator.

The A/Swine/Spain/01/2010 H1N1 and the A/Swine/Spain/SF32071/2007 H3N2 viruses were propagated in MDCK monolayer cell culture at a multiplicity of infection (MOI) of 0.01 and harvest 48 hours later. Virus cells entry was facilitated by 10 μg/mL of porcine trypsin (Sigma-Aldrich, Madrid, Spain) addition. For both virus titrations, serial dilutions in MDCK cells were carried out to calculate the 50% tissue culture infection dose ($TCID_{50}$) [168].

In the present study, the commercial inactivated SIV vaccine (RESPIPORC FLU3, IDT®, Dessau-Rosslau, Germany) was used. Vaccine formulation include the H1N1 (Haselünne/IDT2617/2003), H3N2 (Bakum/IDT1769/2003), and H1N2 (Bakum/1832/2000) strains.

### 5.3.2 Experiment Design

Twenty 5-week-old domestic pigs free of SIV and its antibodies were selected. Animals were equally distributed in two different boxes, box 1 and 2 of the animal biosafety level 3 (aBSL3) facilities at IRTA-CReSA . In box one, seeders animals H1N1 (1 and 2), seeders animals H3N2 (5 and 6) and animals from group A (9 to 14) were allocated. Whereas seeders H1N1 (3 and 4), seeders H3N2 (7 and 8), and animals from group B (15 to 20) were housed in box two.

After an acclimation period of one week, animals from group A received the first dose of the vaccine according to manufacturer's instruction, by 2 mL intramuscular administration in the neck muscle. In parallel, animals from group B received 2 mL of phosphate buffered saline (PBS) in the same manner. Twenty-one days post-vaccination (21 dpv), animals from group A and B, received the second dose of the vaccine and PBS, respectively.

Three weeks after the second vaccination dose (42 dpv), animals 1 to 4 and 5 to 8 were challenged with A/swine/Spain/SF11131/2007 (H1N1) and A/Swine/Spain/SF32071/2007 (H3N2), respectively. For the inoculation, two administration routes, intranasal and endotracheal, were used with a viral concentration of $10^7$ $TCID_{50}$ in a final volume of 2 and 5 mL, respectively. For the intranasal administration, 1 mL of inoculum per nostril was inoculated with a diffuser device (MAD Nasal, Teleflex, Morrisville, NC, USA). On the other hand, for the endotracheal administration animal was intubated. For both, a nose snare was used to restrain animals [235]. Experimentally inoculated animals were separated from the rest by a physical barrier. One day post inoculation (1 dpi), barriers were lifted to allow direct contact.

After the challenge, animals were daily monitoring for rectal temperature, clinical signs and animal behavior in a blind manner by trained veterinarians. Clinical signs were scored as previously described[173]. Moreover, after the first day post-contact (1 dpc), the SIV load in nasal swab samples was daily measured by RTq-PCR (explained below). When viral loads started to drop animals were euthanized.

Nasal swab samples were collected before first and second vaccination, at day of challenge and daily from 1 dpc to animal euthanasia. Blood samples were collected at vaccinations, challenge and euthanasia days. From each euthanized animal, lung, nasal turbinate (NT) and broncho-alveolar lavage fluid (BALF) were collected and stored at -80 °C. BALF from each animal were collected after filling the right lung with 150 mL of PBS. By last, an extra lung sample was stored in formalin.

Procedures were approved by the animal ethics committee from the Generalitat de Catalunya, under the project number 10856, preserving the Spanish and European regulations.

### 5.3.3 Evaluation of the Humoral Response Against SIV

Antibody levels against influenza NP was performed by ID Screen®— influenza A Antibody Competition ELISA kit (ID VET, Grabels, France). The inhibition percentages were calculated according to the manufacturer's

instructions were values below 45 % were considered positive, greater than 50 % negative, and between both values doubtful.

Furthermore, the hemagglutination inhibition (HI) assay was performed in samples collected at day of seeders challenge and each pig euthanasia day as previously described [172]. All tested sera sample were first treated with RDE II Seiken (Denka Chemicals, Tokyo, Japan) at 37°C during 18 h and later inactivated at 56°C for 1 h. Unspecific hemadsorption inhibitors were removed by adding a volume of 50 % chicken red blood cells (RBCs) and later diluted in PBS (1:10). Treated pig sera were two-fold diluted, in v-bottomed 96 well plates, with PBS until 1:1024 dilution. Subsequently, twenty-five μL of each viral antigens used on challenge diluted until 4 Hemagglutination Units (HAU), were dispensed in each well in parallel and incubated during 1 h at room temperature. After that, twenty-five μL of 0.5% of chicken RBCs were dispensed and again incubated for 1 h at room temperature. The hemagglutination titer of each serum was established as the reciprocal dilution at which inhibition was complete. Titers ≥1/40 were considered seroprotective.

### 5.3.4 Pathological Analyses and Immunohistochemistry in Lung

The lung parenchyma was macroscopically examined during each animal necropsy. The percentage of lung-affected area was also determined through an image analysis as previously described [175], using ImageJ® software [245].

A sample from each lung collected in formalin was fixed in 10% buffered formalin, dehydrated, and embedded in paraffin wax. Later, two 3–5 μm thick sections were cut for both, hematoxylin-eosin (HE) staining and immunohistochemistry (IHC), for light microscopy examination [176,177]. For IHC, two-step polymer method (Envision TM) was conducted using as primary and secondary antibodies a monoclonal one against influenza A virus (IAV) (Hb65 from the ATCC) and system + HRP-labeled polymer Anti-Mouse (K4001, Dako), respectively [178]. The degree of lung lesion according to the number of airways affected and the amount of immunoreactivity were evaluated, on HE and IHC examination respectively, using a previous described semiquantitative scores [246].

### 5.3.5 SIV Genome Detection

Lung and NT were homogenized in brain heart infusion medium (10% weight/volume) with TissueLyser II (Qiagen, Düsseldorf, Germany). RNA from nasal swab, BALF, lung and NT samples were extracted using the MagAttract 96 Cador Pathogen kit ® (Qiagen, Düsseldorf, Germany) according to manufacturer's instructions. To detect and quantify SIV RNA on each sample a

RT-qPCR based on M segment amplification was performed in the Fast7500 equipment (Applied Biosystem) [132]. Samples with a cycle threshold (Ct) value under 40 were considered positive whereas no fluorescence detection were considered negative [132,235].

### 5.3.6 Whole SIV Genome Sequencing

RNA from A/Swine/Spain/01/2010 H1N1 and A/Swine/Spain/SF32071/2007 H3N2 inoculums, and RNA extracted from nasal swab and BALF samples with a Ct value lower than 35 were proposed for whole genome sequencing [15,235]. First, a whole SIV genome amplification was performed using 0.5 µL of each forward MBTuni-12 and reverse MBTuni-13 primers, both at 0.2 µM. Moreover, 0.5 µL of SuperScript® III One-Step RT-PCR System with Platinum™ Taq High Fidelity DNA Polymerase (Thermo Fisher Scientific, Waltham, MA, USA), 12.5 µL of reaction mix included in the kit, 8.5 µL of RNasa free water and 2.5 µL of SIV RNA. In parallel, a second amplification was performed to enhance biggest SIV segments amplification replacing the forward primer by MBTuni12G, keeping the remaining conditions [180]. Only samples with whole SIV amplification were further selected [15]. For sequencing, a multiplexed sequencing library was prepared per sample following the Nextera-XT DNA Library Prep protocol (Illumina®, San Diego, CA, USA). Subsequently, the libraries sequentiation was performed using Miseq Reagent Kit v2 in a 150-cycle paired-end run on Miseq Instrument (Illumina®, San Diego, CA, USA). Sequencing fastq files data were deposited at the National Center for Biotechnology Information (NCBI, https://www.ncbi.nlm.nih.gov/), with the following accession number (PRJNA902942).

### 5.3.7 Bioinformatic workflow for Quasispecies Genomic and Evolutionary Analysis

In the present study, a bioinformatic workflow was developed to Illumina reads alignment and variant calling, with tools widely used for the study of viral quasispecies [77,90,91]. First, Illumina adapters were automatically removed. Reads quality were checked with FastQC (v 0.11.8) [181] and low-quality reads (Phread < 30) were trimmed by Trimmomatic (v0.39) [182]. To determine SIV H1N1 and H3N2 inoculum consensus sequences, reads from both were aligned against the H1N1 (JX908038-45) [184] and H3N2 (HE774666-73) [248] genome sequences using Burrows-Wheeler alignment (BWA) tool mem function (v0.7.17) [289]. After mapping, unmapped, and low quality mapped (< 30) reads were removed from the analysis using Samtools (v.0.39) [185]. Moreover, PCR duplicates and reads recalibration were performed with the Picard "MArkDuplicatesSpark" and "BaseRecalibrator" options included in GATK4

(v4.1). Indeed, the sequence depth on each genome position was calculated with "-depth" function included on Samtools (v1.9) and plotted using ggplot2 library in Rstudio [186,187]. Subsequently, consensus sequences were generated using consensus option from Bcftools (v.1.9) [185].

All samples were simultaneously aligned, against both inocula consensus, following the previous described workflow. Finally, each sample was again aligned, using only as a reference the segments that were present on each specific sample. In all samples, SNV reported because of misalignment reads due to the high percentage of similarity between H1N1 and H3N2 sequences, were parsed and eliminated using R (v.4.1.2) [187].

All variants found along the whole genome were noted using LoFreq software with default parameters [188]. Moreover, the effect on variant of each substitution noted was predicted with SnpEff software (v.4.3) [189]. Previously, a database for both subtypes was created with "build–gtf22" function, using the previously annotated genomes [184,248]. The following requirements were considered to call a single nucleotide variant (SNV); p value < 0.01 and at least 100 and 10 reads of depth and alternative base count respectively [235]. By last, the nucleotide diversity ($\pi$) per genomic segment per sample were calculated with SNPGenie software [190].

### 5.3.8 Protein structure representation

Allocations of nonsynonymous substitutions with an allele frequency greater than 5 % were pointed in each SIV protein. Lolliplot proteins representation was done with the trackViewer package from Bioconductor [249]. All protein domain delimitation was inferred as previously reported [34,290,291]. Besides, HA and NA 3D protein representations were also performed with the PyMOL Molecular Graphics System (v.4.6).

### 5.3.9 Statistical analysis

T-test was used to compare the distribution of the percentage of competition on the day of the challenge, and ct values from 4 to 9 dpi, between vaccinated and nonvaccinated animals. Chi-squared test was used to study differences in proportions between the numbers of genomic segments detected and synonymous and nonsynonymous percentages in vaccinated and nonvaccinated animals. Subsequently, Bonferroni correction was applied. Finally, an analysis of variance (ANOVA) and subsequent post-hoc Kruskal-Wallis test by rank, were applied to compare $\pi$ means between vaccinated and nonvaccinated animals on different days and in different segments.

## 5.4 Results

### 5.4.1 Humoral response against SIV

Competition percentage means of antibodies against NP were greater at all collection days in vaccinated animals (Figure 5.1). From day of the challenge until the end of the experiment, difference between groups were significant (*t-test; p*= 0.001881). At day of the challenge, 2 out of 6 sera samples collected from vaccinated animals were considered positive.

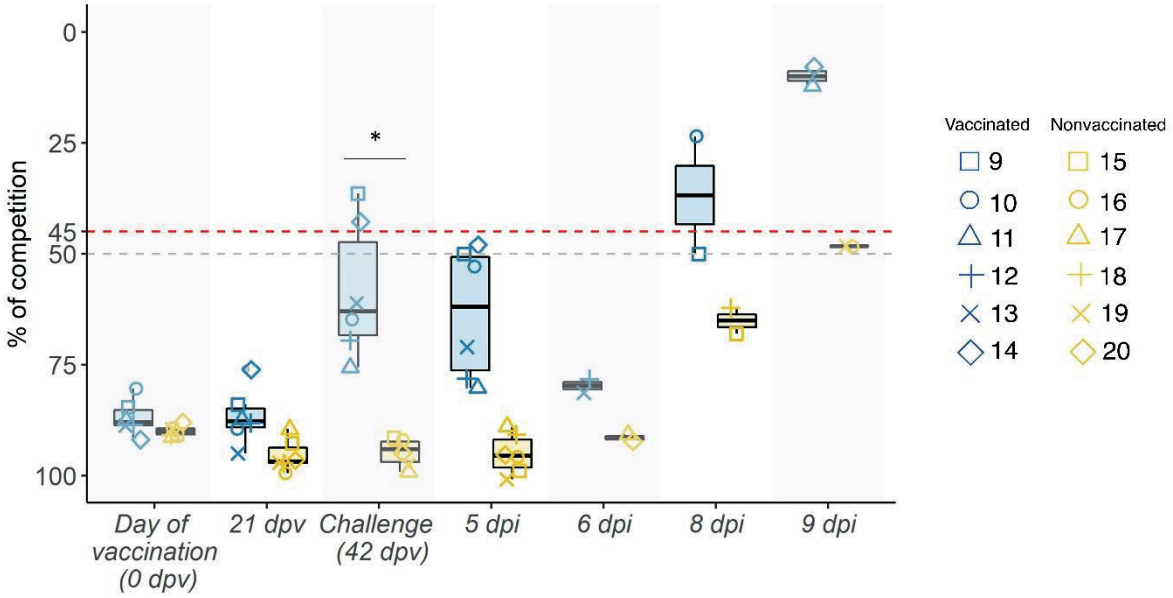


**Figure 5.1. SIV NP antibody kinetics in serum samples boxplot.** The percentage of competition is expressed in the ordinate axis whereas the day on which each serum sample was collected is indicated on abscissas one. Blue boxplots show samples collected from vaccinated animals, whereas the yellow ones represent nonvaccinated ones, and the whiskers show quartile variability. Different shapes illustrate the ID number of each pig. Values above the red line (< 45%), below the grey line (> 50 %) and between both lines are considered positive, negative, and doubtful respectively. * $p < 0.05$

Regarding HI titers against strains used on the challenge at day of the challenge, in sera from vaccinated, animals no positive titers were observed against H1N1 subtype, even though all sera showed positive titers against H3N2 subtype (Table 5.1). On the day of euthanasia, titers against H1N1 subtype were only detected in vaccinated animals, specifically in 3 out of 6 animals. On the other hand, positive titers against H3N2 were observed in all samples collected from vaccinated animals, whereas were only detected in nonvaccinated samples at 8 and 9 dpi with low titers value.

**Table 5.1. HI activity of sera samples against H1N1 and H3N2 strains used on the challenge.** HI titers are shown, titers greater than 40 are considered positive.

| | | HI titers against H1N1 | | | | | HI titers against H3N2 | | | | |
|---|---|---|---|---|---|---|---|---|---|---|---|
| | | | Euthanasia Day | | | | | Euthanasia Day | | | |
| Group | Pig ID | 42 dpv | 6 dpi | 7 dpi | 8 dpi | 9 dpi | 42 dpv | 6 dpi | 7 dpi | 8 dpi | 9 dpi |
| Vaccinated Animals | 9 | 0 | | | 0 | | 160 | | | 80 | |
| | 10 | 0 | | | 20 | | 80 | | | 80 | |
| | 11 | 0 | | | 320 | | 40 | | | 80 | |
| | 12 | 0 | 0 | | | | 80 | 40 | | | |
| | 13 | 0 | 0 | | | | 80 | 160 | | | |
| | 14 | 0 | | | | 160 | 160 | | | | 320 |
| Nonvaccinated Animals | 15 | 0 | | | 0 | | 0 | | | 10 | |
| | 16 | 0 | | | | 0 | 0 | | | | 40 |
| | 17 | 0 | 0 | | | | 0 | 0 | | | |
| | 18 | 0 | | | 0 | | 40 | | | 40 | |
| | 19 | 0 | | | | 0 | 0 | | | | 80 |
| | 20 | 0 | 0 | | | | 0 | 0 | | | |

### 5.4.2 SIV genome was detected in both experimental groups after seeder contact

SIV was detected in nasal swab samples collected from seeders, vaccinated and nonvaccinated animals, from 2 dpi until the end of the experiment (Figure 5.2a, supplementary table S5.1). SIV was not detected in any nasal swab sample collected before the challenge (42 dpv) (figure 5.2a). As an average, lower ct values were detected in samples collected from nonvaccinated animals in comparison with vaccinated ones, being this difference significant at 6 dpi (t-test; $p=0.0186$). In total, 32 and 31 out of 39 and 40 nasal swab samples analysed from vaccinated and nonvaccinated animals respectively were SIV positive. Besides, 23 vaccinated and 26 nonvaccinated samples obtained ct values lower than 35.

Regarding BALF, Lung, and nasal turbinate samples, SIV was detected in all samples except in BALF from vaccinated animals 11 and lung samples from animal 2. No significative differences were observed between groups, showing similar mean values (Figure 5.2b, supplementary table S5.1). All positive BALF samples had a ct value lower than 35.

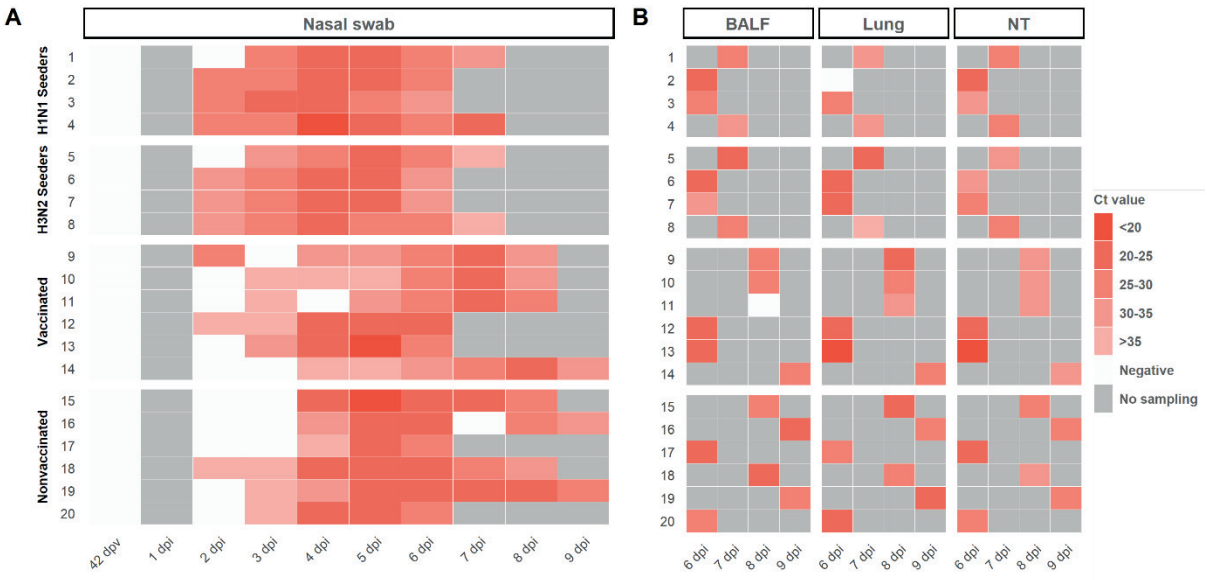


**Figure 5.2. SIV genome detection in samples collected from H1N1 and H3N2 Seeders, Vaccinated and Nonvaccinated animals.** A) Daily SIV RNA detection in samples collected from nasal swabs. B) SIV genome detection in BALF, Lung, and Nasal turbinate samples collected on the day of each animal euthanasia. The Ct values are represented as a heat map where the maximum intense red colors represent higher viral loads and vice versa. RT-qPCR CT values greater than 40 were considered negative, represented in white. No sampling collected was represented as grey. The ID of each animal and the day at which each sample was collected are represented in ordinate and abscissa axes, respectively.

### 5.4.3 Pathological findings

On average, the lung affected area was greater in vaccinated animals, although statistical differences were not found. Vaccinated animals 9 and 10 presented high damage percentages, 17,89 and 31,89 % respectively. The remaining pigs did not exceed 6 % of lung affected area (Table 5.2).

In vaccinated pigs, three animals showed the highest airways affected scoring whereas the remained obtained the second one. By contrast, an average lower microscopic lesions score was detected in nonvaccinated pigs. Regarding immunohistochemistry labelling, all lungs showed scattered amount of immunoreactivity except nonvaccinated animals 16 and 19, with low amounts, and vaccinated pig 11, with the absence of immunoreactivity.

**Table 5.2. Lung pathological results according to the percentage of total lung-affected area, and the semi-quantitative scoring for the degree of airways affectation and amount of immunoreactivity.**

| Group | Pig ID | Euthanasia day | Lung affected area (%) | Airways affected score | Immunoreactivity score |
|---|---|---|---|---|---|
| *Vaccinated Animals* | *9* | 8 dpi | 17.96 | 3 | ++ |
| | *10* | 8 dpi | 31.89 | 3 | ++ |
| | *11* | 8 dpi | 5.52 | 2.5 | - |
| | *12* | 6 dpi | 3.19 | 3 | ++ |
| | *13* | 6 dpi | 0.19 | 2.5 | ++ |
| | *14* | 9 dpi | 6.09 | 2.5 | ++ |
| | | *mean* | 10.81 | 2.75 | |
| *Nonvaccinated Animals* | *15* | 8 dpi | NO DATA | 1.5 | ++ |
| | *16* | 9 dpi | 4.86 | 3 | + |
| | *17* | 6 dpi | 0.48 | 2 | ++ |
| | *18* | 8 dpi | 5.43 | 2.5 | ++ |
| | *19* | 9 dpi | 5.65 | 3 | + |
| | *20* | 6 dpi | 0.62 | 1.5 | ++ |
| | | *mean* | 3.41 | 2.25 | |

*Airways affected scoring: absence (0), few inflammatory cells isolated (0.5), a localized cluster of inflammatory cells (1), several clusters of inflammatory cells (1.5–2), severely several (2.5), and many airways affected (3). Moreover, minimal (1.5), mild (2) interstitial infiltrate, and plus moderate interstitial and alveolar infiltrate (2.5–3). Immunoreactivity scoring: absence (-), low (+), scattered (++), moderate (+++), and abundant (++++) amount of immunoreactivity.*

### 5.4.4 Whole genome sequencing of Inocula, Nasal swab, and BALF collected from vaccinated and nonvaccinated animals

The whole SIV genome from inocula A/swine/Spain/SF11131/2007 (H1N1) and A/Swine/Spain/SF32071/2007 (H3N2) was determined (Figure 5.3a.1). From samples collected after contact challenge, 39 SIV genomes were sequenced, 20 from vaccinated animals and 19 from nonvaccinated ones (Figure 5.3a.2 and 5.3a.3, Supplementary table S5.1). After sequenced samples alignment, a total of 2.467.438 reads against SIV were obtained, 1.347.544 from vaccinated samples and 1.119.899 from nonvaccinated samples, 67 % of these reads matched against H1N1 genome whereas the remaining 33 % did it against H3N2 subtype (Supplementary table S5.2).

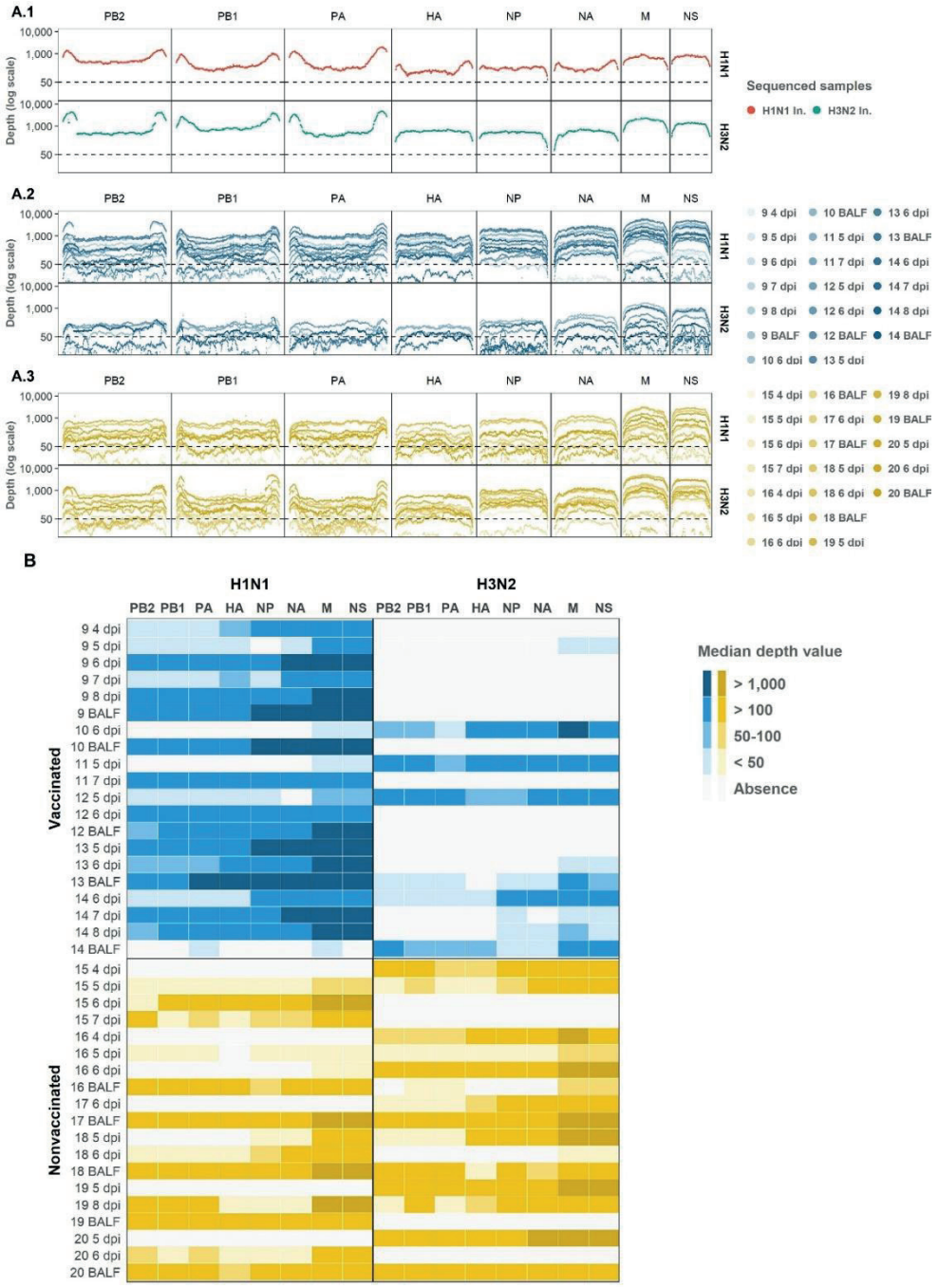


**Figure 5.3. Depth and coverage obtained per SIV genomic segment after both inocula, vaccinated and nonvaccinated pig samples NGS reads alignment against each subtype genomic profile**. (A1) Illumina sequencing profile of SIV H1N1 (plotted in red) and H3N2 (plotted in green) used as inocula. In the x axis each position per genomic segment is indicated whereas the depth of read is indicated in y axis in the logarithm scale. In the upper and lower graphs, profiles against H1N1 and H3N2 subtypes are separated and represented respectively. (A2) Illumina profile of samples collected from vaccinated animals where each sample is represented in different tones of blues. (A3) Illumina profile of samples collected from nonvaccinated animals where each sample is represented in different tones of yellows. (B) Heat map of the median depth value obtained in all sequenced samples from vaccinated and nonvaccinated animals per H1N1 (left) and H3N2 (right) genomic segments. Genomic segments per subtype and samples are indicated in the x and y axes respectively. The name of each sequenced sample indicates the origin and the day of its collection. BALF samples were collected at each pig necropsy.

Regarding the depth per position and the coverage (Figure 5.3), 74.8 % of H1N1 SIV whole genome positions sequenced were represented with a depth of more than 50 reads. On the other hand, the 6 % of the H3N2 position sequenced were also represented by more than 50 reads. Those positions were selected for further variant analysis. In general, segments NS and M segments obtained the greatest median depth values (Figure 5.3), meanwhile, the biggest segments PA, PB1 and PB2 get the lowest values.

### 5.4.5 Determination of H1N1 and H3N2 Genomic Segment per Sample

In relation to the subtype segments profile per sample, in vaccinated animals we obtained 95 H1N1 segments, 18 H3N2 segments, and 41 segments where both subtypes were simultaneously found (Figure 5.4). Meanwhile, in nonvaccinated animals, 42 H1N1 segments, 50 H3N2 segments, and 60 with both subtypes were found (Figure 5.4). The distribution of H1N1 and H3N2 segments was statistically different between groups (chi-squared; $p = 0.0002$, $p = 0.000018$, respectively), being greater the number of H1N1 segments in vaccinated animals and greater the number of H3N2 segments in nonvaccinated ones. Regarding the number of segments in which sequences from both subtypes were found, in vaccinated animals this number is lower than in nonvaccinated ones, although this difference was not significant (chi-squared; $p = 0.0587$).

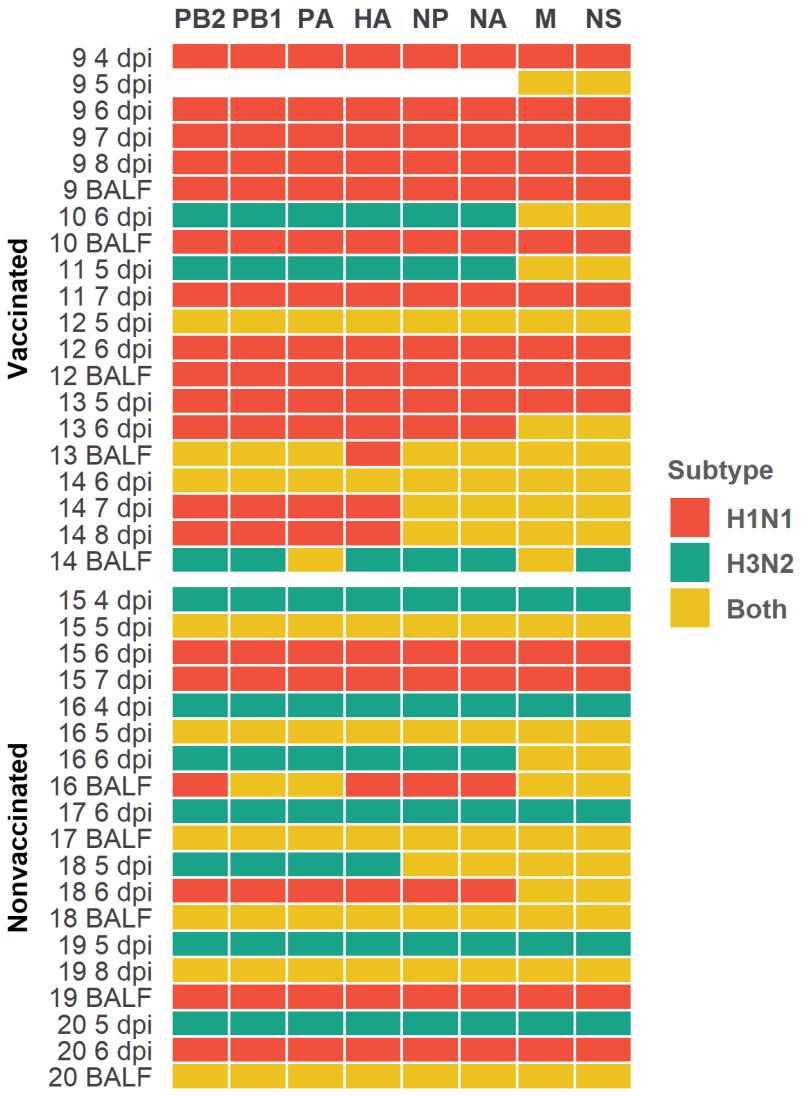


**Figure 5.4. Profile subtype identification per genomic segment in each sequenced sample heatmap.** H1N1 subtype segments are indicated in red cells, H3N2 are indicated in green cells and yellow ones indicate that both subtypes were simultaneously found. Genomic segments and sequence samples collected from vaccinated and nonvaccinated animals are represented on the x and y axes respectively. The number of each sequenced sample indicate the animal from which each sample was collected Sample collection day are also indicated before dpi in nasal swab samples, the BALF samples were collected on the day of animal necropsy.

### 5.4.6 Variants detected in Inocula and its evolution in samples sequenced from infected pigs

From both inocula, 14 and 9 SNV were detected from H1N1 and H3N2 respectively (Table 5.3). In H1N1, 8 out of 14 substitutions found were synonymous, whereas in H3N2 all SNV detected were nonsynonymous. Furthermore, most of the SNV detected in H1N1 (12 out of 14) exceed the 5 % of allele frequency whereas any substitution did it in H3N2 inoculum (Table 5.3).

Table 5.3. SNV detected in H1N1 and H3N2 inocula samples.

| | | Nucleotide change | | Aminoacidic change | | Depth | Alt. Base | Allele | Effect on |
|---|---|---|---|---|---|---|---|---|---|
| | Gene | position | ref. → alt. | position | ref. → alt. | of read | count | frequency | variant |
| Inoculum H1N1 | NS1 | 323 | A → C | 108 | K → T | 860 | 107 | 12.44 | nsyn |
| | | 631 | G → A | 211 | G → R | 731 | 228 | 31.19 | nsyn |
| | M1 | 240 | C → T | 80 | V → V | 681 | 435 | 63.88 | syn |
| | | 261 | T → C | 87 | N → N | 702 | 23 | 3.28 | syn |
| | | 396 | C → T | 132 | Y → Y | 961 | 14 | 1.46 | syn |
| | M2 | 896 | R → A | 70 | X → K | 603 | 312 | 51.74 | nsyn |
| | | 896 | R → G | 70 | X → E | 603 | 291 | 48.26 | nsyn |
| | NA | 150 | T → A | 50 | N → K | 274 | 56 | 20.44 | nsyn |
| | PA | 1055 | A → G | 352 | E → G | 189 | 10 | 5.29 | nsyn |
| | PB1 | 1146 | T → C | 382 | N → N | 244 | 52 | 21.31 | syn |
| | | 1185 | C → T | 395 | L → L | 256 | 48 | 18.75 | syn |
| | | 1254 | Y → C | 418 | V → V | 322 | 132 | 40.99 | syn |
| | PB2 | 1054 | T → C | 352 | L → L | 405 | 98 | 24.2 | syn |
| | | 168 | G → A | 56 | P → P | 990 | 224 | 22.63 | syn |
| Inoculum H3N2 | HA | 1111 | C → T | 371 | H → Y | 589 | 15 | 2.55 | nsyn |
| | PA | 1046 | A → G | 349 | E → G | 369 | 15 | 4.06 | nsyn |
| | | 290 | C → T | 97 | T → I | 574 | 13 | 2.26 | nsyn |
| | | 2047 | C → A | 683 | L → I | 4042 | 161 | 3.98 | nsyn |
| | | 1852 | G → A | 618 | V → I | 760 | 10 | 1.32 | nsyn |
| | PB1 | 1308 | C → T | 436 | Y → Y | 827 | 12 | 1.45 | nsyn |
| | PB2 | 153 | G → A | 51 | M → I | 3026 | 33 | 1.09 | nsyn |
| | | 395 | C → T | 132 | P → L | 440 | 15 | 3.41 | nsyn |
| | | 2033 | A → C | 678 | D → A | 1044 | 11 | 1.05 | nsyn |

*Abbreviations: alt. (alternative), ref. (reference), nsyn (Nonsynonymous) and syn (Synonymous).*

These SNV were later detected in samples collected from vaccinated and nonvaccinated animals in HN1 inoculum (Figure 5). In most of the sequenced samples the SNVs G211R (NS1), V80V (M1), X70E (M2), L395L, and V418 (PB1) increased its allele frequency over time. On the other hand, allele frequencies of NS1 K108T, M1 N87N and Y132Y, NA N50K, PA E325G, PB1 N382N, and PB2 substitutions tend to be decreased beyond detection with some exceptions (Figure 5.5). Notably, any SNV detected in H3N2 inoculum was later detected in sequenced samples.

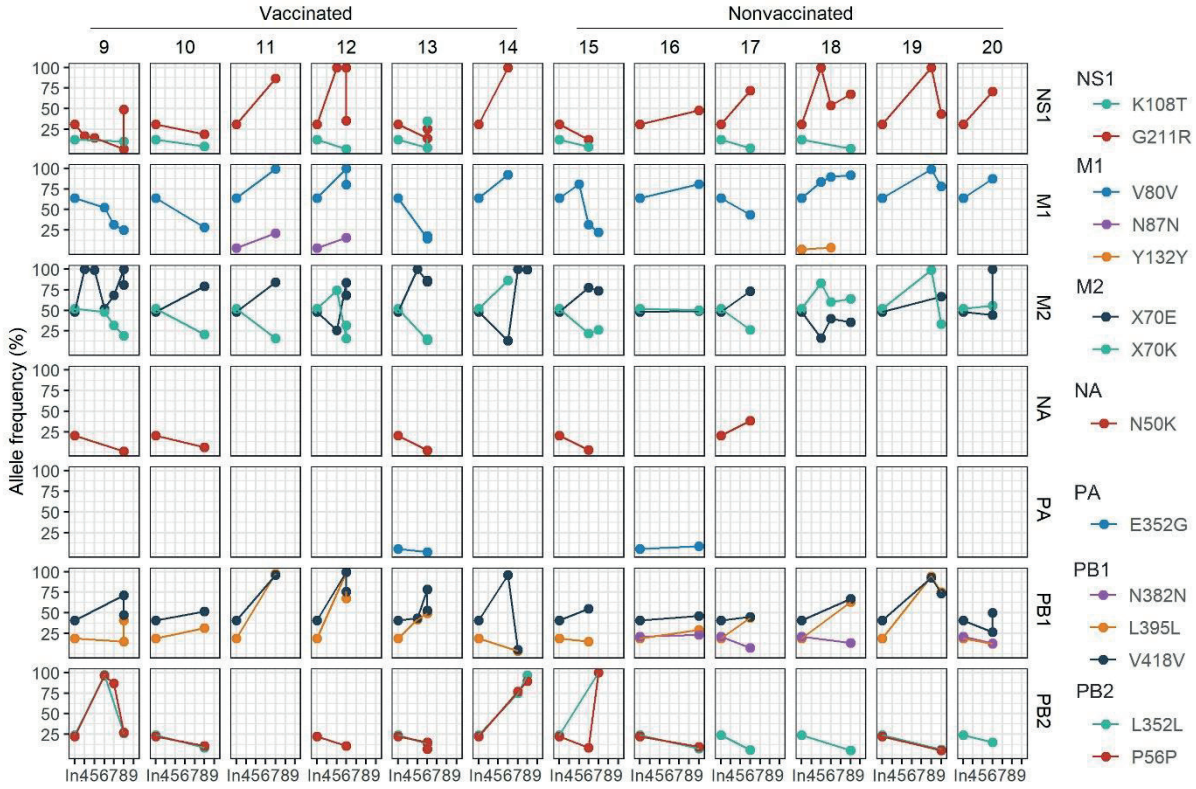


**Figure 5.5. Evolution of the allele frequencies of nonsynonymous substitutions detected in H1N1 inoculum and later in samples collected from both experimental groups.** The day of variant detection and the allele frequency percentage is represented in ordinate and abscissa axes respectively. The "In." in x axis indicates the percentage obtained in the inoculum, whereas 4 to 9 numbers indicate the day after inoculation at which frequency was observed in the sample. In each column, the different animals are represented whereas, in each row NS1, M1, M2, NA, PA, PB1, and PB2 proteins are indicated. Each mutation is plotted in different colours.

### 5.4.7 *De novo* SNVs identification; Synonymous and Nonsynonymous proportion and allocation along SIV Genome. segments

A total of 313 SNVs were found in all analysed samples, 187 in vaccinated animals and 126 in nonvaccinated ones (Figure 5.6 and Figure 5.7). In vaccinated pigs, 172 were found in H1N1 and 15 in H3N2 subtypes, meanwhile, in nonvaccinated animals 67 and 59 were identified per subtype respectively. Regarding SNVs per subtype, 239 were found in H1N1 and 74 in H3N2 (Figure 5.6).

The proportions of the total synonymous and nonsynonymous de novo SNV were studied from 1 to 10 % allele frequency in sequenced samples from vaccinated and nonvaccinated animals (Figure 5.6). Regarding the H1N1 subtype, in all allele frequencies analysed the proportion of nonsynonymous variants was greater than synonymous ones in both experimental groups. This difference was greater in vaccinated animals although no statistical differences between groups were found (Figure 5.6a). By contrast, in nonvaccinated animals

these proportions were very close to 50%, being this trend consolidated throughout the allele frequencies analysed. In H3N2, the proportion of nonsynonymous SNVs was greater in both scenarios, specifically in samples from nonvaccinated animals (Figure 5.6b).

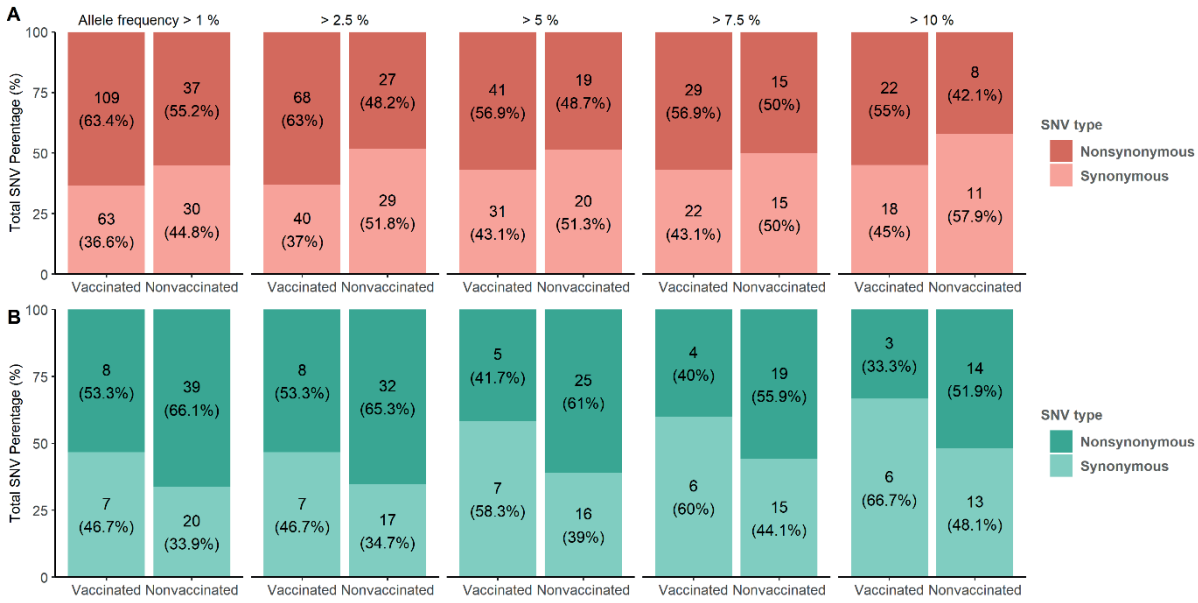


**Figure 5.6. De novo synonymous and nonsynonymous SNV proportion bars in samples from vaccinated and nonvaccinated animals at different allele frequencies.** (A) SNV proportions found in H1N1 subtype, represented in red bars (B) SNV proportions found in H3N2 subtype, represented in green bars. The total number of SNV and its percentages are indicated in each bar. Dark and soft colours represent nonsynonymous and synonymous SNV, respectively.

Considering those variants whose allele frequency was greater than 1%, SNVs were allocated along the whole genome of both studied subtypes (Figure 5.7, Supplementary table S5.3). In general, in H1N1 subtype, more substitutions were found in samples from vaccinated animals (Figure 5.7a). Specifically, a total of 54 de novo nonsynonymous variants were found in polymerase segments in samples from vaccinated animals, while only 14 were reported in nonvaccinated samples. In the HA and NA segments, 12 and 13 nonsynonymous substitutions were reported from vaccinated animals while only 3 and 5 were found in the other group respectively. Regarding the NS, a total of 17 nonsynonymous variants were identified in vaccinated animals and 9 in nonvaccinated. By last, segments in which the least nonsynonymous substitutions appear were the M and the NP, with 6 ,7 in vaccinated pigs and 4, 2 in nonvaccinated ones, respectively (Figure 5.7a).

Regarding SNV found in H3N2 subtype, only 8 nonsynonymous substitutions were found in vaccinated animals, 2 in PB2, 2 in PB1, 2 in M, and

only 1 in NA and NS. Nevertheless, no nonsynonymous substitutions were reported in PA, HA, and NP (Figure 5.7 b). On the other hand, in the nonvaccinated group, the largest number of nonsynonymous variants were also found in the polymerase segments, 11 in PA, 11 in PB1 and 8 in PB2. In the remaining segments, 4 nonsynonymous variants were detected in NS, 2 in M, and in HA, NA, and NP only one was reported in each (Figure 5.7 b).

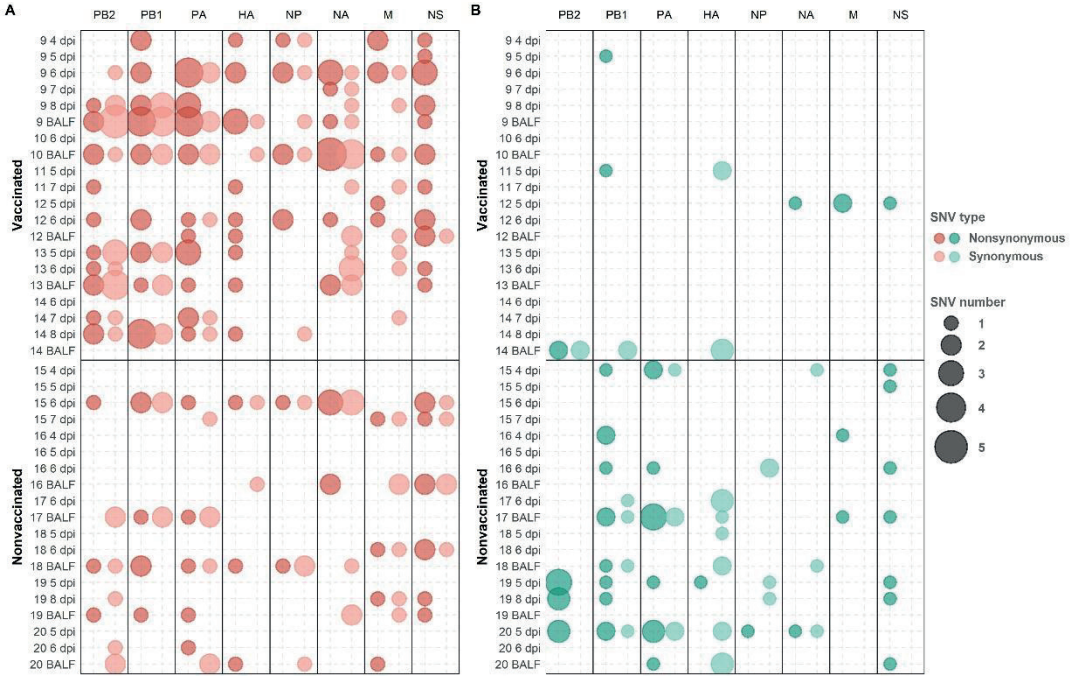


**Figure 5.7. De novo synonymous and nonsynonymous SNV with an allele frequency greater than 1% allocation along SIV genome.** (A) SNV was found in H1N1 subtype represented in green circles. (B) SNV found in H3N2 subtype indicated in red circles. Nonsynonymous and synonymous substitutions are represented in dark and light colours, respectively. Circle size indicates the total number of SNV found per genomic segment and samples, in abscissa and ordinate axes respectively.

### 5.4.8 De novo nonsynonymous SNV with an allele frequency greater than 5 % allocated on protein domains

In H1N1, in vaccinated animals the following nonsynonymous SNV, that exceed the 5 %of allele frequency, were reported in PB2 (L77V, D195N, T364K, I394T, Q566L and D671G), in PB1 (R187G, A370V, F512C, C625G, S642N, W666L and S720F), in PB1-F2 (K29R and P33L), PA-X (E114K,R208K and V218A), PA(T528I, V645A and V645I), HA (E111K, N275S, S278P, T408A, V466I and K467R), NP(A286T, T360A, S407N and V456L), NA (V394I), ion channel (M2) (I51N and G58D) and NS1(T91I and L146P). Meanwhile, in nonvaccinated animals, substitutions were allocated in PB2 (D195N), in PB1 (A370V and K388R), in PB1-F2 (F57Y), PA-X (R208K), PA (I407V and V505I), HA (V216I and V466I),

NA (S90P and N209K), matrix protein (M1) (Q158L and E204V), M2(G58D) and NS1(K66E, L79I and F137Y) (Figure 5.8 and 5.9).

Regarding substitutions found in H3N2, in vaccinated pigs, SNVs were noted in PB2 (N9D and P14S) and PB1-F2 (H15L). On the other hand, in nonvaccinated animals substitutions found were allocated in PB2 (N71T, T215P, N659I, L665R, and K702E), in PB1 (T57S, Q202K. C625G, A652D, and F699L), in PB1-F2 (H15L), PA (I120L, G316E, W317L, S388G, Y393C, I407V andM561V), HA (I351K), NA(S33G), nuclear export protein (NS2) (T33I) and NS1(W102L and R211G) (Figure 5.8 and figure 5.9). All the substitutions found in the present study were noted in supplementary table 5.3.

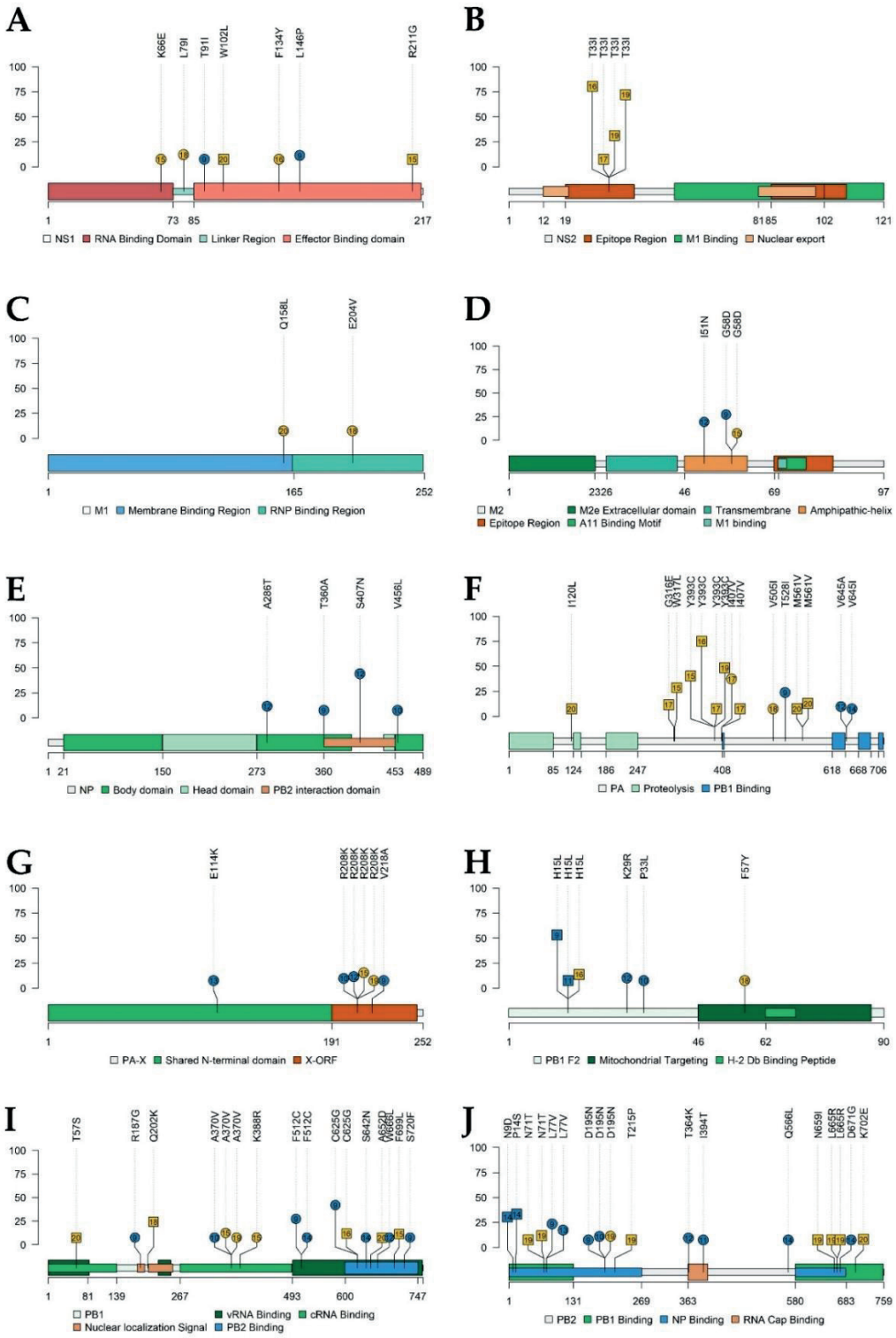


**Figure 8. Nonsynonymous SNV allocation on SIV proteins lolliplot representation. Substitutions found in NS1(A), NS2 (B), M1 (C), M2 (D), NP (E), PA (F), PA-X (G), PB2-F2 (H), PB1(I) and PB2 (J) proteins with an allele frequency greater than 5 %.** In ordinate axis, the allele frequency of each substitution is indicated. Substitutions noted in blue and yellow show substitutions found in vaccinated and nonvaccinated animals. Besides, the circle shape indicates that substitution was reported in H1N1 subtype, whereas substitutions found in H3N2 are represented by square shapes. Number inside each shape indicates the pig ID of each reported substitution. Figure legends indicate the most important domains of each protein.

Regarding substitutions found in H3N2, in vaccinated pigs, SNVs were noted in PB2 (N9D and P14S) and PB1-F2 (H15L). On the other hand, in nonvaccinated animals substitutions found were allocated in PB2 (N71T, T215P, N659I, L665R, and K702E), in PB1 (T57S, Q202K. C625G, A652D, and F699L), in PB1-F2 (H15L), PA (I120L, G316E, W317L, S388G, Y393C, I407V andM561V), HA (I351K), NA(S33G), nuclear export protein (NS2) (T33I) and NS1(W102L and R211G) (Figure 5.8 and figure 5.9). All the substitutions found in the present study were noted in supplementary table 5.3.

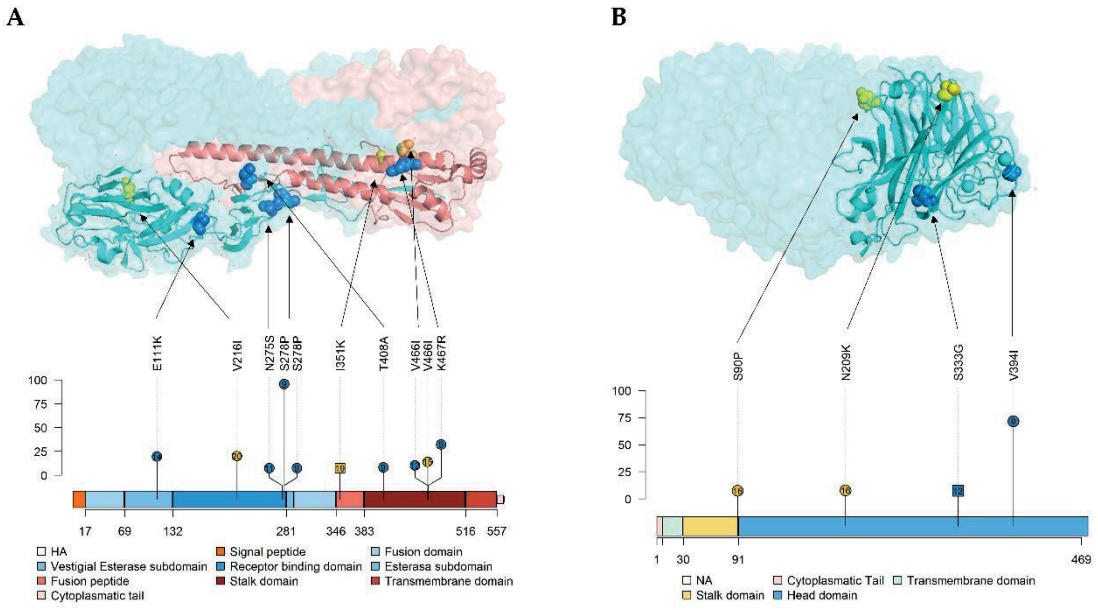


**Figure 9. Localization of nonsynonymous substitutions, with an allele frequency greater than 5 %, found in HA and NA surface glycoproteins on 3D and lolliplot proteins representation.** (A) HA trimer structure (PDB accession no. 3LZG [208]) and domains representation by lolliplot. HA1 and HA2 domains are represented in different tones of blues and reds respectively. (B) NA tetramer structure (PDB accession no. 4B7Q [209]) and domains representation by lolliplot. In both 3D representations substitutions are highlighted in blue, yellow and orange if it were found in samples from vaccinated, nonvaccinated and both respectively. In lolliplot representation, substitutions are plotted in blue and yellow (vaccinated or nonvaccinated origin group), circle and squared shapes (H1N1, H3N2 subtype) and number on shapes indicate the animal in which each substitution was found. In the ordinate axis, the substitution allele frequency is indicated. The different surface glycoprotein domains are indicated in the lolliplot legends.

### 5.4.9 Nucleotide Diversity

In the H1N1 subtype, the nucleotide diversity (μ) values fluctuated over time in both experimental groups (Figure 5.10a). The μ significantly increased in vaccinated animals from 5 dpi to 6 dpi, and from 7 dpi to 8 dpi (kruskal-wallis; $p$ = 0.03134 and 0.003948 respectively). However, μ decreased at 5 and 7 dpi in comparison with each previous day, although this decrease is not significant. In

H3N2 subtype the μ only significantly increased from 5 to 6 dpi (kruskal-wallis; $p = 0.0002218$). In general, μ means are greater in vaccinated animals. However, the μ mean in nonvaccinated animals was slightly higher at 7 dpi, and significantly higher at.9 dpi (kruskal-wallis; $p = 0.04804$). On the other hand, in H3N2 subtype, higher levels of μ were observed in samples from nonvaccinated animals, whereas in vaccinated animals the highest levels of μ were observed at 9dpi.

Regarding μ per genomic segment per group, the diversity is higher in H1N1 in comparison with H3N2 (Figure 5.10 b). In the H1N1 subtype greater μ mean were observed in all segments in vaccinated animals, except in M and NS segments. The highest μ were found in the HA. No significant differences per genomic segment per group were observed.

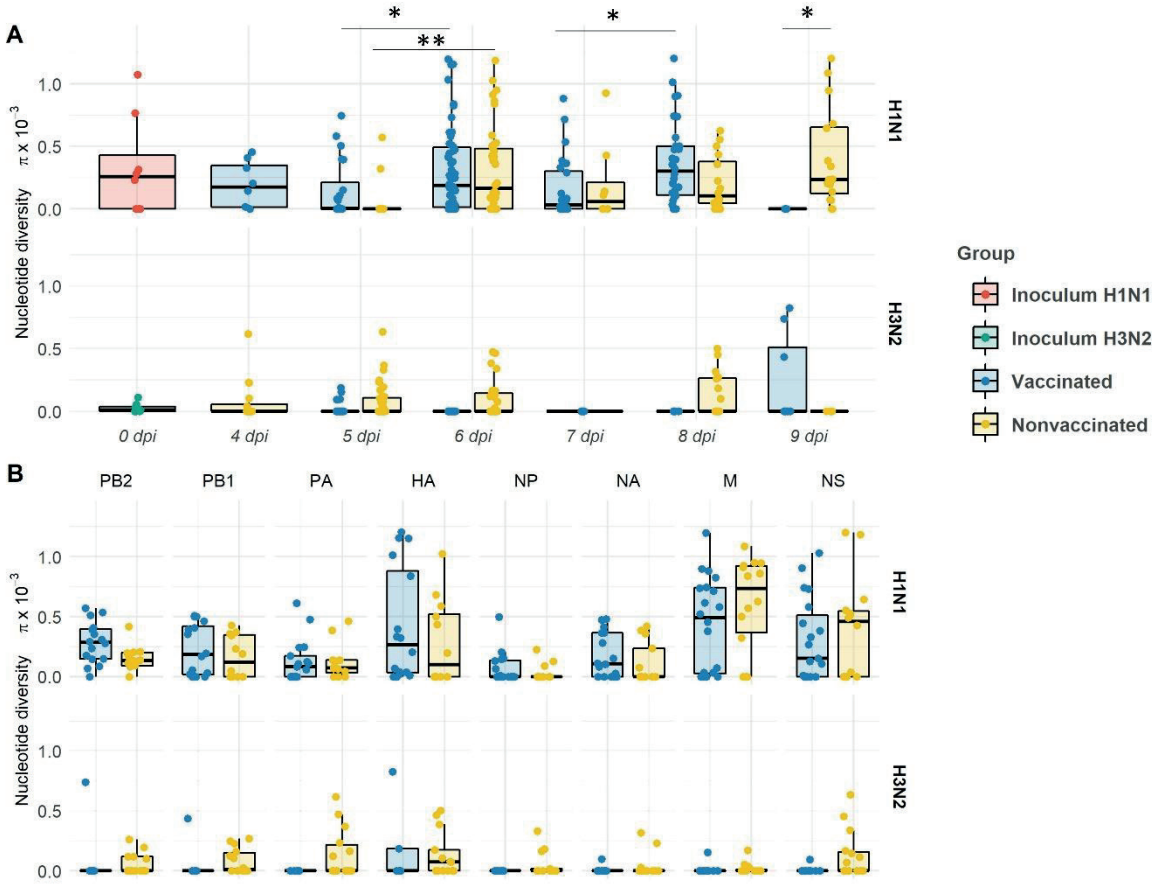


**Figure 5.10. Evolution of the nucleotide diversity (π) in H1N1 and H3N2 viral quasispecies in vaccinated and nonvaccinated animals over time (A) and per genomic segment (B).** Dots in the boxplot indicates μ in each genomic segment. Boxplots indicate means, lower and upper quartile, and standard deviation. The nucleotide diversity of H1N1 and H3N2 inocula, and samples collected from vaccinated and nonvaccinated animals are represented in red, green, blue, and yellow respectively. * $p < 0.05$ *and* **$p < 0.001$.

## 5.5 Discussion

The influenza virus is a worldwide distributed pathogen that infects many species of mammals and birds [64]. Interspecies transmission poses a continuous threat to animal and human health. In 2009, a swine-origin pandemic virus A (H1N1) pdm09 with avian, human, and swine segments, arose in Mexico because of the genomic reassortments between two previous circulating strains among swine [161]. From that moment, the pigs as "mixing vessels" hypothesis became specially more relevant, highlighting these animals as a possible intermediate host in the adaptation of human IAV to avian and vice versa [113,116]. Currently, in Europe, there are 4 main swine strains circulating among the swine population, the EA (*avian-like*) H1N1, *human-like* H3N2, *human-like* H1N2, and the A(H1N1) pdm09 [106,166]. This, together with the high density of the pig population in European farms, increases the possibility of new genomic reassortments that could cause again a new pandemic strain [153]. Nowadays, vaccine application, although limited, is one of the most extended practices to avoid swine influenza and reduce viral shedding [149,150]. Previous studies have shown different evolution patterns on H1N1 and H3N2 SIV subtypes, that may be caused by different host immune humoral pressures [235,288]. However, how immune pressure can shape the viral evolution during different subtypes SIVs coinfection, has not been studied in deeper detail. Therefore, due to the importance of SIV evolution, in the present study, previously H1N1 and H3N2 inoculated pigs, were put in contact with vaccinated and nonvaccinated animals. Subsequently, quasispecies and the intra and its genetic diversity were studied by NGS.

In this work, a commercial trivalent vaccine was applied to immunize animals from the vaccinated group. On the day of the seeders challenge, higher levels of antibodies against NP SIV protein were detected in vaccinated animals, being detected the highest percentage of competition in pig 9. Regarding HI activity, before the challenge, only sera from vaccinated animals presented hemagglutinating titers against H3N2 subtype. On the contrary, any sera had IH activity against H1N1, although it was only detected in vaccinated animals 10, 11, and 12 at necropsy day. According to SIV detection, the virus was detected in seeders, vaccinated, and nonvaccinated animals. Hence, in the present study, the reproduction of experimental infection by contact with SIV was correctly carried out. Besides, the CT values means indicate that from 4 to 9 dpi, the viral loads are greater in nonvaccinated animals, especially at 6 dpi. Therefore, the vaccine has an effect in terms of reducing viral seeding, although it is not sterilizing, so selective pressure is feasible due to humoral immunity caused by vaccination [225,235,288].

On the contrary, the effect of the vaccine was not as effective regarding the pathological findings, as the percentage lung affected area and airways affected score means were greater in vaccinated animals, meanwhile similar results between groups were observed in relation to the immunoreactivity score. In vaccinated animals, animals 9 and 10, we obtained the highest percentage of lung lesions with 17.96 and 31.89 %, respectively. The remaining animals have similar values to animals from the nonvaccinated groups. Hence, animals 9 and 10 can be considered outliers. In both animals may be occurring vaccine-associated enhanced respiratory disease (VAERD), that has been previously described in influenza [129–131] This adverse effect is produced when the inactivated vaccine strain and the infection strain are the same subtypes but with heterologous antigenicity. Together, the vaccine works in terms of viral shedding reduction, but it did not avoid the SIV clinical manifestations.

Herein, 41 SIV quasispecies were analyzed by NGS, 2 inocula, 20 samples from vaccinated animals, and 19 from nonvaccinated ones. First, in samples from vaccinated animals, H1N1 alone segments were more widely detected in each genomic profile, meanwhile, H3N2 segments alone were barely detected 8 times. On the contrary, in the nonvaccinated group, the presence of both segments simultaneously found was the most frequent profile detected, followed by H3N2 alone. These results indicate that vaccination is causing an effect on viral populations, while in vaccinated animals the H1N1 subtype was dominant, it decreases the probability that two subtypes simultaneously coexist, resulting in a decreased probability that a genomic reassortment will take place. Contrary, because of the dominant presence of H1N1, in these animals there was a greater increase in SIV nucleotide diversity, and the greatest number of *de novo* SNVs were found, in total 170 (Figure 6). Notably, the reduction in the presence of H3N2 segments also is reflected in the number of *de novo* SNV in this subtype, being only 15 detected. Thus, in this scenario, the application of the vaccine is causing the H1N1 SIV prevails over H3N2, which has an impact on its evolution. Hence, in one hand in vaccinated pigs, the probability of reassortments was reduced, as has been previously reported [292] although on the other hand, SIV H1N1 genetic variability increased, allowing viral genomic diversification which could result in immune escape mutants, as previously reported in IAV [293–298]. The identity percentage matrix among HAs and NAs from both, challenge, and vaccine strains, are available in the supplementary Table S5.4.

Regarding the SNV and the nucleotide diversity found in both inocula, H1N1 strain is more genetically diverse than H3N2, since more SNVs were reported, and they are also represented with a higher allele frequency. Substitutions found in H1N1 inoculum were later detected in samples collected

from both experimental groups, although SNVs allele frequencies were later decreasing over time, or they were no longer detected. However, there are also some substitutions such as, PB2 P56P, PB1 V418V, M1 V80V, M2 X70K/E, and NS1 G211R, whose allele frequencies increased in some samples. These variants continue to belong to the viral population despite having suffered a bottleneck effect. Considering the quasispecies hypothesis, these mutants could have a beneficial on virus fitness, since they were present in the initial viral population mutant spectrum, and they remained after a selection event, meanwhile the remaining disappeared. On the other hand, all SNVs detected on inoculum H3N2 viral quasispecies spectrum were no longer detected in virus collected from pig samples. All variants detected in both inocula were probably generated, and maintained over time, during virus passages in MDCK cells, because of virus adaptation to cells. Thus, the loss of these variants is probably due to the re-adaptation of the virus to its natural host.

The proportion of nonsynonymous and synonymous *de novo* SNV found may indicate whether the viral quasispecies evolution is under selective pressure. In the H1N1 subtype, in vaccinated animals the proportion is greater, indicating that viral evolution is under positive selection in this scenario [196,197]. However, neutral selection may be acting in nonvaccinated animals, as the same proportion of SNVs was detected [299]. Therefore, in both scenarios, genetic diversification is occurring. Many of the new mutations generated in SIV during the experimental trial, probably play a neutral role in viral fitness, such as the synonymous variants, while others are generated because of the viral readaptation from cell culture to its natural host. However, a higher proportion of nonsynonymous substitutions were generated in vaccinated animals, which could be indicating that additionally, the humoral immune pressure is acting as an evolutionary selection force. By contrast, in the H3N2 subtype, in nonvaccinated animals, the highest proportion of nonsynonymous mutations may be indicating that the virus is also under positive selection. Similar results have been previously found with the same strain; therefore, virions may be poorly adapted to swine hosts, probably because of the readaptation from cell culture [77,288]. In vaccinated animals, as previously mentioned, the viral shedding was greatly reduced, consequently, not enough variants have been detected. Therefore, the main force that drives viral evolution in this scenario could not be inferred.

In this study, the rapid evolutionary capacity and plasticity of SIV are again evidenced, since 313 *de novo* synonymous and nonsynonymous SNV were reported from all the quasispecies herein analyzed (Supplementary Table S5.3) [225,235,288,300,301]. During virus replication, many generated mutations are

not liable for the virus progeny, so they are lost. However, those mutations that are beneficial for viral fitness are naturally selected and will increase their allelic representation in the viral quasispecies [70]. With this regard, in the present study, most of the substitutions were not detected with an allele frequency greater than 5 %, so they do not pose an adaptive evolutionary advantage for the virus. For instance, in the H1N1 subtype in vaccinated animals, only 63 % of all nonsynonymous SNVs found did not exceed the 5% of allele frequency. By contrast, 41 (H1N1) and 4 (H3N2) nonsynonymous substitutions with an allele frequency greater than 5 % were found in viral samples from vaccinated animals. Thus, these substitutions may pose a viral benefice under host immune pressure. These substitutions were allocated in all SIV proteins, except in M1 and NS2 (Figure 8 and Figure 9). Regarding the polymerase segments (PB2, PB1, PA), in H1N1 subtype 25 nonsynonymous substitutions were found in vaccinated animals. Single substitutions reported from these proteins, were related to an increase in IAV polymerase activity, raising its virulence, and in jump interspecies host [302–305]. In the H1N1 NS1 protein, two substitutions were found in the effector binding domain, and both were detected in animal 9. Substitution T91I is allocated in the domain that recruits the host eukaryotic translation initiation factor 4G1 (eIF4G), favouring viral mRNA translation instead of host mRNA [57,200]. In addition, substitution L146P is allocated in the nuclear export signal, according to a previous study leucine at this position is required for NS1 cytoplasmatic localization, although it was detected in the study, it was only found on day 5 dpi with an allele frequency of 13% [206]. In relation to the NP, 4 nonsynonymous substitutions were found in H1N1, while none were detected in H3N2. These results were previously detected in previous studies carried out in our group, where the evolutionary capacity of H1N1 and H3N2 was separately evaluated, and 6 nonsynonymous substitutions were detected in H1N1 and none in H3N2 [235,288].

Surface glycoproteins HA and NA proteins are highly immunogenic, constituting the main target to generate neutralizing antibodies by the host after IAV infection or vaccination [106,197,306]. Thus, both proteins are under high immune pressure when a previously immunized host becomes infected with the virus, which triggers a greater genetic drift [197,223]. The HA is a viral surface glycoprotein that attaches to sialic acid allocated in the swine host respiratory tract, allowing virus cell entry [102]. In the present study, 6 *de novo* substitutions with an allele frequency greater than 5 % have been detected in nonvaccinated animals (Figure 9). The E111K in the vestigial esterase subdomain is allocated in a previously described epitope region of the protein[307,308]. Both substitutions, N275S, and S278P were found in the receptor binding domain (RBD) of the

protein, where the main antigenic sites of the virus are allocated [208,309]. Besides, single substitutions in this domain are related to the virus interspecies switch [225,310,311]. Notably, N275S substitution was reported, with a 97,58 % of allele frequency, in vaccinated animal 9 at 4 dpi, although its allele frequency decreased to 5.58 % in BALF at necropsy (Supplementary table S5.3). Finally, the remaining 3 *de novo* substitutions T408A, V466I, and K467R were allocated on the stalk domain of the protein. Two of these substitutions were also reported from animal 4, reaching 36.64 % of allele frequency in K467R. In a previous similar experiment, substitutions in this domain were also found in the H3N2 subtype in vaccinated animals, finding exactly one substitution at position 467 (T467I) [288]. Notably, relevant nonsynonymous substitutions in vaccinated animals were not found on the H3N2 HA protein.

Regarding NA, this surface glycoprotein plays an important role in virion progeny realising [34]. In vaccinated animals, only two nonsynonymous substitutions, whose allele frequency exceeds 5 %, were reported, both in the head domain of the protein (Figure 9). These substitutions, S333G in HA H3N2 and V394I in HA H1N1, were located on the exposed part of the protein. The first one is allocated in epitope region F'329–339 [281], while V394I is nearby to previously described epitopes[312,313]. Interestingly, V394I was also detected with 73.7 % in viral samples from animal 9. Therefore, in this animal, 4 important substitutions have been detected in both surface glycoproteins. Besides, together with pig 10, the highest pathological scores were reported from this animal. Therefore, in this animal, apart from the VAERD effect, these mutations may be affecting viral fitness, increasing its replicative capacity, and so its virulence. Altogether, all substitutions found in both HA and NA, may have an impact on evading the immune system by the virus, although further analyses with reverse genetic technology would be required [283].

Our findings support the wide capacity of evolution and adaptation to changing environments of SIV. In the present study, a lower probability of viral reassortment was observed in vaccinated animals, as has been recently reported [292]. However, the vaccine did not avoid the genetic diversification of SIV. Herein, nonsynonymous substitutions were found in viral quasispecies collected in vaccinated animals, and the role that they could play in the evasion of the immune system was hypothesized according to previous literature. Thus, genetic reverse studies are further needed to prove the role of this substitution on virus populations. Finally, this study underlines the importance of performing surveillance and genomic studies of SIV, as well as increasing the vaccination rate in pigs, to prevent the circulation of the virus in the field as much as possible,

preventing its evolution, reducing the reassortment events and minimizing the risk of pandemics in both, humans, and pigs.

# Part III

# General discussion and conclusions

# Chapter 6
# General discussion

The high capacity of mutation and adaptability of IAVs, the wide host range, and their interspecies transmission, make of IAVs a constant threat to both, human and animal health. Due to the important role of swine in human-to-avian IAVs adaptation, the study of SIVs evolution might be of great value in understanding their genetic diversity and interaction with the host to avoid new strain emergence. Therefore, this doctoral thesis focuses on the study of the evolution of SIV in swine host under the effect of the most widely used vaccine in the field, with the aim of studying the viral quasispecies and their evolutionary dynamics under this scenario. Previous similar studies have been performed in vaccinated and nonvaccinated pigs, although they are only focused on HA and NA evolution [225,300], meanwhile herein the SIV whole genome is analyzed.

In this thesis, the study of the evolution of SIV in animals with pre-existing immunity against influenza and naïve animals has been addressed through NGS. To that aim, three experiments have been carried out, where vaccinated and nonvaccinated animals were challenged with SIV EA H1N1 and/or "human-like" H3N2, being two of the most current circulating subtypes among the swine population in Europe [106]. Interestingly, different evolutionary patterns were observed between H1N1 and H3N2 strains. In the study with the H3N2 subtype, natural infection with A(H1N1)pdm09 occurred, this fact enriched the analysis since it is a situation that can happen on the farm. It allowed us to analyze the evolution of the virus in previously infected and vaccinated animals. For this study, a third group with naïve animals would allow us to understand the virus evolution without immune pressure, although this insight can already be observed in study III. Additionally, from the study III, where animals were coinfected with both subtypes, remarkable information was inferred about the genomic reassortments dynamics in vaccinated animals. Due to the importance of these genetic events in new pandemic viruses generation, to complete the knowledge about these dynamics, a similar experiment could be carried out using the A(H1N1) virus, since new SIVs strains harbouring pandemic segments have recently emerged [122,314,315]. By last, it should be highlighted that in the present study our main objective was to simulate as much as possible a real situation on the farm. Thus, the most widely used vaccine was selected for the experimental designs. Probably, using the same strain from both, vaccination, and challenge, would be very interesting to study escape mutants, but autogenous vaccines are forbidden in Europe, so this situation would not be real in the field.

Regarding the genetic diversification found in the present work, the implication that may have the nonsynonymous substitutions with higher allele frequency on virus fitness has been theoretically studied according to previous

literature. Therefore, two important factors should be deeply analysed, first, whether the substitution or set of substitutions found have a real impact on viral fitness as suggested. Second, the transmission capacity of these variants among the pig population. For addressing the first question, infectious clones with the most relevant nonsynonymous substitutions found should be created using reverse genetics technology, and subsequently, test *in vitro* its possible contribution to the improvement of viral fitness[283,316,317]. To study if substitutions, especially in HA and NA, could have a major impact on viral antigenicity, the hemagglutinating titers of pigs sera collected in these experiment animals against the whole infectious clones could be studied by hemagglutination inhibition assays. The role of substitutions on pathogenicity could be also assessed by reverse genetic technology, studying the interferon response levels, viral replication ability, and cytokines production in infected cells, as previously reported, especially in NS1 protein[267,318–322]. Subsequently, an experimental infection in pigs could be proposed, using an infectious clone with the most relevant mutations found, as a challenge strain. On the other hand, an experimental design with serial infections must be carried out to determine its transmittance *in vivo.* By last, the genomic evolutionary monitoring of the SIV strains, herein studied, in the field would add great value to this work, to evidence if these substitutions were also generated in natural conditions and fixed on the population.

Regarding the synonymous substitutions found in this study, all have been quantitatively analyzed to determine which was the greatest force that explained the virus evolution under different scenarios, natural, purifying, or neutral selection. However, future analyses on this kind of substitution could provide a better understanding of the virus genetic drift and its host interaction through codon usage bias studies [323–325].

Considering nonsynonymous substitutions found, the present thesis provides novel insight into the distribution and allocation of *de novo* nonsynonymous substitutions in viral proteins. In studies I and II, 5 nonsynonymous substitutions were reported in the NS1 protein of each analyzed subtype. Four substitutions were allocated nearby or in the flexible linker region of the protein, while the remaining were reported in the effector domain. Previous studies reported that substitutions on the linker region could have an impact on molecule conformation, affecting its activity by interaction with other host substrates [60]. On the other hand, according to previous literature, substitutions on the effector domain herein reported, could be involved in type I INF regulation and viral mRNA translation enhancement, and as a result virus replication and virulence increasement [57,58,213,267,268]. Hence, it could be

hypothesized that the plasticity of the NS1 could facilitate the rapid adaptability of the virus under immune pressure. However, in viral samples analyzed in study III, 2 out of 7 substitutions found in NS1 were reported from vaccinated animals.

In the NP, different patterns have been found between subtypes H1N1 and H3N2. On one hand, in the study I synonymous and nonsynonymous SNVs were detected in H1N1 subtype, in both allele frequencies analyzed, 1 and 5 %. Interestingly, in study II only one nonsynonymous substitution with an allele frequency lower than 5 % was detected in H3N2 subtype. Hence, from these results could be inferred that NP plasticity is greater in H1N1 subtype, while H3N2 NP seems less susceptible to nonsynonymous mutations, being more conserved. These results are very consistent, as this pattern was again observed in SNVs reported from study III. Therefore, as mentioned in the discussion from study II, the results from this thesis suggest the conserved state of NP H3N2 protein indicating that this protein is a good target for the design of novel antivirals and vaccines [275,326]. However, in H1N1 SNVs were detected despite protein preservation. Many studies comparing NP sequences underlined that NP is a highly conserved protein between subtypes, being a good candidate for the development of a universal IAV vaccine[327].

The nonsynonymous substitutions found in the surface glycoproteins, HA and NA, could have an impact on the change of the antigenicity of the protein and could have arisen in response to immune pressure in vaccinated animals. In the HA, substitutions such as D200N, E111K, N275S, and S278P were reported in viral samples from vaccinated animals, and they are allocated in or nearby previously described antigenic protein regions of the HA of the H1N1 subtype (study I and III)[208,307,309]. In H3N2 (study II), only substitution V239I was found in a previously reported epitope region [276]. Notably, no relevant substitutions were found in HA protein in H3N2 subtype in study III. Interestingly, in all studies, relevant substitutions were found in the stalk domain of the protein in samples from vaccinated animals. Although this region is characterized by slow evolution and independent of immune pressure[279], according to our results this domain evolution could also be under positive selection because of vaccination. In study I, two substitutions in the transmembrane region of the stalk domain (I513V and V521M) could be involved in the antigenicity of the molecule. As previously reported, changes in this region variates the exposure of HA in the virion, therefore it could play an important role in changing the antigenicity of the protein[226]. Although substitutions T467I, and N505S in H3N2 (study II), and V408A, V466I, and K67R in H1N1 (study III), were not found in the transmembrane domain, they may be causing

the same effect due to their proximity. Consequently, further studies that could improve the understanding of these substitutions role on the antigenicity of the molecule would be highly desirable.

Few SNVs were found in NA protein in comparison with other viral proteins such as HA. Thus, NA seems to evolve slower than HA, as previously reported [328–330]. However, substitutions were found in NA in all studies. The highest number of nonsynonymous SNVs on NA was reported in the H3N2 subtype in study II, in which a total of 6 nonsynonymous substitutions with an allele frequency greater than 5 % were reported. Specifically, two substitutions, V303I and N329S were allocated on the previously described epitope regions E'302-308 and F'329-339 of N2 protein[281]. Furthermore, in study III, V394I and S333G substitutions were reported in the head domain of the NA in H1N1 and H3N2 subtypes respectively. V394I is allocated on the protein surface nearby the previously described epitope region [312,313] with a very high allelic frequency (73.74%). On the other hand, S333G is in epitope region F'329–339 [281]. Hence, all these substitutions reported in NA could be involved in its antigenic drift.

Taken together, the results of the present thesis provide insight into the evolutionary dynamics of H1N1 and H3N2 subtypes in different scenarios of pig vaccination, nonvaccination, and natural infection. In all the cases studied, the genetic diversification of the virus genome occurs, suggesting that natural selection is playing the main role in shaping viral evolution in vaccinated animals. Furthermore, interesting nonsynonymous variants that could be playing an important role in the antigenicity of the virus, its replicative capacity, and virulence were pointed out. Notably, in vaccinated animals, these substitutions were allocated in the effector domain of the NS1 protein, in the head domain of the NA, and in both the head and the stalk domains of the HA. Nevertheless, the implication of the nonsynonymous substitutions herein found in the virus fitness must be further analyzed. In addition, in study III the dynamics of reassortment events under vaccination were assessed, finding out a lower probability of genomic reassortment in vaccinated animals. This agrees with the conclusions obtained in the recent work of Li et al [292].

Finally, all these results highlight the wide evolution and plasticity capacity of IAVs, assuming an evolutionary success due to the quick adaptation of viruses to different environments. All this triggers a continuous IAVs circulation through ecosystems and evolution, posing a threat to global health. Hence, the improvement of biosecurity conditions on farms, sustainable meat consumption to reduce livestock population, the increase in genetic and surveillance studies, further expand the use of current vaccines against IAV and the development of

universal vaccines are necessary measures to minimize virus circulation and therefore reduce it endemic and pandemic risk.

# Chapter 7
# Conclusions

1. Vaccination against swine influenza affects the evolution pattern of H1N1 and H3N2 viruses where positive selection may act in vaccinated animals.

2. *De novo* substitutions in NS1 from H1N1 subtype were only detected in samples collected from vaccinated animals. Substitutions E65G and E67N, located in the linker region, may be changing the plasticity of the molecule being able to join to different host substrates. Substitutions found in the effector domain, G161E, E179A, and E81S could affect both, mRNA viral translation, replication, and pathogenesis (Study I).

3. The variation capacity of the NP from H3N2 subtype, in both vaccinated and nonvaccinated animals, is lesser than that of H1N1 subtype.

4. In the head domain of the hemagglutinin protein, substitutions D200N, E111K, N275S, and S278P found in vaccinated animals may be involved in the antigenic drift of the H1N1 subtype (Study I and III). On the other hand, substitution V239I found in a previously infected animal with A(H1N1)pdm09 could also have a similar evasion effect (Study II).

5. In the stalk domain of the hemagglutinin, relevant nonsynonymous substitutions were only detected in viral samples collected from vaccinated animals. Therefore, changes in this region could also be contributing to molecule antigenicity, particularly I513V and V521M allocated in the transmembrane region.

6. In neuraminidase from H3N2, substitutions V303I, N329S, and S333G, found in viral samples collected from previously immunized animals, were allocated in previously described epitope regions. Regarding H1N1 subtype, substitution V394I was observed on the surface of the NA. Hence, all these substitutions could be involved in the antigenic drift of the protein.

7. In vaccinated animals, the possibility of genomic reassortments between H1N1 and H3N2 subtypes is reduced although genetic diversification increases, particularly in H1N1.

# References

1. Types of Influenza Viruses | CDC Available online: https://www.cdc.gov/flu/about/viruses/types.htm (accessed on 7 October 2022).

2. Long, J.S.; Mistry, B.; Haslam, S.M.; Barclay, W.S. Host and Viral Determinants of Influenza A Virus Species Specificity. *Nat Rev Microbiol* 2019, *17*, 67–81.

3. Zaraket, H.; Hurt, A.C.; Clinch, B.; Barr, I.; Lee, N. Burden of Influenza B Virus Infection and Considerations for Clinical Management. *Antiviral Res* **2021**, *185*, 104970, doi:10.1016/J.ANTIVIRAL.2020.104970.

4. Koutsakos, M.; Nguyen, T.H.; Barclay, W.S.; Kedzierska, K. Knowns and Unknowns of Influenza B Viruses. *http://dx.doi.org/10.2217/fmb.15.120* **2015**, *11*, 119–135, doi:10.2217/FMB.15.120.

5. Bodewes, R.; Morick, D.; de Mutsert, G.; Osinga, N.; Bestebroer, T.; van der Vliet, S.; Smits, S.L.; Kuiken, T.; Rimmelzwaan, G.F.; Fouchier, R.A.M.; et al. Recurring Influenza B Virus Infections in Seals. *Emerg Infect Dis* **2013**, *19*, 511, doi:10.3201/EID1903.120965.

6. Lee, H.S.; Lim, S.; Noh, J.Y.; Song, J.Y.; Cheong, H.J.; Lee, J.H.; Woo, S. il; Kim, W.J. Identification of Influenza C Virus in Young South Korean Children, from October 2013 to September 2016. *Journal of Clinical Virology* **2019**, *115*, 47, doi:10.1016/J.JCV.2019.03.016.

7. Sederdahl, B.K.; Williams, J. v. Epidemiology and Clinical Characteristics of Influenza C Virus. *Viruses* **2020**, *12*, doi:10.3390/V12010089.

8. Manuguerra, J.C.; Hannoun, C. Natural Infection of Dogs by Influenza C Virus. *Res Virol* **1992**, *143*, 199–204, doi:10.1016/S0923-2516(06)80104-4.

9. Zhang, H.; Porter, E.; Lohman, M.; Lu, N.; Peddireddi, L.; Hanzlicek, G.; Marthaler, D.; Liu, X.; Bai, J. Influenza C Virus in Cattle with Respiratory Disease, United States, 2016-2018. *Emerg Infect Dis* **2018**, *24*, 1926–1929, doi:10.3201/EID2410.180589.

10. Yuanji, G.; Fengen, J.; Ping, W. Isolation of Influenza C Virus from Pigs and Experimental Infection of Pigs with Influenza C Virus. *J Gen Virol* **1983**, *64 (Pt 1)*, 177–182, doi:10.1099/0022-1317-64-1-177.

11. Kimura, H.; Abiko, C.; Peng, G.; Muraki, Y.; Sugawara, K.; Hongo, S.; Kitame, F.; Mizuta, K.; Numazaki, Y.; Suzuki, H.; et al. Interspecies Transmission of Influenza C Virus between Humans and Pigs. *Virus Res* **1997**, *48*, 71–79, doi:10.1016/S0168-1702(96)01427-X.

12. Liu, R.; Sheng, Z.; Huang, C.; Wang, D.; Li, F. Influenza D Virus. *Curr Opin Virol* **2020**, *44*, 154–161, doi:10.1016/J.COVIRO.2020.08.004.

13. Hause, B.M.; Collin, E.A.; Liu, R.; Huang, B.; Sheng, Z.; Lu, W.; Wang, D.; Nelson, E.A.; Li, F. Characterization of a Novel Influenza Virus in Cattle and Swine: Proposal for a New Genus in the Orthomyxoviridae Family. *mBio* **2014**, *5*, doi:10.1128/MBIO.00031-14/SUPPL_FILE/MBO001141760ST2.DOC.

14. Hause, B.M.; Ducatez, M.; Collin, E.A.; Ran, Z.; Liu, R.; Sheng, Z.; Armien, A.; Kaplan, B.; Chakravarty, S.; Hoppe, A.D.; et al. Isolation of a Novel Swine Influenza Virus from Oklahoma in 2011 Which Is Distantly Related to Human Influenza C Viruses. *PLoS Pathog* **2013**, *9*, e1003176, doi:10.1371/JOURNAL.PPAT.1003176.

15. Zhou, B.; Donnelly, M.E.; Scholes, D.T.; st. George, K.; Hatta, M.; Kawaoka, Y.; Wentworth, D.E. Single-Reaction Genomic Amplification Accelerates Sequencing and Vaccine Production for Classical and Swine Origin Human Influenza A Viruses. *J Virol* **2009**, *83*, 10309–10313, doi:10.1128/jvi.01109-09.

16. Palese, P. The Genes of Influenza Virus. *Cell* **1977**, *10*, 1–10, doi:10.1016/0092-8674(77)90133-7.

17. Lamb, R.A.; Lai, C.J.; Choppin, P.W. Sequences of MRNAs Derived from Genome RNA Segment 7 of Influenza Virus: Colinear and Interrupted MRNAs Code for Overlapping Proteins. *Proc Natl Acad Sci U S A* **1981**, *78*, 4170–4174, doi:10.1073/pnas.78.7.4170.

18. Lamb, R.A.; Choppin, P.W.; Chanock, R.M.; Lai, C.J. Mapping of the Two Overlapping Genes for Polypeptides NS1 and NS2 on RNA Segment 8 of Influenza Virus Genome. *Proc Natl Acad Sci U S A* **1980**, *77*, 1857–1861, doi:10.1073/pnas.77.4.1857.

19. Hao, W.; Wang, L.; Li, S. Roles of the Non-Structural Proteins of Influenza A Virus. *Pathogens* **2020**, *9*, 1–19, doi:10.3390/PATHOGENS9100812.

20. Wise, H.M.; Foeglein, A.; Sun, J.; Dalton, R.M.; Patel, S.; Howard, W.; Anderson, E.C.; Barclay, W.S.; Digard, P. A Complicated Message: Identification of a Novel PB1-Related Protein Translated from Influenza A Virus Segment 2 MRNA. *J Virol* **2009**, *83*, 8021, doi:10.1128/JVI.00826-09.

21. Chen, W.; Calvo, P.A.; Malide, D.; Gibbs, J.; Schubert, U.; Bacik, I.; Basta, S.; O'Neill, R.; Schickli, J.; Palese, P.; et al. A Novel Influenza A Virus Mitochondrial Protein That Induces Cell Death. *Nat Med* **2001**, *7*, 1306–1312, doi:10.1038/NM1201-1306.

22. Jagger, B.W.; Wise, H.M.; Kash, J.C.; Walters, K.A.; Wills, N.M.; Xiao, Y.L.; Dunfee, R.L.; Schwartzman, L.M.; Ozinsky, A.; Bell, G.L.; et al. An Overlapping Protein-Coding Region in Influenza A Virus Segment 3 Modulates the Host Response. *Science* **2012**, *337*, 199–204, doi:10.1126/SCIENCE.1222213.

23. Muramoto, Y.; Noda, T.; Kawakami, E.; Akkina, R.; Kawaoka, Y. Identification of Novel Influenza A Virus Proteins Translated from PA MRNA. *J Virol* **2013**, *87*, 2455–2462, doi:10.1128/JVI.02656-12/ASSET/2B2A6BB4-7B61-4A81-9014-1671D0F9ED1D/ASSETS/GRAPHIC/ZJV9990972740006.JPEG.

24. Selman, M.; Dankar, S.K.; Forbes, N.E.; Jia, J.J.; Brown, E.G. Adaptive Mutation in Influenza A Virus Non-Structural Gene Is Linked to Host Switching and Induces a Novel Protein by Alternative Splicing. *Emerg Microbes Infect* **2012**, *1*, e42, doi:10.1038/EMI.2012.38.

25. Wise, H.M.; Hutchinson, E.C.; Jagger, B.W.; Stuart, A.D.; Kang, Z.H.; Robb, N.; Schwartzman, L.M.; Kash, J.C.; Fodor, E.; Firth, A.E.; et al. Identification of a Novel Splice Variant Form of the Influenza A Virus M2 Ion Channel with an Antigenically Distinct Ectodomain. *PLoS Pathog* **2012**, *8*, doi:10.1371/JOURNAL.PPAT.1002998.

26. Noda, T. Native Morphology of Influenza Virions. *Front Microbiol* **2012**, *2*, 269, doi:10.3389/FMICB.2011.00269/BIBTEX.

27. Roberts, P.C.; Compans, R.W. Host Cell Dependence of Viral Morphology. *Proceedings of the National Academy of Sciences* **1998**, *95*, 5746–5751, doi:10.1073/PNAS.95.10.5746.

28. Sugita, Y.; Noda, T.; Sagara, H.; Kawaoka, Y. Ultracentrifugation Deforms Unfixed Influenza A Virions. *J Gen Virol* **2011**, *92*, 2485, doi:10.1099/VIR.0.036715-0.

29. Elleman, C.J.; Barclay, W.S. The M1 Matrix Protein Controls the Filamentous Phenotype of Influenza A Virus. *Virology* **2004**, *321*, 144–153, doi:10.1016/J.VIROL.2003.12.009.

30. Smirnov, Y.A.; Kuznetsova, M.A.; Kaverin, N. v. The Genetic Aspects of Influenza Virus Filamentous Particle Formation. *Archives of Virology 1991 118:3* **1991**, *118*, 279–284, doi:10.1007/BF01314038.

31. ADA, G.L.; PERRY, B.T.; ABBOT, A. Biological and Physical Properties of the Ryan Strain of Filamentous Influenza Virus. *J Gen Microbiol* **1958**, *19*, 23–39, doi:10.1099/00221287-19-1-23/CITE/REFWORKS.

32. Smirnov, Y.A.; Kuznetsova, M.A.; Kaverin, N. v. The Genetic Aspects of Influenza Virus Filamentous Particle Formation. *Archives of Virology 1991 118:3* **1991**, *118*, 279–284, doi:10.1007/BF01314038.

33. Russell, C.J. Hemagglutinin Stability and Its Impact on Influenza A Virus Infectivity, Pathogenicity, and Transmissibility in Avians, Mice, Swine, Seals, Ferrets, and Humans. *Viruses* **2021**, *13*, 746, doi:10.3390/v13050746.

34. McAuley, J.L.; Gilbertson, B.P.; Trifkovic, S.; Brown, L.E.; McKimm-Breschkin, J.L. Influenza Virus Neuraminidase Structure and Functions. *Front Microbiol* **2019**, *0*, 39, doi:10.3389/FMICB.2019.00039.

35. Pielak, R.M.; Chou, J.J. Influenza M2 Proton Channels. *Biochim Biophys Acta* **2011**, *1808*, 522, doi:10.1016/J.BBAMEM.2010.04.015.

36. Lamb, R.A.; Zebedee, S.L.; Richardson, C.D. Influenza Virus M2 Protein Is an Integral Membrane Protein Expressed on the Infected-Cell Surface. *Cell* **1985**, *40*, 627–633, doi:10.1016/0092-8674(85)90211-9.

37. Maciej Serda; Becker, F.G.; Cleary, M.; Team, R.M.; Holtermann, H.; The, D.; Agenda, N.; Science, P.; Sk, S.K.; Hinnebusch, R.; et al. Orthomyxoviridae: The Viruses and Their Replication. *Uniwersytet śląski* **1996**, *7*, 343–354, doi:10.2/JQUERY.MIN.JS.

38. Zebedee, S.L.; Lamb, R.A. Influenza A Virus M2 Protein: Monoclonal Antibody Restriction of Virus Growth and Detection of M2 in Virions. *J Virol* **1988**, *62*, 2762–2772, doi:10.1128/JVI.62.8.2762-2772.1988.

39. Noda, T.; Kawaoka, Y. Structure of Influenza Virus Ribonucleoprotein Complexes and Their Packaging into Virions. *Rev Med Virol* **2010**, *20*, 380, doi:10.1002/RMV.666.

40. Obayashi, E.; Yoshida, H.; Kawai, F.; Shibayama, N.; Kawaguchi, A.; Nagata, K.; Tame, J.R.H.; Park, S.Y. The Structural Basis for an Essential Subunit Interaction in Influenza Virus RNA Polymerase. *Nature 2008 454:7208* **2008**, *454*, 1127–1131, doi:10.1038/nature07225.

41. He, X.; Zhou, J.; Bartlam, M.; Zhang, R.; Ma, J.; Lou, Z.; Li, X.; Li, J.; Joachimiak, A.; Zeng, Z.; et al. Crystal Structure of the Polymerase PAC–PB1N Complex from an Avian Influenza H5N1 Virus. *Nature 2008 454:7208* **2008**, *454*, 1123–1126, doi:10.1038/nature07120.

42. Ruigrok, R.W.H.; Baudin, F. Structure of Influenza Virus Ribonucleoprotein Particles. II. Purified RNA-Free Influenza Virus Ribonucleoprotein Forms Structures That Are Indistinguishable from the Intact Influenza Virus Ribonucleoprotein Particles. *Journal of General Virology* **1995**, *76*, 1009–1014, doi:10.1099/0022-1317-76-4-1009/CITE/REFWORKS.

43. Compans, R.W.; Content, J.; Duesberg, P.H. Structure of the Ribonucleoprotein of Influenza Virus. *J Virol* **1972**, *10*, 795–800, doi:10.1128/JVI.10.4.795-800.1972.

44. Baudin, F.; Bach, C.; Cusack, S.; Ruigrok, R.W.H. Structure of Influenza Virus RNP. I. Influenza Virus Nucleoprotein Melts Secondary Structure in Panhandle RNA and Exposes the Bases to the Solvent. *EMBO J* **1994**, *13*, 3158–3165, doi:10.1002/J.1460-2075.1994.TB06614.X.

45. Klumpp, K.; Ruigrok, R.W.H.; Baudin, F. Roles of the Influenza Virus Polymerase and Nucleoprotein in Forming a Functional RNP Structure. *EMBO J* **1997**, *16*, 1248–1257, doi:10.1093/EMBOJ/16.6.1248.

46. Krammer, F.; Smith, G.J.D.; Fouchier, R.A.M.; Peiris, M.; Kedzierska, K.; Doherty, P.C.; Palese, P.; Shaw, M.L.; Treanor, J.; Webster, R.G.; et al. Influenza. *Nat Rev Dis Primers* 2018, *4*, 1–21.

47. Chauhan, R.P.; Gordon, M.L. An Overview of Influenza A Virus Genes, Protein Functions, and Replication Cycle Highlighting Important Updates. *Virus Genes* **2022**, *58*, 255–269, doi:10.1007/s11262-022-01904-w.

48. Rust, M.J.; Lakadamyali, M.; Zhang, F.; Zhuang, X. Assembly of Endocytic Machinery around Individual Influenza Viruses during Viral Entry. *Nat Struct Mol Biol* **2004**, *11*, 567–573, doi:10.1038/NSMB769.

49. de Vries, E.; Tscherne, D.M.; Wienholts, M.J.; Cobos-Jiménez, V.; Scholte, F.; García-Sastre, A.; Rottier, P.J.M.; de Haan, C.A.M. Dissection of the Influenza A Virus Endocytic Routes Reveals Macropinocytosis as an Alternative Entry Pathway. *PLoS Pathog* **2011**, *7*, doi:10.1371/JOURNAL.PPAT.1001329.

50. Banerjee, I.; Yamauchi, Y.; Helenius, A.; Horvath, P. High-Content Analysis of Sequential Events during the Early Phase of Influenza A Virus Infection. *PLoS One* **2013**, *8*, doi:10.1371/JOURNAL.PONE.0068450.

51. Stewart, M. Molecular Mechanism of the Nuclear Protein Import Cycle. *Nature Reviews Molecular Cell Biology 2007 8:3* **2007**, *8*, 195–208, doi:10.1038/NRM2114.

52. Martín-Benito, J.; Ortín, J. Influenza Virus Transcription and Replication. *Adv Virus Res* **2013**, *87*, 113–137, doi:10.1016/B978-0-12-407698-3.00004-1.

53. Eisfeld, A.J.; Neumann, G.; Kawaoka, Y. At the Centre: Influenza A Virus Ribonucleoproteins. *Nat Rev Microbiol* **2015**, *13*, 28, doi:10.1038/NRMICRO3367.

54. Dou, D.; Revol, R.; Östbye, H.; Wang, H.; Daniels, R. Influenza A Virus Cell Entry, Replication, Virion Assembly and Movement. *Front Immunol* **2018**, *9*, 1581, doi:10.3389/FIMMU.2018.01581/BIBTEX.

55. Chen, B.J.; Leser, G.P.; Jackson, D.; Lamb, R.A. The Influenza Virus M2 Protein Cytoplasmic Tail Interacts with the M1 Protein and Influences Virus Assembly at the Site of Virus Budding. *J Virol* **2008**, *82*, 10059–10070, doi:10.1128/JVI.01184-08.

56. Lai, J.C.C.; Chan, W.W.L.; Kien, F.; Nicholls, J.M.; Peiris, J.S.M.; Garcia, J.M. Formation of Virus-like Particles from Human Cell Lines Exclusively Expressing Influenza Neuraminidase. *Journal of General Virology* **2010**, *91*, 2322–2330, doi:10.1099/VIR.0.019935-0/CITE/REFWORKS.

57. Aragón, T.; de la Luna, S.; Novoa, I.; Carrasco, L.; Ortín, J.; Nieto, A. Eukaryotic Translation Initiation Factor 4GI Is a Cellular Target for NS1 Protein, a Translational Activator of Influenza Virus. *Mol Cell Biol* **2000**, *20*, 6259–6268, doi:10.1128/MCB.20.17.6259-6268.2000.

58. Nemeroff, M.E.; Barabino, S.M.L.; Li, Y.; Keller, W.; Krug, R.M. Influenza Virus NS1 Protein Interacts with the Cellular 30 KDa Subunit of CPSF and Inhibits 3′ End Formation of Cellular Pre-MRNAs. *Mol Cell* **1998**, *1*, 991–1000, doi:10.1016/S1097-2765(00)80099-4.

59. Cho, J.H.; Zhao, B.; Shi, J.; Savage, N.; Shen, Q.; Byrnes, J.; Yang, L.; Hwang, W.; Li, P. Molecular Recognition of a Host Protein by NS1 of Pandemic and Seasonal Influenza A Viruses. *Proc Natl Acad Sci U S A* **2020**, *117*, 6550–6558, doi:10.1073/PNAS.1920582117/-/DCSUPPLEMENTAL.

60. Mitra, S.; Kumar, D.; Hu, L.; Sankaran, B.; Moosa, M.M.; Rice, A.P.; Ferreon, J.C.; Ferreon, A.C.M.; Prasad, B.V.V. Influenza A Virus Protein NS1 Exhibits Strain-Independent Conformational Plasticity. *J Virol* **2019**, *93*, 917–936, doi:10.1128/JVI.00917-19.

61. Gibbs, J.S.; Malide, D.; Hornung, F.; Bennink, J.R.; Yewdell, J.W. The Influenza A Virus PB1-F2 Protein Targets the Inner Mitochondrial Membrane via a Predicted Basic Amphipathic Helix That Disrupts Mitochondrial Function. *J Virol* **2003**, *77*, 7214–7224, doi:10.1128/JVI.77.13.7214-7224.2003.

62. Mcauley, J.L.; Chipuk, J.E.; Boyd, K.L.; van de Velde, N.; Green, D.R.; Jonathan, A.M.C. PB1-F2 Proteins from H5N1 and 20th Century Pandemic Influenza Viruses Cause Immunopathology. *PLoS Pathog* **2010**, *6*, e1001014, doi:10.1371/JOURNAL.PPAT.1001014.

63. Hayashi, T.; MacDonald, L.A.; Takimoto, T. Influenza A Virus Protein PA-X Contributes to Viral Growth and Suppression of the Host Antiviral and Immune Responses. *J Virol* **2015**, *89*, 6442–6452, doi:10.1128/JVI.00319-15.

64. Joseph, U.; Su, Y.C.F.; Vijaykrishna, D.; Smith, G.J.D. The Ecology and Adaptive Evolution of Influenza A Interspecies Transmission. *Influenza Other Respir Viruses* **2017**, *11*, 74–84, doi:10.1111/IRV.12412.

65. Tong, S.; Zhu, X.; Li, Y.; Shi, M.; Zhang, J.; Bourgeois, M.; Yang, H.; Chen, X.; Recuenco, S.; Gomez, J.; et al. New World Bats Harbor Diverse Influenza A Viruses. *PLoS Pathog* **2013**, *9*, e1003657, doi:10.1371/JOURNAL.PPAT.1003657.

66. A Revision of the System of Nomenclature for Influenza Viruses: A WHO Memorandum. *Bull World Health Organ* **1980**, *58*, 585.

67. Schuster, P. Quasispecies on Fitness Landscapes. *Curr Top Microbiol Immunol* **2016**, *392*, 61–120, doi:10.1007/82_2015_469.

68. Bull, J.J.; Meyers, L.A.; Lachmann, M. Quasispecies Made Simple. *PLoS Comput Biol* **2005**, *1*, 0450–0460, doi:10.1371/JOURNAL.PCBI.0010061.

69. Lauring, A.S.; Andino, R. Quasispecies Theory and the Behavior of RNA Viruses. *PLoS Pathog* **2010**, *6*, 1–8, doi:10.1371/JOURNAL.PPAT.1001005.

70. Domingo, E.; Perales, C. Viral Quasispecies. *PLoS Genet* **2019**, *15*, doi:10.1371/JOURNAL.PGEN.1008271.

71. Eigen, M. Selforganization of Matter and the Evolution of Biological Macromolecules. *Naturwissenschaften 1971 58:10* **1971**, *58*, 465–523, doi:10.1007/BF00623322.

72. Eigen, M.; Schuster, P. A Principle of Natural Self-Organization. *Naturwissenschaften 1977 64:11* **1977**, *64*, 541–565, doi:10.1007/BF00450633.

73. Domingo, E.; Sheldon, J.; Perales, C. Viral Quasispecies Evolution. *Microbiology and Molecular Biology Reviews* **2012**, *76*, 159–216, doi:10.1128/mmbr.05023-11.

74. Huang, S.W.; Hung, S.J.; Wang, J.R. Application of Deep Sequencing Methods for Inferring Viral Population Diversity. *J Virol Methods* 2019, *266*, 95–102.

75. Ahlquist, P. RNA-Dependent RNA Polymerases, Viruses, and RNA Silencing. *Science* **2002**, *296*, 1270–1273, doi:10.1126/SCIENCE.1069132.

76. FAOSTAT Available online: https://www.fao.org/faostat/en/#data/QCL (accessed on 27 April 2022).

77. Sobel Leonard, A.; McClain, M.T.; Smith, G.J.D.; Wentworth, D.E.; Halpin, R.A.; Lin, X.; Ransier, A.; Stockwell, T.B.; Das, S.R.; Gilbert, A.S.; et al. Deep Sequencing of Influenza A Virus from a Human Challenge Study Reveals a Selective Bottleneck and Only Limited Intrahost Genetic Diversification. *J Virol* **2016**, *90*, 11247–11258, doi:10.1128/jvi.01657-16.

78. Moncla, L.H.; Bedford, T.; Dussart, P.; Horm, S.V.; Rith, S.; Buchy, P.; Karlsson, E.A.; Li, L.; Liu, Y.; Zhu, H.; et al. Quantifying Within-Host Diversity of H5N1 Influenza Viruses in Humans and Poultry in Cambodia. *PLoS Pathog* **2020**, *16*, e1008191, doi:10.1371/journal.ppat.1008191.

79. Shao, W.; Li, X.; Goraya, M.U.; Wang, S.; Chen, J.L. Evolution of Influenza a Virus by Mutation and Re-Assortment. *Int J Mol Sci* 2017, *18*.

80. Nelson, M.I.; Holmes, E.C. The Evolution of Epidemic Influenza. *Nat Rev Genet* **2007**, *8*, 196–205, doi:10.1038/NRG2053.

81. Russell, C.A.; Jones, T.C.; Barr, I.G.; Cox, N.J.; Garten, R.J.; Gregory, V.; Gust, I.D.; Hampson, A.W.; Hay, A.J.; Hurt, A.C.; et al. Influenza Vaccine Strain Selection and Recent Studies on the Global Migration of Seasonal Influenza Viruses. *Vaccine* **2008**, *26 Suppl 4*, doi:10.1016/J.VACCINE.2008.07.078.

82. Scholtissek, C.; Rohde, W.; von Hoyningen, V.; Rott, R. On the Origin of the Human Influenza Virus Subtypes H2N2 and H3N2. *Virology* **1978**, *87*, 13–20, doi:10.1016/0042-6822(78)90153-8.

83. Kawaoka, Y.; Krauss, S.; Webster, R.G. Avian-to-Human Transmission of the PB1 Gene of Influenza A Viruses in the 1957 and 1968 Pandemics. *J Virol* **1989**, *63*, 4608, doi:10.1128/JVI.63.11.4603-4608.1989.

84. Belshe, R.B. The Origins of Pandemic Influenza — Lessons from the 1918 Virus. *https://doi.org/10.1056/NEJMp058281* **2005**, *353*, 2209–2211, doi:10.1056/NEJMP058281.

85. Smith, G.J.D.; Vijaykrishna, D.; Bahl, J.; Lycett, S.J.; Worobey, M.; Pybus, O.G.; Ma, S.K.; Cheung, C.L.; Raghwani, J.; Bhatt, S.; et al. Origins and Evolutionary Genomics of the 2009 Swine-Origin H1N1 Influenza a Epidemic. *Nature* **2009**, *459*, 1122–1125, doi:10.1038/nature08182.

86. Chare, E.R.; Gould, E.A.; Holmes, E.C. Phylogenetic Analysis Reveals a Low Rate of Homologous Recombination in Negative-Sense RNA Viruses. *J Gen Virol* **2003**, *84*, 2691–2703, doi:10.1099/VIR.0.19277-0.

87. He, C.Q.; Han, G.Z.; Wang, D.; Liu, W.; Li, G.R.; Liu, X.P.; Ding, N.Z. Homologous Recombination Evidence in Human and Swine Influenza A Viruses. *Virology* **2008**, *380*, 12–20, doi:10.1016/J.VIROL.2008.07.014.

88. Lu, I.N.; Muller, C.P.; He, F.Q. Applying Next-Generation Sequencing to Unravel the Mutational Landscape in Viral Quasispecies. *Virus Res* **2020**, *283*, doi:10.1016/J.VIRUSRES.2020.197963.

89. Knyazev, S.; Hughes, L.; Skums, P.; Zelikovsky, A. Epidemiological Data Analysis of Viral Quasispecies in the Next-Generation Sequencing Era. *Brief Bioinform* **2021**, *22*, 96–108, doi:10.1093/BIB/BBAA101.

90. Cacciabue, M.; Currá, A.; Carrillo, E.; König, G.; Gismondi, M.I. A Beginner's Guide for FMDV Quasispecies Analysis: Sub-Consensus Variant Detection and Haplotype Reconstruction Using next-Generation Sequencing. *Brief Bioinform* **2020**, *21*, 1766–1775, doi:10.1093/bib/bbz086.

91. Borges, V.; Pinheiro, M.; Pechirra, P.; Guiomar, R.; Gomes, J.P. INSaFLU: An Automated Open Web-Based Bioinformatics Suite "from-Reads" for Influenza Whole-Genome-Sequencing-Based Surveillance. *Genome Med* **2018**, *10*, doi:10.1186/S13073-018-0555-0.

92. Webster, R.G.; Bean, W.J.; Gorman, O.T.; Chambers, T.M.; Kawaoka, Y. Evolution and Ecology of Influenza A Viruses. *Microbiol Rev* **1992**, *56*, 152–179, doi:10.1128/MR.56.1.152-179.1992.

93. Naguib, M.M.; Verhagen, J.H.; Samy, A.; Eriksson, P.; Fife, M.; Lundkvist, Å.; Ellström, P.; Järhult, J.D. Avian Influenza Viruses at the Wild-Domestic Bird Interface in Egypt. *Infect Ecol Epidemiol* **2019**, *9*, doi:10.1080/20008686.2019.1575687.

94. Ramey, A.M.; Reeves, A.B. Ecology of Influenza A Viruses in Wild Birds and Wetlands of Alaska. *https://doi.org/10.1637/0005-2086-64.2.109* **2020**, *64*, 109–122, doi:10.1637/0005-2086-64.2.109.

95. Webster, R.G.; Yakhno, M.; Hinshaw, V.S.; Bean, W.J.; Copal Murti, K. Intestinal Influenza: Replication and Characterization of Influenza Viruses in Ducks. *Virology* **1978**, *84*, 268–278, doi:10.1016/0042-6822(78)90247-7.

96. Hall, J.S.; Dusek, R.J.; Nashold, S.W.; TeSlaa, J.L.; Allen, R.B.; Grear, D.A. Avian Influenza Virus Prevalence in Marine Birds Is Dependent on Ocean Temperatures. *Ecological Applications* **2020**, *30*, doi:10.1002/EAP.2040.

97. Chatziprodromidou, I.P.; Arvanitidou, M.; Guitian, J.; Apostolou, T.; Vantarakis, G.; Vantarakis, A. Global Avian Influenza Outbreaks 2010-2016: A Systematic Review of Their Distribution, Avian Species and Virus Subtype. *Syst Rev* **2018**, *7*, 1–12, doi:10.1186/S13643-018-0691-Z/FIGURES/6.

98. Short, K.R.; Richard, M.; Verhagen, J.H.; van Riel, D.; Schrauwen, E.J.A.; van den Brand, J.M.A.; Mänz, B.; Bodewes, R.; Herfst, S. One Health, Multiple Challenges: The Inter-Species Transmission of Influenza A Virus. *One Health* **2015**, *1*, 1, doi:10.1016/J.ONEHLT.2015.03.001.

99. Verhagen, J.H.; Fouchier, R.A.M.; Lewis, N. Highly Pathogenic Avian Influenza Viruses at the Wild-Domestic Bird Interface in Europe: Future Directions for Research and Surveillance. *Viruses* **2021**, *13*, doi:10.3390/V13020212.

100. Frymus, T.; Belák, S.; Egberink, H.; Hofmann-Lehmann, R.; Marsilio, F.; Addie, D.D.; Boucraut-Baralon, C.; Hartmann, K.; Lloret, A.; Lutz, H.; et al. Influenza Virus Infections in Cats. *Viruses* **2021**, *13*, 1435, doi:10.3390/V13081435.

101. Harder, T.C.; Siebert, U.; Wohlsein, P.; Vahlenkamp, T. Influenza A Virus Infections in Marine Mammals and Terrestrial Carnivores. *Berl Munch Tierarztl Wochenschr* **2013**, *126*, 500–508.

102. Russell, C.J. Hemagglutinin Stability and Its Impact on Influenza A Virus Infectivity, Pathogenicity, and Transmissibility in Avians, Mice, Swine, Seals, Ferrets, and Humans. *Viruses* **2021**, *13*, doi:10.3390/V13050746.

103. Parrish, C.R.; Murcia, P.R.; Holmes, E.C. Influenza Virus Reservoirs and Intermediate Hosts: Dogs, Horses, and New Possibilities for Influenza Virus Exposure of Humans. *J Virol* **2015**, *89*, 2990–2994, doi:10.1128/JVI.03146-14.

104. Chambers, T.M. Equine Influenza. *Cold Spring Harb Perspect Med* **2022**, *12*, doi:10.1101/CSHPERSPECT.A038331.

105. Peteranderl, C.; Herold, S.; Schmoldt, C. Respiratory Viral Infections: Human Influenza Virus Infections. *Semin Respir Crit Care Med* **2016**, *37*, 487, doi:10.1055/S-0036-1584801.

106. Ma, W. *Swine Influenza Virus: Current Status and Challenge*; Elsevier B.V., 2020; Vol. 288, p. 198118;.

107. Taubenberger, J.K.; Reid, A.H.; Krafft, A.E.; Bijwaard, K.E.; Fanning, T.G. Initial Genetic Characterization of the 1918 "Spanish" Influenza Virus. *Science* **1997**, *275*, 1793–1796, doi:10.1126/SCIENCE.275.5307.1793.

108. Johnson, N.P.A.S.; Mueller, J. Updating the Accounts: Global Mortality of the 1918-1920 "Spanish" Influenza Pandemic. *Bull Hist Med* **2002**, *76*, 105–115, doi:10.1353/BHM.2002.0022.

109. 1918 Pandemic (H1N1 Virus) | Pandemic Influenza (Flu) | CDC Available online: https://www.cdc.gov/flu/pandemic-resources/1918-pandemic-h1n1.html (accessed on 18 October 2022).

110. Honigsbaum, M. Revisiting the 1957 and 1968 Influenza Pandemics. *Lancet* **2020**, *395*, 1824, doi:10.1016/S0140-6736(20)31201-0.

111. Rozo, M.; Gronvall, G.K. The Reemergent 1977 H1N1 Strain and the Gain-of-Function Debate. *mBio* **2015**, *6*, doi:10.1128/MBIO.01013-15.

112. Ito, T.; Couceiro, J.N.S.S.; Kelm, S.; Baum, L.G.; Krauss, S.; Castrucci, M.R.; Donatelli, I.; Kida, H.; Paulson, J.C.; Webster, R.G.; et al. Molecular Basis for the Generation in Pigs of Influenza A Viruses with Pandemic Potential. *J Virol* **1998**, *72*, 7367–7373, doi:10.1128/JVI.72.9.7367-7373.1998.

113. Ma, W.; Kahn, R.E.; Richt, J.A. The Pig as a Mixing Vessel for Influenza Viruses: Human and Veterinary Implications. *J Mol Genet Med* **2009**, *3*, 158, doi:10.4172/1747-0862.1000028.

114. Brown, I.H. The Epidemiology and Evolution of Influenza Viruses in Pigs. *Vet Microbiol* **2000**, *74*, 29–46, doi:10.1016/S0378-1135(00)00164-4.

115. Ma, W.; Kahn, R.E.; Richt, J.A. The Pig as a Mixing Vessel for Influenza Viruses: Human and Veterinary Implications. *J Mol Genet Med* **2009**, *3*, 166, doi:10.4172/1747-0862.1000028.

116. Scholtissek, C. Pigs as 'Mixing Vessels' for the Creation of New Pandemic Influenza A Viruses. *Medical Principles and Practice* **1990**, *2*, 65–71, doi:10.1159/000157337.

117. Medina, R.A. 1918 Influenza Virus: 100 Years on, Are We Prepared against the next Influenza Pandemic? *Nature Reviews Microbiology 2018 16:2* **2018**, *16*, 61–62, doi:10.1038/nrmicro.2017.174.

118. Swine Influenza - WOAH - World Organisation for Animal Health Available online: https://www.woah.org/en/disease/swine-influenza/ (accessed on 4 August 2022).

119. Hennig, C.; Graaf, A.; Petric, P.P.; Graf, L.; Schwemmle, M.; Beer, M.; Harder, T. Are Pigs Overestimated as a Source of Zoonotic Influenza Viruses? *Porcine Health Manag* **2022**, *8*, doi:10.1186/S40813-022-00274-X.

120. Top, F.H.; Russell, P.K. Swine Influenza A at Fort Dix, New Jersey (January-February 1976). IV. Summary and Speculation. *J Infect Dis* **1977**, *136 Suppl*, S376–S380, doi:10.1093/INFDIS/136.SUPPLEMENT_3.S376.

121. Myers, K.P.; Olsen, C.W.; Gray, G.C. Cases of Swine Influenza in Humans: A Review of the Literature. *Clin Infect Dis* **2007**, *44*, 1084–1088, doi:10.1086/512813.

122. Sun, H.; Xiao, Y.; Liu, J.; Wang, D.; Li, F.; Wang, C.; Li, C.; Zhu, J.; Song, J.; Sun, H.; et al. Prevalent Eurasian Avian-like H1N1 Swine Influenza Virus with 2009 Pandemic Viral Genes Facilitating Human Infection. *Proc Natl Acad Sci U S A* **2020**, *117*, 17204–17210, doi:10.1073/pnas.1921186117.

123. Swine Influenza - WOAH - World Organisation for Animal Health Available online: https://www.woah.org/en/disease/swine-influenza/ (accessed on 24 October 2022).

124. Barbé, F.; Atanasova, K.; van Reeth, K. Cytokines and Acute Phase Proteins Associated with Acute Swine Influenza Infection in Pigs. *Vet J* **2011**, *187*, 48–53, doi:10.1016/J.TVJL.2009.12.012.

125. Li, Y.; Robertson, I. The Epidemiology of Swine Influenza. *Animal Diseases 2021 1:1* **2021**, *1*, 1–14, doi:10.1186/S44149-021-00024-6.

126. Er, C.; Lium, B.; Tavornpanich, S.; Hofmo, P.O.; Forberg, H.; Hauge, A.G.; Grøntvedt, C.A.; Framstad, T.; Brun, E. Adverse Effects of Influenza A(H1N1)Pdm09 Virus Infection on Growth Performance of Norwegian Pigs - a Longitudinal Study at a Boar Testing Station. *BMC Vet Res* **2014**, *10*, doi:10.1186/S12917-014-0284-6.

127. Saade, G.; Deblanc, C.; Bougon, J.; Marois-Créhan, C.; Fablet, C.; Auray, G.; Belloc, C.; Leblanc-Maridor, M.; Gagnon, C.A.; Zhu, J.; et al. Coinfections and Their

Molecular Consequences in the Porcine Respiratory Tract. *Vet Res* **2020**, *51*, doi:10.1186/S13567-020-00807-8.

128. White, M. Porcine Respiratory Disease Complex (PRDC). *Livestock* **2011**, *16*, 40, doi:10.1111/J.2044-3870.2010.00025.X.

129. Vincent, A.L.; Lager, K.M.; Janke, B.H.; Gramer, M.R.; Richt, J.A. Failure of Protection and Enhanced Pneumonia with a US H1N2 Swine Influenza Virus in Pigs Vaccinated with an Inactivated Classical Swine H1N1 Vaccine. *Vet Microbiol* **2008**, *126*, 310–323, doi:10.1016/J.VETMIC.2007.07.011.

130. Gauger, P.C.; Vincent, A.L.; Loving, C.L.; Lager, K.M.; Janke, B.H.; Kehrli, M.E.; Roth, J.A. Enhanced Pneumonia and Disease in Pigs Vaccinated with an Inactivated Human-like (δ-Cluster) H1N2 Vaccine and Challenged with Pandemic 2009 H1N1 Influenza Virus. *Vaccine* **2011**, *29*, 2712–2719, doi:10.1016/J.VACCINE.2011.01.082.

131. Kimble, J.B.; Wymore Brand, M.; Kaplan, B.S.; Gauger, P.; Coyle, E.M.; Chilcote, K.; Khurana, S.; Vincent, A.L. Vaccine-Associated Enhanced Respiratory Disease Following Influenza Virus Infection in Ferrets Recapitulates the Model in Pigs. *J Virol* **2022**, *96*, doi:10.1128/JVI.01725-21/ASSET/428F8F3C-3754-4717-AA6E-1ADA592C7ACC/ASSETS/IMAGES/LARGE/JVI.01725-21-F006.JPG.

132. Spackman, E.; Senne, D.A.; Myers, T.J.; Bulaga, L.L.; Garber, L.P.; Perdue, M.L.; Lohman, K.; Daum, L.T.; Suarez, D.L. Development of a Real-Time Reverse Transcriptase PCR Assay for Type A Influenza Virus and the Avian H5 and H7 Hemagglutinin Subtypes. *J Clin Microbiol* **2002**, *40*, 3256–3260, doi:10.1128/JCM.40.9.3256-3260.2002.

133. Zell, R.; Scholtissek, C.; Ludwig, S. Genetics, Evolution, and the Zoonotic Capacity of European Swine Influenza Viruses. **2012**, 29–55, doi:10.1007/82_2012_267.

134. Hinshaw, V.S.; Webster, R.G.; Turner, B. Novel Influenza A Viruses Isolated from Canadian Feral Ducks: Including Strains Antigenically Related to Swine Influenza (Hsw1N1) Viruses. *Journal of General Virology* **1978**, *41*, 115–127, doi:10.1099/0022-1317-41-1-115.

135. Zhu, H.; Webby, R.; Lam, T.T.Y.; Smith, D.K.; Peiris, J.S.M.; Guan, Y. History of Swine Influenza Viruses in Asia. *Curr Top Microbiol Immunol* **2013**, *370*, 57–68, doi:10.1007/82_2011_179.

136. Schrader, C.; Süss, J. Molecular Epidemiology of Porcine H3N2 Influenza A Viruses Isolated in Germany between 1982 and 2001. *Intervirology* **2004**, *47*, 72–77, doi:10.1159/000077829.

137. Brown, I.H.; Harris, P.A.; McCauley, J.W.; Alexander, D.J. Multiple Genetic Reassortment of Avian and Human Influenza A Viruses in European Pigs, Resulting in the Emergence of an H1N2 Virus of Novel Genotype. *J Gen Virol* **1998**, *79 ( Pt 12)*, 2947–2955, doi:10.1099/0022-1317-79-12-2947.

138. Boni, A.; Vaccari, G.; di Trani, L.; Zaccaria, G.; Alborali, G.L.; Lelli, D.; Cordioli, P.; Moreno, A.M. Genetic Characterization and Evolution of H1N1pdm09 after Circulation in a Swine Farm. *Biomed Res Int* **2014**, *2014*, doi:10.1155/2014/598732.

139. Grøntvedt, C.A.; Er, C.; Gjerset, B.; Hauge, A.G.; Brun, E.; Jørgensen, A.; Lium, B.; Framstad, T. Influenza A(H1N1)Pdm09 Virus Infection in Norwegian Swine Herds 2009/10: The Risk of Human to Swine Transmission. *Prev Vet Med* **2013**, *110*, 429–434, doi:10.1016/J.PREVETMED.2013.02.016.

140. Saavedra-Montañez, M.; Vaca, L.; Ramírez-Mendoza, H.; Gaitán-Peredo, C.; Bautista-Martínez, R.; Segura-Velázquez, R.; Cervantes-Torres, J.; Sánchez-Betancourt, J.I. Identification and Genomic Characterization of Influenza Viruses with Different Origin in Mexican Pigs. *Transbound Emerg Dis* **2019**, *66*, 186–194, doi:10.1111/TBED.12998.

141. Danilenko, D.M.; Komissarov, A.B.; Fadeev, A. v.; Bakaev, M.I.; Ivanova, A.A.; Petrova, P.A.; Vassilieva, A.D.; Komissarova, K.S.; Zheltukhina, A.I.; Konovalova, N.I.; et al. Antigenic and Genetic Characterization of Swine Influenza Viruses Identified in the European Region of Russia, 2014-2020. *Front Microbiol* **2021**, *12*, doi:10.3389/FMICB.2021.662028.

142. Tarnagda, Z.; Yougbaré, I.; Ilboudo, A.K.; Kagoné, T.; Sanou, A.M.; Cissé, A.; Médah, I.; Yelbéogo, D.; Nzussouo, N.T. Sentinel Surveillance of Influenza in Burkina Faso: Identification of Circulating Strains during 2010-2012. *Influenza Other Respir Viruses* **2014**, *8*, 524–529, doi:10.1111/IRV.12259.

143. Watson, S.J.; Langat, P.; Reid, S.M.; Lam, T.T.-Y.; Cotten, M.; Kelly, M.; van Reeth, K.; Qiu, Y.; Simon, G.; Bonin, E.; et al. Molecular Epidemiology and Evolution of Influenza Viruses Circulating within European Swine between 2009 and 2013. *J Virol* **2015**, *89*, 9920–9931, doi:10.1128/JVI.00840-15.

144. Anderson, T.K.; Campbell, B.A.; Nelson, M.I.; Lewis, N.S.; Janas-Martindale, A.; Killian, M.L.; Vincent, A.L. Characterization of Co-Circulating Swine Influenza A Viruses in North America and the Identification of a Novel H1 Genetic Clade with Antigenic Significance. *Virus Res* **2015**, *201*, 24–31, doi:10.1016/J.VIRUSRES.2015.02.009.

145. Chepkwony, S.; Parys, A.; Vandoorn, E.; Stadejek, W.; Xie, J.; King, J.; Graaf, A.; Pohlmann, A.; Beer, M.; Harder, T.; et al. Genetic and Antigenic Evolution of H1 Swine Influenza A Viruses Isolated in Belgium and the Netherlands from 2014 through 2019. *Sci Rep* **2021**, *11*, doi:10.1038/S41598-021-90512-Z.

146. Nelson, M.I.; Vincent, A.L.; Kitikoon, P.; Holmes, E.C.; Gramer, M.R. Evolution of Novel Reassortant A/H3N2 Influenza Viruses in North American Swine and Humans, 2009-2011. *J Virol* **2012**, *86*, 8872–8878, doi:10.1128/JVI.00259-12.

147. Song, Y.; Zhang, Y.; Zhang, B.; Chen, L.; Zhang, M.; Wang, J.; Jiang, Y.; Yang, C.; Jiang, T. Identification, Genetic Analysis, and Pathogenicity of Classical Swine H1N1 and Human-Swine Reassortant H1N1 Influenza Viruses from Pigs in China. *Viruses* **2020**, *12*, doi:10.3390/V12010055.

148. Han, J.Y.; Park, S.J.; Kim, H.K.; Rho, S.; van Nguyen, G.; Song, D.; Kang, B.K.; Moon, H.J.; Yeom, M.J.; Park, B.K. Identification of Reassortant Pandemic H1N1 Influenza Virus in Korean Pigs. *J Microbiol Biotechnol* **2012**, *22*, 699–707, doi:10.4014/JMB.1106.05062.

149. Salvesen, H.A.; Whitelaw, C.B.A. Current and Prospective Control Strategies of Influenza A Virus in Swine. *Porcine Health Manag* **2021**, *7*, doi:10.1186/S40813-021-00196-0.

150. Reeth, K. van; Vincent, A.L.; Lager, K.M. Vaccines and Vaccination for Swine Influenza: Differing Situations in Europe and the USA. In *Animal Influenza*; John Wiley & Sons, Inc.: Hoboken, NJ, USA, 2016; pp. 480–501.

151. Ma, W.; Richt, J.A. Swine Influenza Vaccines: Current Status and Future Perspectives. *Anim Health Res Rev* **2010**, *11*, 81–96, doi:10.1017/S146625231000006X.

152. Holzer, B.; Martini, V.; Edmans, M.; Tchilian, E. T and B Cell Immune Responses to Influenza Viruses in Pigs. *Front Immunol* **2019**, *10*, 98, doi:10.3389/FIMMU.2019.00098.

153. Mostafa, A.; Abdelwhab, E.M.; Mettenleiter, T.C.; Pleschka, S. Zoonotic Potential of Influenza A Viruses: A Comprehensive Overview. *Viruses* 2018, *10*.

154. Reeth, K. van; Ma, W. Swine Influenza Virus Vaccines: To Change or Not to Change—That's the Question. *Curr Top Microbiol Immunol* **2012**, *370*, 173–200, doi:10.1007/82_2012_266.

155. Pleguezuelos, O.; James, E.; Fernandez, A.; Lopes, V.; Rosas, L.A.; Cervantes-Medina, A.; Cleath, J.; Edwards, K.; Neitzey, D.; Gu, W.; et al. Efficacy of FLU-v, a Broad-

Spectrum Influenza Vaccine, in a Randomized Phase IIb Human Influenza Challenge Study. *NPJ Vaccines* **2020**, *5*, doi:10.1038/S41541-020-0174-9.

156. Sun, W.; Luo, T.; Liu, W.; Li, J. Progress in the Development of Universal Influenza Vaccines. *Viruses 2020, Vol. 12, Page 1033* **2020**, *12*, 1033, doi:10.3390/V12091033.

157. Swine Influenza: OIE - World Organisation for Animal Health Available online: https://www.oie.int/en/animal-health-in-the-world/animal-diseases/Swine-influenza/ (accessed on 5 March 2021).

158. Das, K.; Aramini, J.M.; Ma, L.-C.; Krug, R.M.; Arnold, E. Structures of Influenza A Proteins and Insights into Antiviral Drug Targets. *Nat Struct Mol Biol* **2010**, *17*, 530–538, doi:10.1038/nsmb.1779.

159. Bouvier, N.M.; Palese, P. The Biology of Influenza Viruses. *Vaccine* **2008**, *26 Suppl 4*, D49-53, doi:10.1016/j.vaccine.2008.07.039.

160. 2009 H1N1 Pandemic (H1N1pdm09 Virus) | Pandemic Influenza (Flu) | CDC Available online: https://www.cdc.gov/flu/pandemic-resources/2009-h1n1-pandemic.html (accessed on 5 March 2021).

161. Garten, R.J.; Davis, C.T.; Russell, C.A.; Shu, B.; Lindstrom, S.; Balish, A.; Sessions, W.M.; Xu, X.; Skepner, E.; Deyde, V.; et al. Antigenic and Genetic Characteristics of Swine-Origin 2009 A(H1N1) Influenza Viruses Circulating in Humans. *Science* **2009**, *325*, 197–201, doi:10.1126/science.1176225.

162. Bergmann, M.; Garcia-Sastret, A.; Palese, P. *Transfection-Mediated Recombination of Influenza A Virus*; 1992; Vol. 66;.

163. CARRAT, F.; FLAHAULT, A. Influenza Vaccine: The Challenge of Antigenic Drift. *Vaccine* **2007**, *25*, 6852–6862, doi:10.1016/j.vaccine.2007.07.027.

164. Nichol, K.L.; Treanor, J.J. Vaccines for Seasonal and Pandemic Influenza. *J Infect Dis* **2006**, *194*, S111–S118, doi:10.1086/507544.

165. Reeth, K. van; Brown, I.H.; Dürrwald, R.; Foni, E.; Labarque, G.; Lenihan, P.; Maldonado, J.; Markowska-Daniel, I.; Pensaert, M.; Pospisil, Z.; et al. Seroprevalence of H1N1, H3N2 and H1N2 Influenza Viruses in Pigs in Seven European Countries in 2002–2003. *Influenza Other Respir Viruses* **2008**, *2*, 99, doi:10.1111/J.1750-2659.2008.00043.X.

166. Simon, G.; Larsen, L.E.; Dürrwald, R.; Foni, E.; Harder, T.; van Reeth, K.; Markowska-Daniel, I.; Reid, S.M.; Dan, A.; Maldonado, J.; et al. European Surveillance Network for Influenza in Pigs: Surveillance Programs, Diagnostic Tools and Swine Influenza Virus Subtypes Identified in 14 European Countries from 2010 to 2013. *PLoS One* **2014**, *9*, e115815, doi:10.1371/journal.pone.0115815.

167. Thacker, E.; Janke, B. Swine Influenza Virus: Zoonotic Potential and Vaccination Strategies for the Control of Avian and Swine Influenzas. *J Infect Dis* **2008**, *197*, S19–S24, doi:10.1086/524988.

168. Reed, LJ.; Muench, H. A Simple Method of Estimating Fifty per Cent Endpoints. *Antioch Review* **1938**, *27*, 493–497, doi:10.7723/antiochreview.72.3.0546.

169. Crisci, E.; Fraile, L.; Valentino, S.; Martínez-Guinó, L.; Bottazzi, B.; Mantovani, A.; Montoya, M. Immune Characterization of Long Pentraxin 3 in Pigs Infected with Influenza Virus. *Vet Microbiol* **2014**, *168*, 185–192, doi:10.1016/J.VETMIC.2013.10.004.

170. Bohorquez, J.A.; Muñoz-González, S.; Pérez-Simó, M.; Revilla, C.; Domínguez, J.; Ganges, L. Identification of an Immunosuppressive Cell Population during Classical Swine Fever Virus Infection and Its Role in Viral Persistence in the Host. *Viruses 2019, Vol. 11, Page 822* **2019**, *11*, 822, doi:10.3390/V11090822.

171. Lopez, E.; Bosch-Camós, L.; Ramirez-Medina, E.; Vuono, E.; Navas, M.J.; Muñoz, M.; Accensi, F.; Zhang, J.; Alonso, U.; Argilaguet, J.; et al. Deletion Mutants of the Attenuated Recombinant ASF Virus, BA71ΔCD2, Show Decreased Vaccine Efficacy. *Viruses 2021, Vol. 13, Page 1678* **2021**, *13*, 1678, doi:10.3390/V13091678.

172. López-Serrano, S.; Cordoba, L.; Pérez-Maillo, M.; Pleguezuelos, P.; Remarque, E.J.; Ebensen, T.; Guzmán, C.A.; Christensen, D.; Segalés, J.; Darji, A. Immune Responses to Pandemic H1N1 Influenza Virus Infection in Pigs Vaccinated with a Conserved Hemagglutinin HA1 Peptide Adjuvanted with CAF®01 or CDA/AGalCerMPEG. *Vaccines (Basel)* **2021**, *9*, 751, doi:10.3390/vaccines9070751.

173. Galindo-Cardiel, I.; Ballester, M.; Solanes, D.; Nofrarías, M.; López-Soria, S.; Argilaguet, J.M.; Lacasta, A.; Accensi, F.; Rodríguez, F.; Segalés, J. Standardization of Pathological Investigations in the Framework of Experimental ASFV Infections. *Virus Res* **2013**, *173*, 180–190, doi:10.1016/j.virusres.2012.12.018.

174. Nielsen, J.; Bøtner, A.; Tingstedt, J.E.; Aasted, B.; Johnsen, C.K.; Riber, U.; Lind, P. In Utero Infection with Porcine Reproductive and Respiratory Syndrome Virus Modulates Leukocyte Subpopulations in Peripheral Blood and Bronchoalveolar Fluid of Surviving Piglets. *Vet Immunol Immunopathol* **2003**, *93*, 135–151, doi:10.1016/S0165-2427(03)00068-0.

175. Sibila, M.; Aragón, V.; Fraile, L.; Segalés, J. Comparison of Four Lung Scoring Systems for the Assessment of the Pathological Outcomes Derived from Actinobacillus Pleuropneumoniae Experimental Infections. *BMC Vet Res* **2014**, *10*, doi:10.1186/1746-6148-10-165.

176. Busquets, N.; Segalés, J.; Córdoba, L.; Mussá, T.; Crisci, E.; Martín-Valls, G.E.; Simon-Grifé, M.; Pérez-Simó, M.; Pérez-Maíllo, M.; Núñez, J.I.; et al. Experimental Infection with H1N1 European Swine Influenza Virus Protects Pigs from an Infection with the 2009 Pandemic H1N1 Human Influenza Virus. *Vet Res* **2010**, *41*, 74, doi:10.1051/vetres/2010046.

177. Sisteré-Oró, M.; López-Serrano, S.; Veljkovic, V.; Pina-Pedrero, S.; Vergara-Alert, J.; Córdoba, L.; Pérez-Maillo, M.; Pleguezuelos, P.; Vidal, E.; Segalés, J.; et al. DNA Vaccine Based on Conserved HA-Peptides Induces Strong Immune Response and Rapidly Clears Influenza Virus Infection from Vaccinated Pigs. *PLoS One* **2019**, *14*, doi:10.1371/journal.pone.0222201.

178. Sabattini, E.; Bisgaard, K.; Ascani, S.; Poggi, S.; Piccioli, M.; Ceccarelli, C.; Pieri, F.; Fraternali-Orcioni, G.; Pileri, S.A. The EnVision(TM)+ System: A New Immunohistochemical Method for Diagnostics and Research. Critical Comparison with the APAAP, ChemMate(TM), CSA, LABC, and SABC Techniques. *J Clin Pathol* **1998**, *51*, 506–511, doi:10.1136/jcp.51.7.506.

179. Detmer, S.E.; Gunvaldsen, R.E.; Harding, J.C. Comparison of Influenza A Virus Infection in High- and Low-birth-weight Pigs Using Morphometric Analysis. *Influenza Other Respir Viruses* **2013**, *7*, 2, doi:10.1111/IRV.12199.

180. Lycett, S.J.; Baillie, G.; Coulter, E.; Bhatt, S.; Kellam, P.; McCauley, J.W.; Wood, J.L.N.; Brown, I.H.; Pybus, O.G.; Brown Leigh, A.J. Estimating Reassortment Rates in Co-Circulating Eurasian Swine Influenza Viruses. *Journal of General Virology* **2012**, *93*, 2326–2336, doi:10.1099/vir.0.044503-0.

181. Andrews, S. FastQC: A Quality Control Tool for High Throughput Sequence Data. Available online: https://www.bioinformatics.babraham.ac.uk/projects/fastqc/ (accessed on 1 September 2021).

182. Bolger, A.M.; Lohse, M.; Usadel, B. Trimmomatic: A Flexible Trimmer for Illumina Sequence Data. *Bioinformatics* **2014**, *30*, 2114–2120, doi:10.1093/bioinformatics/btu170.

183. Langmead, B.; Salzberg, S.L. Fast Gapped-Read Alignment with Bowtie 2. *Nat Methods* **2012**, *9*, 357–359, doi:10.1038/nmeth.1923.

184. Martín-Valls, G.E.; Simon-Grifé, M.; van Boheemen, S.; de Graaf, M.; Bestebroer, T.M.; Busquets, N.; Martín, M.; Casal, J.; Fouchier, R.A.M.; Mateu, E. Phylogeny of Spanish Swine Influenza Viruses Isolated from Respiratory Disease Outbreaks and Evolution of Swine Influenza Virus within an Endemically Infected Farm. *Vet Microbiol* **2014**, *170*, 266–277, doi:10.1016/j.vetmic.2014.02.031.

185. Danecek, P.; Bonfield, J.K.; Liddle, J.; Marshall, J.; Ohan, V.; Pollard, M.O.; Whitwham, A.; Keane, T.; McCarthy, S.A.; Davies, R.M.; et al. Twelve Years of SAMtools and BCFtools. *Gigascience* **2021**, *10*, 1–4, doi:10.1093/gigascience/giab008.

186. Wickham, H. *Ggplot2: Elegant Graphics for Data Analysis*; Springer-Verlag New York, 2016; ISBN 978-3-319-24277-4.

187. RStudio | Open Source & Professional Software for Data Science Teams - RStudio Available online: https://www.rstudio.com/ (accessed on 1 September 2021).

188. Wilm, A.; Aw, P.P.K.; Bertrand, D.; Yeo, G.H.T.; Ong, S.H.; Wong, C.H.; Khor, C.C.; Petric, R.; Hibberd, M.L.; Nagarajan, N. LoFreq: A Sequence-Quality Aware, Ultra-Sensitive Variant Caller for Uncovering Cell-Population Heterogeneity from High-Throughput Sequencing Datasets. *Nucleic Acids Res* **2012**, *40*, 11189, doi:10.1093/NAR/GKS918.

189. Cingolani, P.; Platts, A.; Wang, L.L.; Coon, M.; Nguyen, T.; Wang, L.; Land, S.J.; Lu, X.; Ruden, D.M. A Program for Annotating and Predicting the Effects of Single Nucleotide Polymorphisms, SnpEff: SNPs in the Genome of Drosophila Melanogaster Strain W1118; Iso-2; Iso-3. *Fly (Austin)* **2012**, *6*, 80–92, doi:10.4161/fly.19695.

190. Nelson, C.W.; Moncla, L.H.; Hughes, A.L. SNPGenie: Estimating Evolutionary Parameters to Detect Natural Selection Using Pooled next-Generation Sequencing Data. *Bioinformatics* **2015**, *31*, 3709–3711, doi:10.1093/bioinformatics/btv449.

191. Nelson, C.W.; Hughes, A.L. Within-Host Nucleotide Diversity of Virus Populations: Insights from next-Generation Sequencing. *Infect Genet Evol* **2015**, *30*, 1–7, doi:10.1016/j.meegid.2014.11.026.

192. VanderWaal, K.; Deen, J. Global Trends in Infectious Diseases of Swine. *Proc Natl Acad Sci U S A* **2018**, *115*, 11495–11500, doi:10.1073/pnas.1806068115.

193. Wang, R.; Chen, J.; Gao, K.; Wei, G.W. Vaccine-Escape and Fast-Growing Mutations in the United Kingdom, the United States, Singapore, Spain, India, and Other COVID-19-Devastated Countries. *Genomics* **2021**, *113*, 2158–2170, doi:10.1016/j.ygeno.2021.05.006.

194. Wu, N.C.; Thompson, A.J.; Lee, J.M.; Su, W.; Arlian, B.M.; Xie, J.; Lerner, R.A.; Yen, H.L.; Bloom, J.D.; Wilson, I.A. Different Genetic Barriers for Resistance to HA Stem Antibodies in Influenza H3 and H1 Viruses. *Science (1979)* **2020**, *368*, 1335–1340, doi:10.1126/science.aaz5143.

195. Mancera Gracia, J.C.; Pearce, D.S.; Masic, A.; Balasch, M. Influenza A Virus in Swine: Epidemiology, Challenges and Vaccination Strategies. *Front Vet Sci* **2020**, *7*, doi:10.3389/FVETS.2020.00647/FULL.

196. Fitch, W.M.; Leiter, J.M.; Li, X.Q.; Palese, P. Positive Darwinian Evolution in Human Influenza A Viruses. *Proc Natl Acad Sci U S A* **1991**, *88*, 4270–4274, doi:10.1073/pnas.88.10.4270.

197. Li, W.; Shi, W.; Qiao, H.; Ho, S.Y.W.; Luo, A.; Zhang, Y.; Zhu, C. Positive Selection on Hemagglutinin and Neuraminidase Genes of H1N1 Influenza Viruses. *Virol J* **2011**, *8*, doi:10.1186/1743-422X-8-183.

198. Machkovech, H.M.; Bedford, T.; Suchard, M.A.; Bloom, J.D. Positive Selection in CD8 + T-Cell Epitopes of Influenza Virus Nucleoprotein Revealed by a Comparative Analysis of Human and Swine Viral Lineages . *J Virol* **2015**, *89*, 11275–11283, doi:10.1128/jvi.01571-15.

199. Pérez, L.J.; Díaz de Arce, H.; Perera, C.L.; Rosell, R.; Frías, M.T.; Percedo, M.I.; Tarradas, J.; Dominguez, P.; Núñez, J.I.; Ganges, L. Positive Selection Pressure on the B/C Domains of the E2-Gene of Classical Swine Fever Virus in Endemic Areas under C-Strain Vaccination. *Infection, Genetics and Evolution* **2012**, *12*, 1405–1412, doi:10.1016/j.meegid.2012.04.030.

200. de la Luna, S.; Fortes, P.; Beloso, A.; Ortín, J. Influenza Virus NS1 Protein Enhances the Rate of Translation Initiation of Viral MRNAs. *J Virol* **1995**, *69*, 2427–2433, doi:10.1128/jvi.69.4.2427-2433.1995.

201. Noah, D.L.; Twu, K.Y.; Krug, R.M. Cellular Antiviral Responses against Influenza A Virus Are Countered at the Posttranscriptional Level by the Viral NS1A Protein via Its Binding to a Cellular Protein Required for the 3′ End Processing of Cellular Pre-MRNAS. *Virology* **2003**, *307*, 386–395, doi:10.1016/S0042-6822(02)00127-7.

202. White, H.N. B-Cell Memory Responses to Variant Viral Antigens. *Viruses* **2021**, *13*, 565, doi:10.3390/v13040565.

203. Fernandez-Sesma, A.; Marukian, S.; Ebersole, B.J.; Kaminski, D.; Park, M.-S.; Yuen, T.; Sealfon, S.C.; García-Sastre, A.; Moran, T.M. Influenza Virus Evades Innate and Adaptive Immunity via the NS1 Protein. *J Virol* **2006**, *80*, 6295–6304, doi:10.1128/JVI.02381-05.

204. Carrillo, B.; Choi, J.-M.; Bornholdt, Z.A.; Sankaran, B.; Rice, A.P.; Prasad, B.V.V. The Influenza A Virus Protein NS1 Displays Structural Polymorphism. *J Virol* **2014**, *88*, 4113, doi:10.1128/JVI.03692-13.

205. Qian, X.Y.; Chien, C.Y.A.; Lu, Y.; Montelione, G.T.; Krug, R.M. *An Amino-Terminal Polypeptide Fragment of the Influenza Virus NS1 Protein Possesses Specific RNA-Binding Activity and Largely Helical Backbone Structure*; Cold Spring Harbor Laboratory Press, 1995; Vol. 1, pp. 948–956;.

206. Li, Y.; Yamakita, Y.; Krug, R.M. Regulation of a Nuclear Export Signal by an Adjacent Inhibitory Sequence: The Effector Domain of the Influenza Virus NS1 Protein. *Proceedings of the National Academy of Sciences* **1998**, *95*, 4864–4869, doi:10.1073/PNAS.95.9.4864.

207. Ye, Q.; Krug, R.M.; Tao, Y.J. The Mechanism by Which Influenza A Virus Nucleoprotein Forms Oligomers and Binds RNA. *Nature* **2006**, *444*, 1078–1082, doi:10.1038/nature05379.

208. Xu, R.; Ekiert, D.C.; Krause, J.C.; Hai, R.; Crowe, J.E.; Wilson, I.A. Structural Basis of Preexisting Immunity to the 2009 H1N1 Pandemic Influenza Virus. *Science (1979)* **2010**, *328*, 357–360, doi:10.1126/science.1186430.

209. van der Vries, E.; Collins, P.J.; Vachieri, S.G.; Xiong, X.; Liu, J.; Walker, P.A.; Haire, L.F.; Hay, A.J.; Schutten, M.; Osterhaus, A.D.M.E.; et al. H1N1 2009 Pandemic Influenza Virus: Resistance of the I223R Neuraminidase Mutant Explained by Kinetic and Structural Analysis. *PLoS Pathog* **2012**, *8*, doi:10.1371/journal.ppat.1002914.

210. Kochs, G.; García-Sastre, A.; Martínez-Sobrido, L. Multiple Anti-Interferon Actions of the Influenza A Virus NS1 Protein. *J Virol* **2007**, *81*, 7011, doi:10.1128/JVI.02581-06.

211. Zhou, H.Z.; Zhu, J.Z.; Tu, J.T.; Wei, Z.; Yong, H.; Zhengjun, Y.; Wensi, Y.; Yongtao, L.; Anding, Z.; Yurong, W.; et al. Effect on Virulence and Pathogenicity of H5N1 Influenza A Virus through Truncations of NS1 EIF4GI Binding Domain. *J Infect Dis* **2010**, *202*, 1338–1346, doi:10.1086/656536.

212. Gianfrani, C.; Oseroff, C.; Sidney, J.; Chesnut, R.W.; Sette, A. Human Memory CTL Response Specific for Influenza A Virus Is Broad and Multispecific. *Hum Immunol* **2000**, *61*, 438–452, doi:10.1016/S0198-8859(00)00105-1.

213. Nogales, A.; Chauché, C.; DeDiego, M.L.; Topham, D.J.; Parrish, C.R.; Murcia, P.R.; Martínez-Sobrido, L. The K186E Amino Acid Substitution in the Canine Influenza Virus H3N8 NS1 Protein Restores Its Ability To Inhibit Host Gene Expression. *J Virol* **2017**, *91*, 877–894, doi:10.1128/JVI.00877-17.

214. Chauché, C.; Nogales, A.; Zhu, H.; Goldfarb, D.; Ahmad Shanizza, A.I.; Gu, Q.; Parrish, C.R.; Martínez-Sobrido, L.; Marshall, J.F.; Murcia, P.R. Mammalian Adaptation of an Avian Influenza A Virus Involves Stepwise Changes in NS1. *J Virol* **2018**, *92*, doi:10.1128/JVI.01875-17.

215. Jiao, P.; Tian, G.; Li, Y.; Deng, G.; Jiang, Y.; Liu, C.; Liu, W.; Bu, Z.; Kawaoka, Y.; Chen, H. A Single-Amino-Acid Substitution in the NS1 Protein Changes the Pathogenicity of H5N1 Avian Influenza Viruses in Mice. *J Virol* **2008**, *82*, 1146–1154, doi:10.1128/JVI.01698-07.

216. Li, J.J.; Zhang, K.; Chen, Q.; Zhang, X.; Sun, Y.; Bi, Y.; Zhang, S.; Gu, J.; Li, J.J.; Liu, D.; et al. Three Amino Acid Substitutions in the NS1 Protein Change the Virus Replication of H5N1 Influenza Virus in Human Cells. *Virology* **2018**, *519*, 64–73, doi:10.1016/j.virol.2018.04.004.

217. Wang, S.; Zhang, L.; Zhang, R.; Chi, X.; Yang, Z.; Xie, Y.; Shu, S.; Liao, Y.; Chen, J.-L. Identification of Two Residues within the NS1 of H7N9 Influenza A Virus That Critically Affect the Protein Stability and Function. *Vet Res* **2018**, *49*, 98, doi:10.1186/s13567-018-0594-y.

218. Portela, A.; Digard, P. The Influenza Virus Nucleoprotein: A Multifunctional RNA-Binding Protein Pivotal to Virus Replication. *Journal of General Virology* **2002**, *83*, 723–734, doi:10.1099/0022-1317-83-4-723.

219. Li, Z.; Watanabe, T.; Hatta, M.; Watanabe, S.; Nanbo, A.; Ozawa, M.; Kakugawa, S.; Shimojima, M.; Yamada, S.; Neumann, G.; et al. Mutational Analysis of Conserved Amino Acids in the Influenza A Virus Nucleoprotein. *J Virol* **2009**, *83*, 4153–4162, doi:10.1128/JVI.02642-08.

220. Biswas, S.K.; Boutz, P.L.; Nayak, D.P. Influenza Virus Nucleoprotein Interacts with Influenza Virus Polymerase Proteins. *J Virol* **1998**, *72*, 5493–5501, doi:10.1128/JVI.72.7.5493-5501.1998.

221. Pagani, I.; di Pietro, A.; Oteiza, A.; Ghitti, M.; Mechti, N.; Naffakh, N.; Vicenzi, E. Mutations Conferring Increased Sensitivity to Tripartite Motif 22 Restriction Accumulated Progressively in the Nucleoprotein of Seasonal Influenza A (H1N1) Viruses between 1918 and 2009. *mSphere* **2018**, *3*, doi:10.1128/mSphere.00110-18.

222. Pietro, A. di; Kajaste-Rudnitski, A.; Oteiza, A.; Nicora, L.; Towers, G.J.; Mechti, N.; Vicenzi, E. TRIM22 Inhibits Influenza A Virus Infection by Targeting the Viral Nucleoprotein for Degradation. *J Virol* **2013**, *87*, 4523, doi:10.1128/JVI.02548-12.

223. Krammer, F. The Human Antibody Response to Influenza A Virus Infection and Vaccination. *Nature Reviews Immunology 2019 19:6* **2019**, *19*, 383–397, doi:10.1038/s41577-019-0143-6.

224. Gamblin, S.J.; Haire, L.F.; Russell, R.J.; Stevens, D.J.; Xiao, B.; Ha, Y.; Vasisht, N.; Steinhauer, D.A.; Daniels, R.S.; Elliot, A.; et al. The Structure and Receptor Binding Properties of the 1918 Influenza Hemagglutinin. *Science* **2004**, *303*, 1838–1842, doi:10.1126/science.1093155.

225. Murcia, P.R.; Hughes, J.; Battista, P.; Lloyd, L.; Baillie, G.J.; Ramirez-Gonzalez, R.H.; Ormond, D.; Oliver, K.; Elton, D.; Mumford, J.A.; et al. Evolution of an Eurasian Avian-like Influenza Virus in Naïve and Vaccinated Pigs. *PLoS Pathog* **2012**, *8*, e1002730, doi:10.1371/journal.ppat.1002730.

226. Kubiszewski-Jakubiak, S.; Worch, R. Influenza A H1 and H3 Transmembrane Domains Interact Differently with Each Other and with Surrounding Membrane Lipids. *Viruses* **2020**, *12*, doi:10.3390/V12121461.

227. Gilchuk, I.M.; Bangaru, S.; Gilchuk, P.; Irving, R.P.; Kose, N.; Bombardi, R.G.; Thornburg, N.J.; Creech, C.B.; Edwards, K.M.; Li, S.; et al. Influenza H7N9 Virus Neuraminidase-Specific Human Monoclonal Antibodies Inhibit Viral Egress and Protect from Lethal Influenza Infection in Mice. *Cell Host Microbe* **2019**, *26*, 715-728.e8, doi:10.1016/j.chom.2019.10.003.

228. Östbye, H.; Gao, J.; Martinez, M.R.; Wang, H.; de Gier, J.-W.; Daniels, R. N-Linked Glycan Sites on the Influenza A Virus Neuraminidase Head Domain Are Required for Efficient Viral Incorporation and Replication. *J Virol* **2020**, *94*, doi:10.1128/JVI.00874-20.

229. Swine Influenza - OIE - World Organisation for Animal Health Available online: https://www.oie.int/en/disease/swine-influenza/ (accessed on 22 February 2022).

230. Li, Y.; Robertson, I. The Epidemiology of Swine Influenza. *Animal Diseases* **2021**, *1*, doi:10.1186/S44149-021-00024-6.

231. Breen, M.; Nogales, A.; Baker, S.F.; Martínez-Sobrido, L. Replication-Competent Influenza A Viruses Expressing Reporter Genes. *Viruses* **2016**, *8*, 1–28, doi:10.3390/V8070179.

232. Skehel, J.J.; Wiley, D.C. Receptor Binding and Membrane Fusion in Virus Entry: The Influenza Hemagglutinin. *Annu Rev Biochem* **2000**, *69*, 531–569, doi:10.1146/ANNUREV.BIOCHEM.69.1.531.

233. Varghese, J.N.; McKimm-Breschkin, J.L.; Caldwell, J.B.; Kortt, A.A.; Colman, P.M. The Structure of the Complex between Influenza Virus Neuraminidase and Sialic Acid, the Viral Receptor. *Proteins* **1992**, *14*, 327–332, doi:10.1002/PROT.340140302.

234. Lewis, N.S.; Russell, C.A.; Langat, P.; Anderson, T.K.; Berger, K.; Bielejec, F.; Burke, D.F.; Dudas, G.; Fonville, J.M.; Fouchier, R.A.M.; et al. The Global Antigenic Diversity of Swine Influenza A Viruses. *Elife* **2016**, *5*, doi:10.7554/ELIFE.12217.

235. López-Valiñas, Á.; Sisteré-Oró, M.; López-Serrano, S.; Baioni, L.; Darji, A.; Chiapponi, C.; Segalés, J.; Ganges, L.; Núñez, J.I. Identification and Characterization of Swine Influenza Virus H1n1 Variants Generated in Vaccinated and Nonvaccinated, Challenged Pigs. *Viruses* **2021**, *13*, 2087, doi:10.3390/V13102087/S1.

236. Fulton, B.O.; Sachs, D.; Beaty, S.M.; Won, S.T.; Lee, B.; Palese, P.; Heaton, N.S. Mutational Analysis of Measles Virus Suggests Constraints on Antigenic Variation of the Glycoproteins. *Cell Rep* **2015**, *11*, 1331, doi:10.1016/J.CELREP.2015.04.054.

237. Cobey, S. Pathogen Evolution and the Immunological Niche. *Ann N Y Acad Sci* **2014**, *1320*, 1, doi:10.1111/NYAS.12493.

238. Doud, M.B.; Lee, J.M.; Bloom, J.D. How Single Mutations Affect Viral Escape from Broad and Narrow Antibodies to H1 Influenza Hemagglutinin. *Nature Communications 2018 9:1* **2018**, *9*, 1–12, doi:10.1038/s41467-018-03665-3.

239. Prachanronarong, K.L.; Canale, A.S.; Liu, P.; Somasundaran, M.; Hou, S.; Poh, Y.-P.; Han, T.; Zhu, Q.; Renzette, N.; Zeldovich, K.B.; et al. Mutations in Influenza A Virus Neuraminidase and Hemagglutinin Confer Resistance against a Broadly Neutralizing Hemagglutinin Stem Antibody. *J Virol* **2019**, *93*, doi:10.1128/JVI.01639-18.

240. Kirkpatrick Roubidoux, E.; McMahon, M.; Carreño, J.M.; Capuano, C.; Jiang, K.; Simon, V.; van Bakel, H.; Wilson, P.; Krammer, F. Identification and Characterization of Novel Antibody Epitopes on the N2 Neuraminidase. *mSphere* **2021**, *6*, doi:10.1128/MSPHERE.00958-20.

241. Park, J.K.; Xiao, Y.; Ramuta, M.D.; Rosas, L.A.; Fong, S.; Matthews, A.M.; Freeman, A.D.; Gouzoulis, M.A.; Batchenkova, N.A.; Yang, X.; et al. Pre-Existing Immunity to Influenza Virus Hemagglutinin Stalk Might Drive Selection for Antibody-Escape Mutant Viruses in a Human Challenge Model. *Nature Medicine 2020 26:8* **2020**, *26*, 1240–1246, doi:10.1038/s41591-020-0937-x.

242. Zhou, N.N.; Senne, D.A.; Landgraf, J.S.; Swenson, S.L.; Erickson, G.; Rossow, K.; Liu, L.; Yoon, K.; Krauss, S.; Webster, R.G. Genetic Reassortment of Avian, Swine, and Human Influenza A Viruses in American Pigs. *J Virol* **1999**, *73*, 8851–8856, doi:https://doi.org/10.1128/JVI.73.10.8851-8856.1999.

243. Baratelli, M.; Córdoba, L.; Pérez, L.J.; Maldonado, J.; Fraile, L.; Núñez, J.I.; Montoya, M. Genetic Characterization of Influenza A Viruses Circulating in Pigs and Isolated in North-East Spain during the Period 2006–2007. *Res Vet Sci* **2014**, *96*, 380–388, doi:10.1016/J.RVSC.2013.12.006.

244. Vincent, A.L.; Ma, W.; Lager, K.M.; Janke, B.H.; Richt, J.A. Chapter 3 Swine Influenza Viruses: A North American Perspective. *Adv Virus Res* **2008**, *72*, 127–154, doi:10.1016/S0065-3527(08)00403-X.

245. ImageJ Available online: https://imagej.nih.gov/ij/ (accessed on 14 January 2022).

246. Detmer, S.E.; Gunvaldsen, R.E.; Harding, J.C. Comparison of Influenza a Virus Infection in High- and Low-Birth-Weight Pigs Using Morphometric Analysis. *Influenza Other Respir Viruses* **2013**, *7*, 2–9, doi:10.1111/irv.12199.

247. Bankevich, A.; Nurk, S.; Antipov, D.; Gurevich, A.A.; Dvorkin, M.; Kulikov, A.S.; Lesin, V.M.; Nikolenko, S.I.; Pham, S.; Prjibelski, A.D.; et al. Original Articles SPAdes: A New Genome Assembly Algorithm and Its Applications to Single-Cell Sequencing. *J. Comput. Biol.* **2012**, *19*, 455–477, doi:10.1089/cmb.2012.0021.

248. Mussá, T.; Ballester, M.; Silva-Campa, E.; Baratelli, M.; Busquets, N.; Lecours, M.P.; Dominguez, J.; Amadori, M.; Fraile, L.; Hernández, J.; et al. Swine, Human or Avian Influenza Viruses Differentially Activates Porcine Dendritic Cells Cytokine Profile. *Vet Immunol Immunopathol* **2013**, *154*, 25–35, doi:10.1016/J.VETIMM.2013.04.004.

249. Ou, J.; Zhu, L.J. TrackViewer: A Bioconductor Package for Interactive and Integrative Visualization of Multi-Omics Data. *Nature Methods 2019 16:6* **2019**, *16*, 453–454, doi:10.1038/s41592-019-0430-y.

250. Fan, H.; Wang, B.; Zhang, Y.; Zhu, Y.; Song, B.; Xu, H.; Zhai, Y.; Qiao, M.; Sun, F. A Cryo-Electron Microscopy Support Film Formed by 2D Crystals of Hydrophobin HFBI. *Nature Communications 2021 12:1* **2021**, *12*, 1–13, doi:10.1038/s41467-021-27596-8.

251. Zhu, X.; McBride, R.; Nycholat, C.M.; Yu, W.; Paulson, J.C.; Wilson, I.A. Influenza Virus Neuraminidases with Reduced Enzymatic Activity That Avidly Bind Sialic Acid Receptors. *J Virol* **2012**, *86*, 13371, doi:10.1128/JVI.01426-12.

252. Kyriakis, C.S.; Rose, N.; Foni, E.; Maldonado, J.; Loeffen, W.L.A.; Madec, F.; Simon, G.; van Reeth, K. Influenza A Virus Infection Dynamics in Swine Farms in Belgium, France, Italy and Spain, 2006-2008. *Vet Microbiol* **2013**, *162*, 543–550, doi:10.1016/J.VETMIC.2012.11.014.

253. Torremorell, M.; Allerson, M.; Corzo, C.; Diaz, A.; Gramer, M. Transmission of Influenza A Virus in Pigs. *Transbound Emerg Dis* **2012**, *59*, 68–84, doi:10.1111/J.1865-1682.2011.01300.X.

254. Simon-Grifé, M.; Martín-Valls, G.E.; Vilar, M.J.; García-Bocanegra, I.; Mora, M.; Martín, M.; Mateu, E.; Casal, J. Seroprevalence and Risk Factors of Swine Influenza in Spain. *Vet Microbiol* **2011**, *149*, 56–63, doi:10.1016/J.VETMIC.2010.10.015.

255. Qiu, Y.; de Hert, K.; van Reeth, K. Cross-Protection against European Swine Influenza Viruses in the Context of Infection Immunity against the 2009 Pandemic H1N1 Virus: Studies in the Pig Model of Influenza. *Vet Res* **2015**, *46*, doi:10.1186/S13567-015-0236-6.

256. Qi, L.; Davis, A.S.; Jagger, B.W.; Schwartzman, L.M.; Dunham, E.J.; Kash, J.C.; Taubenberger, J.K. Analysis by Single-Gene Reassortment Demonstrates That the 1918 Influenza Virus Is Functionally Compatible with a Low-Pathogenicity Avian Influenza Virus in Mice. *J Virol* **2012**, *86*, 9211–9220, doi:10.1128/JVI.00887-12.

257. Zhang, Q.; Shi, J.; Deng, G.; Guo, J.; Zeng, X.; He, X.; Kong, H.; Gu, C.; Li, X.; Liu, J.; et al. H7N9 Influenza Viruses Are Transmissible in Ferrets by Respiratory Droplet. *Science* **2013**, *341*, 410–414, doi:10.1126/SCIENCE.1240532.

258. Domingo, E.; García-Crespo, C.; Lobo-Vega, R.; Perales, C. Mutation Rates, Mutation Frequencies, and Proofreading-Repair Activities in RNA Virus Genetics. *Viruses* **2021**, *13*, doi:10.3390/V13091882.

259. Poole, E.; Elton, D.; Medcalf, L.; Digard, P. Functional Domains of the Influenza A Virus PB2 Protein: Identification of NP- and PB1-Binding Sites. *Virology* **2004**, *321*, 120–133, doi:10.1016/J.VIROL.2003.12.022.

260. Xiao, C.; Ma, W.; Sun, N.; Huang, L.; Li, Y.; Zeng, Z.; Wen, Y.; Zhang, Z.; Li, H.; Li, Q.; et al. PB2-588 V Promotes the Mammalian Adaptation of H10N8, H7N9 and H9N2 Avian Influenza Viruses. *Sci Rep* **2016**, *6*, doi:10.1038/SREP19474.

261. Lina, L.; Saijuan, C.; Chengyu, W.; Yuefeng, L.; Shishan, D.; Ligong, C.; Kangkang, G.; Zhendong, G.; Jiakai, L.; Jianhui, Z.; et al. Adaptive Amino Acid Substitutions Enable Transmission of an H9N2 Avian Influenza Virus in Guinea Pigs. *Sci Rep* **2019**, *9*, doi:10.1038/S41598-019-56122-6.

262. Wang, C.; Lee, H.H.Y.; Yang, Z.F.; Mok, C.K.P.; Zhang, Z. PB2-Q591K Mutation Determines the Pathogenicity of Avian H9N2 Influenza Viruses for Mammalian Species. *PLoS One* **2016**, *11*, doi:10.1371/JOURNAL.PONE.0162163.

263. Cao, Z.; Zeng, W.; Hao, X.; Huang, J.; Cai, M.; Zhou, P.; Zhang, G. Continuous Evolution of Influenza A Viruses of Swine from 2013 to 2015 in Guangdong, China. *PLoS One* **2019**, *14*, doi:10.1371/JOURNAL.PONE.0217607.

264. Chen, W.; Xu, Q.; Zhong, Y.; Yu, H.; Shu, J.; Ma, T.; Li, Z. Genetic Variation and Co-Evolutionary Relationship of RNA Polymerase Complex Segments in Influenza A Viruses. *Virology* **2017**, *511*, 193–206, doi:10.1016/J.VIROL.2017.07.027.

265. Rolling, T.; Koerner, I.; Zimmermann, P.; Holz, K.; Haller, O.; Staeheli, P.; Kochs, G. Adaptive Mutations Resulting in Enhanced Polymerase Activity Contribute to High Virulence of Influenza A Virus in Mice. *J Virol* **2009**, *83*, 6673–6680, doi:10.1128/JVI.00212-09.

266. Slaine, P.D.; MacRae, C.; Kleer, M.; Lamoureux, E.; McAlpine, S.; Warhuus, M.; Comeau, A.M.; McCormick, C.; Hatchette, T.; Khaperskyy, D.A. Adaptive Mutations in Influenza A/California/07/2009 Enhance Polymerase Activity and Infectious Virion Production. *Viruses* **2018**, *10*, doi:10.3390/V10050272.

267. Thepmalee, C.; Sanguansermsri, P.; Suwanankhon, N.; Chamnanpood, C.; Chamnanpood, P.; Pongcharoen, S.; R. Niumsap, P.; Surangkul, D.; Sanguansermsri, D. Changes in the NS1 Gene of Avian Influenza Viruses Isolated in Thailand Affect Expression of Type I Interferon in Primary Chicken Embryonic Fibroblast Cells. *Indian Journal of Virology* **2013**, *24*, 365, doi:10.1007/S13337-013-0158-8.

268. Jia, D.; Rahbar, R.; Chan, R.W.Y.; Lee, S.M.Y.; Chan, M.C.W.; Wang, B.X.; Baker, D.P.; Sun, B.; Malik Peiris, J.S.; Nicholls, J.M.; et al. Influenza Virus Non-Structural Protein 1 (NS1) Disrupts Interferon Signaling. *PLoS One* **2010**, *5*, 13927, doi:10.1371/JOURNAL.PONE.0013927.

269. Koliopoulos, M.G.; Lethier, M.; van der Veen, A.G.; Haubrich, K.; Hennig, J.; Kowalinski, E.; Stevens, R. v.; Martin, S.R.; Reis E Sousa, C.; Cusack, S.; et al. Molecular Mechanism of Influenza A NS1-Mediated TRIM25 Recognition and Inhibition. *Nat Commun* **2018**, *9*, doi:10.1038/S41467-018-04214-8.

270. Pereira, C.F.; Wise, H.M.; Kurian, D.; Pinto, R.M.; Amorim, M.J.; Gill, A.C.; Digard, P. Effects of Mutations in the Effector Domain of Influenza A Virus NS1 Protein. *BMC Res Notes* **2018**, *11*, 673, doi:10.1186/S13104-018-3779-6.

271. Lopes, A.M.; Domingues, P.; Zell, R.; Hale, B.G. Structure-Guided Functional Annotation of the Influenza A Virus NS1 Protein Reveals Dynamic Evolution of the P85β-Binding Site during Circulation in Humans. *J Virol* **2017**, *91*, 1081–1098, doi:10.1128/JVI.01081-17.

272. Shin, Y.-K.; Li, Y.; Liu, Q.; Anderson, D.H.; Babiuk, L.A.; Zhou, Y. SH3 Binding Motif 1 in Influenza A Virus NS1 Protein Is Essential for PI3K/Akt Signaling Pathway Activation. *J Virol* **2007**, *81*, 12730–12739, doi:10.1128/JVI.01427-07.

273. Rossman, J.S.; Lamb, R.A. Influenza Virus Assembly and Budding. *Virology* **2011**, *411*, 229, doi:10.1016/J.VIROL.2010.12.003.

274. Knight, M.L.; Fan, H.; Bauer, D.L.V.; Grimes, J.M.; Fodor, E.; Keown, J.R. Structure of an H3N2 Influenza Virus Nucleoprotein. *Acta Crystallogr F Struct Biol Commun* **2021**, *77*, 208, doi:10.1107/S2053230X2100635X.

275. Hu, Y.; Sneyd, H.; Dekant, R.; Wang, J. Influenza A Virus Nucleoprotein: A Highly Conserved Multi-Functional Viral Protein as a Hot Antiviral Drug Target. *Curr Top Med Chem* **2017**, *17*, doi:10.2174/1568026617666170224122508.

276. Zhong, J.; Liang, L.; Huang, P.; Zhu, X.; Zou, L.; Yu, S.; Zhang, X.; Zhang, Y.; Ni, H.; Yan, J. Genetic Mutations in Influenza H3N2 Viruses from a 2012 Epidemic in Southern China. *Virol J* **2013**, *10*, 345, doi:10.1186/1743-422X-10-345.

277. Lang, A.S.; Kelly, A.; Runstadler, J.A. Prevalence and Diversity of Avian Influenza Viruses in Environmental Reservoirs. *J Gen Virol* **2008**, *89*, 509–519, doi:10.1099/VIR.0.83369-0.

278. Kalhoro, D.H.; Liang, S.; Kalhoro, M.S.; Pirzado, S.A.; Rajput, N.; Naeem, M.; Parveen, F.; Liu, Y. Identification and Genetic Evolution Analysis of One Strain of H3N2 Canine Influenza Virus Isolated from Nanjing, China. *Pak J Zool* **2018**, *50*, 817–824, doi:10.17582/JOURNAL.PJZ/2018.50.3.817.824.

279. Kirkpatrick, E.; Qiu, X.; Wilson, P.C.; Bahl, J.; Krammer, F. The Influenza Virus Hemagglutinin Head Evolves Faster than the Stalk Domain. *Sci Rep* **2018**, *8*, doi:10.1038/S41598-018-28706-1.

280. Hussain, S.; Daniels, R.S.; Wharton, S.A.; Howell, S.; Halai, C.; Kunzelmann, S.; Whittaker, L.; McCauley, J.W. Reduced Sialidase Activity of Influenza A(H3N2) Neuraminidase Associated with Positively Charged Amino Acid Substitutions. *Journal of General Virology* **2021**, *102*, 001648, doi:10.1099/JGV.0.001648/CITE/REFWORKS.

281. Ge, J.; Lin, X.; Guo, J.; Liu, L.; Li, Z.; Lan, Y.; Liu, L.; Guo, J.; Lu, J.; Huang, W.; et al. The Antibody Response Against Neuraminidase in Human Influenza A (H3N2) Virus Infections During 2018/2019 Flu Season: Focusing on the Epitopes of 329-N-Glycosylation and E344 in N2. *Front Microbiol* **2022**, *13*, 590, doi:10.3389/FMICB.2022.845088/BIBTEX.

282. Korsun, N.; Trifonova, I.; Voleva, S.; Grigorova, I.; Angelova, S. Genetic Characterisation of the Influenza Viruses Circulating in Bulgaria during the 2019–2020 Winter Season. *Virus Genes* **2021**, *57*, 401–412, doi:10.1007/S11262-021-01853-W/TABLES/1.

283. Li, Z.; Zhong, L.; He, J.; Huang, Y.; Zhao, Y. Development and Application of Reverse Genetic Technology for the Influenza Virus. *Virus Genes* **2021**, *57*, 151, doi:10.1007/S11262-020-01822-9.

284. Breen, M.; Nogales, A.; Baker, S.F.; Martínez-Sobrido, L. Replication-Competent Influenza A Viruses Expressing Reporter Genes. *Viruses 2016, Vol. 8, Page 179* **2016**, *8*, 179, doi:10.3390/V8070179.

285. Domingoid, E.; Perales, C. Viral Quasispecies. **2019**, doi:10.1371/journal.pgen.1008271.

286. Chen, R.; Holmes, E.C. Avian Influenza Virus Exhibits Rapid Evolutionary Dynamics. *Mol Biol Evol* **2006**, *23*, 2336–2341, doi:10.1093/MOLBEV/MSL102.

287. Trifonov, V.; Khiabanian, H.; Rabadan, R. Geographic Dependence, Surveillance, and Origins of the 2009 Influenza A (H1N1) Virus. *https://doi.org/10.1056/NEJMp0904572* **2009**, *361*, 115–119, doi:10.1056/NEJMP0904572.

288. López-Valiñas, Á.; Baioni, L.; Córdoba, L.; Darji, A.; Chiapponi, C.; Segalés, J.; Ganges, L.; Núñez, J.I. Evolution of Swine Influenza Virus H3N2 in Vaccinated and Nonvaccinated Pigs after Previous Natural H1N1 Infection. *Viruses* **2022**, *14*, doi:10.3390/V14092008/S1.

289. Li, H.; Durbin, R. Fast and Accurate Short Read Alignment with Burrows-Wheeler Transform. *Bioinformatics* **2009**, *25*, 1754–1760, doi:10.1093/BIOINFORMATICS/BTP324.

290. Hu, Y.J.; Tu, P.C.; Lin, C.S.; Guo, S.T. Identification and Chronological Analysis of Genomic Signatures in Influenza a Viruses. *PLoS One* **2014**, *9*, doi:10.1371/journal.pone.0084638.

291. Sriwilaijaroen, N.; Suzuki, Y. Molecular Basis of the Structure and Function of H1 Hemagglutinin of Influenza Virus. *Proc Jpn Acad Ser B Phys Biol Sci* 2012, *88*, 226–249.

292. Li, C.; Culhane, M.R.; Schroeder, D.C.; Cheeran, M.C.J.; Galina Pantoja, L.; Jansen, M.L.; Torremorell, M. Vaccination Decreases the Risk of Influenza A Virus Reassortment but Not Genetic Variation in Pigs. *Elife* **2022**, *11*, doi:10.7554/ELIFE.78618.

293. Sitaras, I.; Kalthoff, D.; Beer, M.; Peeters, B.; de Jong, M.C.M. Immune Escape Mutants of Highly Pathogenic Avian Influenza H5N1 Selected Using Polyclonal Sera: Identification of Key Amino Acids in the HA Protein. *PLoS One* **2014**, *9*, e84628, doi:10.1371/JOURNAL.PONE.0084628.

294. Yasuhara, A.; Yamayoshi, S.; Soni, P.; Takenaga, T.; Kawakami, C.; Takashita, E.; Sakai-Tagawa, Y.; Uraki, R.; Ito, M.; Iwatsuki-Horimoto, K.; et al. Diversity of Antigenic Mutants of Influenza A(H1N1)Pdm09 Virus Escaped from Human Monoclonal Antibodies. *Scientific Reports 2017 7:1* **2017**, *7*, 1–9, doi:10.1038/s41598-017-17986-8.

295. Sitaras, I.; Spackman, E.; de Jong, M.C.M.; Parris, D.J. Selection and Antigenic Characterization of Immune-Escape Mutants of H7N2 Low Pathogenic Avian Influenza Virus Using Homologous Polyclonal Sera. *Virus Res* **2020**, *290*, 198188, doi:10.1016/J.VIRUSRES.2020.198188.

296. Zharikova, D.; Mozdzanowska, K.; Feng, J.; Zhang, M.; Gerhard, W. Influenza Type A Virus Escape Mutants Emerge In Vivo in the Presence of Antibodies to the Ectodomain of Matrix Protein 2. *J Virol* **2005**, *79*, 6644–6654, doi:10.1128/JVI.79.11.6644-6654.2005/ASSET/88AD9789-EC47-4B46-86DA-635D0D9B6BA8/ASSETS/GRAPHIC/ZJV0110563030008.JPEG.

297. Park, J.K.; Xiao, Y.; Ramuta, M.D.; Rosas, L.A.; Fong, S.; Matthews, A.M.; Freeman, A.D.; Gouzoulis, M.A.; Batchenkova, N.A.; Yang, X.; et al. Pre-Existing Immunity to Influenza Virus Hemagglutinin Stalk Might Drive Selection for Antibody-Escape Mutant Viruses in a Human Challenge Model. *Nature Medicine 2020 26:8* **2020**, *26*, 1240–1246, doi:10.1038/s41591-020-0937-x.

298. Xu, C.; Zhang, N.; Yang, Y.; Liang, W.; Zhang, Y.; Wang, J.; Suzuki, Y.; Wu, Y.; Chen, Y.; Yang, H.; et al. Immune Escape Adaptive Mutations in Hemagglutinin Are Responsible for the Antigenic Drift of Eurasian Avian-Like H1N1 Swine Influenza Viruses. *J Virol* **2022**, *96*, doi:10.1128/JVI.00971-22/ASSET/CFE88D01-46C6-4318-805E-8D6BDCE51EB5/ASSETS/IMAGES/LARGE/JVI.00971-22-F004.JPG.

299. Frost, S.D.W.; Magalis, B.R.; Kosakovsky Pond, S.L. Neutral Theory and Rapidly Evolving Viral Pathogens. *Mol Biol Evol* **2018**, *35*, 1348–1354, doi:10.1093/MOLBEV/MSY088.

300. Diaz, A.; Enomoto, S.; Romagosa, A.; Sreevatsan, S.; Nelson, M.; Culhane, M.; Torremorell, M. Genome Plasticity of Triple-Reassortant H1N1 Influenza A Virus during Infection of Vaccinated Pigs. *J Gen Virol* **2015**, *96*, 2982, doi:10.1099/JGV.0.000258.

301. Diaz, A.; Allerson, M.; Culhane, M.; Sreevatsan, S.; Torremorell, M. Antigenic Drift of H1N1 Influenza A Virus in Pigs with and without Passive Immunity. *Influenza Other Respir Viruses* **2013**, *7 Suppl 4*, 52–60, doi:10.1111/IRV.12190.

302. Subbarao, E.K.; London, W.; Murphy, B.R. A Single Amino Acid in the PB2 Gene of Influenza A Virus Is a Determinant of Host Range. *J Virol* **1993**, *67*, 1761–1764, doi:10.1128/JVI.67.4.1761-1764.1993.

303. Cai, M.; Zhong, R.; Qin, C.; Yu, Z.; Wen, X.; Xian, J.; Chen, Y.; Cai, Y.; Yi, H.; Gong, L.; et al. The R251K Substitution in Viral Protein PB2 Increases Viral Replication and Pathogenicity of Eurasian Avian-like H1N1 Swine Influenza Viruses. *Viruses 2020, Vol. 12, Page 52* **2020**, *12*, 52, doi:10.3390/V12010052.

304. Song, J.; Xu, J.; Shi, J.; Li, Y.; Chen, H. Synergistic Effect of S224P and N383D Substitutions in the PA of H5N1 Avian Influenza Virus Contributes to Mammalian Adaptation. *Scientific Reports 2015 5:1* **2015**, *5*, 1–7, doi:10.1038/srep10510.

305. Yu, Z.; Cheng, K.; Sun, W.; Zhang, X.; Li, Y.; Wang, T.; Wang, H.; Zhang, Q.; Xin, Y.; Xue, L.; et al. A PB1 T296R Substitution Enhance Polymerase Activity and Confer a Virulent Phenotype to a 2009 Pandemic H1N1 Influenza Virus in Mice. *Virology* **2015**, *486*, 180–186, doi:10.1016/J.VIROL.2015.09.014.

306. Eichelberger, M.C.; Wan, H. Influenza Neuraminidase as a Vaccine Antigen. *Curr Top Microbiol Immunol* **2014**, *386*, 275–299, doi:10.1007/82_2014_398/COVER.

307. Yewdell, J.W. Monoclonal Antibodies Specific for Discontinuous Epitopes Direct Refolding of Influenza A Virus Hemagglutinin. *Mol Immunol* **2010**, *47*, 1132–1136, doi:10.1016/J.MOLIMM.2009.10.023.

308. Eisenlohr, L.C.; Gerhard, W.; Hackett, C.J. Acid-Induced Conformational Modification of the Hemagglutinin Molecule Alters Interaction of Influenza Virus with Antigen-Presenting Cells. *The Journal of Immunology* **1988**, *141*.

309. Guo, Z.; Wilson, J.R.; York, I.A.; Stevens, J. Biosensor-Based Epitope Mapping of Antibodies Targeting the Hemagglutinin and Neuraminidase of Influenza A Virus. *J Immunol Methods* **2018**, *461*, 23–29, doi:10.1016/J.JIM.2018.07.007.

310. Aytay, S.; Schulze, I.T. Single Amino Acid Substitutions in the Hemagglutinin Can Alter the Host Range and Receptor Binding Properties of H1 Strains of Influenza A Virus. *J Virol* **1991**, *65*, 3022–3028, doi:10.1128/JVI.65.6.3022-3028.1991.

311. Thompson, A.J.; Paulson, J.C. Adaptation of Influenza Viruses to Human Airway Receptors. *J Biol Chem* **2021**, *296*, 100017, doi:10.1074/JBC.REV120.013309.

312. Jiang, L.; Fantoni, G.; Couzens, L.; Gao, J.; Plant, E.; Ye, Z.; Eichelberger, M.C.; Wan, H. Comparative Efficacy of Monoclonal Antibodies That Bind to Different Epitopes of the 2009 Pandemic H1N1 Influenza Virus Neuraminidase. *J Virol* **2016**, *90*, 117–128, doi:10.1128/JVI.01756-15/ASSET/85EF0ACA-5BAA-4F00-A66D-F8D6358AFF8D/ASSETS/GRAPHIC/ZJV9990910630005.JPEG.

313. Wan, H.; Yang, H.; Shore, D.A.; Garten, R.J.; Couzens, L.; Gao, J.; Jiang, L.; Carney, P.J.; Villanueva, J.; Stevens, J.; et al. Structural Characterization of a Protective Epitope Spanning A(H1N1)Pdm09 Influenza Virus Neuraminidase Monomers. *Nature Communications 2015 6:1* **2015**, *6*, 1–10, doi:10.1038/ncomms7114.

314. Bokhari, S.H.; Pomeroy, L.W.; Janies, D.A. Reassortment Networks and the Evolution of Pandemic H1N1 Swine-Origin Influenza. *IEEE/ACM Trans Comput Biol Bioinform* **2012**, *9*, 214–227, doi:10.1109/TCBB.2011.95.

315. Poon, L.L.M.; Mak, P.W.Y.; Li, O.T.W.; Chan, K.H.; Cheung, C.L.; Ma, E.; Yen, H.L.; Vijaykrishna, D.; Guan, Y.; Peiris, J.S.M. Rapid Detection of Reassortment of Pandemic H1N1/2009 Influenza Virus. *Clin Chem* **2010**, *56*, 1340–1344, doi:10.1373/CLINCHEM.2010.149179.

316. Lee, C.W. Reverse Genetics of Influenza Virus. *Methods in Molecular Biology* **2014**, *1161*, 37–50, doi:10.1007/978-1-4939-0758-8_4/FIGURES/2.

317. Hoffmann, E.; Neumann, G.; Kawaoka, Y.; Hobom, G.; Webster, R.G. A DNA Transfection System for Generation of Influenza A Virus from Eight Plasmids. *Proc Natl Acad Sci U S A* **2000**, *97*, 6108, doi:10.1073/PNAS.100133697.

318. Plant, E.P.; Ilyushina, N.A.; Sheikh, F.; Donnelly, R.P.; Ye, Z. Influenza Virus NS1 Protein Mutations at Position 171 Impact Innate Interferon Responses by Respiratory Epithelial Cells. *Virus Res* **2017**, *240*, 81–86, doi:10.1016/J.VIRUSRES.2017.07.021.

319. Cui, X.; Ji, Y.; Wang, Z.; Du, Y.; Guo, H.; Wang, L.; Chen, H.; Zhu, Q. A 113-Amino-Acid Truncation at the NS1 C-Terminus Is a Determinant for Viral Replication of H5N6 Avian Influenza Virus in Vitro and in Vivo. *Vet Microbiol* **2018**, *225*, 6–16, doi:10.1016/J.VETMIC.2018.09.004.

320. Pu, J.; Wang, J.; Zhang, Y.; Fu, G.; Bi, Y.; Sun, Y.; Liu, J. Synergism of Co-Mutation of Two Amino Acid Residues in NS1 Protein Increases the Pathogenicity of Influenza Virus in Mice. *Virus Res* **2010**, *151*, 200–204, doi:10.1016/J.VIRUSRES.2010.05.007.

321. Cheng, J.; Zhang, C.; Tao, J.; Li, B.; Shi, Y.; Liu, H. Effects of the S42 Residue of the H1N1 Swine Influenza Virus NS1 Protein on Interferon Responses and Virus Replication. *Virol J* **2018**, *15*, doi:10.1186/S12985-018-0971-1.

322. Cheng, J.; Tao, J.; Li, B.; Shi, Y.; Liu, H. The Tyrosine 73 and Serine 83 Dephosphorylation of H1N1 Swine Influenza Virus NS1 Protein Attenuates Virus

Replication and Induces High Levels of Beta Interferon. *Virol J* **2019**, *16*, doi:10.1186/S12985-019-1255-0.

323. Cutter, A.D.; Wasmuth, J.D.; Blaxter, M.L. The Evolution of Biased Codon and Amino Acid Usage in Nematode Genomes. *Mol Biol Evol* **2006**, *23*, 2303–2315, doi:10.1093/MOLBEV/MSL097.

324. Goñi, N.; Iriarte, A.; Comas, V.; Soñora, M.; Moreno, P.; Moratorio, G.; Musto, H.; Cristina, J. Pandemic Influenza A Virus Codon Usage Revisited: Biases, Adaptation and Implications for Vaccine Strain Development. *Virol J* **2012**, *9*, doi:10.1186/1743-422X-9-263.

325. Wang, S.F.; Su, M.W.; Tseng, S.P.; Li, M.C.; Tsao, C.H.; Huang, S.W.; Chu, W.C.; Liu, W.T.; Chen, Y.M.A.; Huang, J.C. Analysis of Codon Usage Preference in Hemagglutinin Genes of the Swine-Origin Influenza A (H1N1) Virus. *J Microbiol Immunol Infect* **2016**, *49*, 477–486, doi:10.1016/J.JMII.2014.08.011.

326. Withanage, K.; de Coster, I.; Cools, N.; Viviani, S.; Tourneur, J.; Chevandier, M.; Lambiel, M.; Willems, P.; le Vert, A.; Nicolas, F.; et al. Phase 1 Randomized, Placebo-Controlled, Dose-Escalating Study to Evaluate OVX836, a Nucleoprotein-Based Influenza Vaccine: Intramuscular Results. *J Infect Dis* **2022**, *226*, 119–127, doi:10.1093/INFDIS/JIAB532.

327. Zheng, M.; Luo, J.; Chen, Z. Development of Universal Influenza Vaccines Based on Influenza Virus M and NP Genes. *Infection* **2014**, *42*, 251–262, doi:10.1007/S15010-013-0546-4/TABLES/3.

328. Johansson, B.E.; Brett, I.C. Changing Perspective on Immunization against Influenza. *Vaccine* **2007**, *25*, 3062–3065, doi:10.1016/J.VACCINE.2007.01.030.

329. Webby, R.J.; Swenson, S.L.; Krauss, S.L.; Gerrish, P.J.; Goyal, S.M.; Webster, R.G. Evolution of Swine H3N2 Influenza Viruses in the United States. *J Virol* **2000**, *74*, 8243–8251, doi:10.1128/JVI.74.18.8243-8251.2000/ASSET/ABD41338-4895-45F9-BDB3-FCE2ECD270E6/ASSETS/GRAPHIC/JV1800597004.JPEG.

330. Abdelwhab, E.M.; Arafa, A.S.; Stech, J.; Grund, C.; Stech, O.; Graeber-Gerberding, M.; Beer, M.; Hassan, M.K.; Aly, M.M.; Harder, T.C.; et al. Diversifying Evolution of Highly Pathogenic H5N1 Avian Influenza Virus in Egypt from 2006 to 2011. *Virus Genes* **2012**, *45*, 14–23, doi:10.1007/S11262-012-0758-1/TABLES/2.

# Supplementary Material

The supplementary material of this doctoral thesis was uploaded in Zenodo online repository https://doi.org/10.5281/zenodo.7327040.

**Chapter 1**

**Supplementary table S1.1. IAV genome, protein encoded, function, and domains delimitation.**

**Chapter 3**

**Supplementary table S3.1. Total number of reads obtained in each sequenced sample.** Total number of reads and total number of reads mapped against reference genome after PCR duplicate removal in each influenza genome segment.

**Supplementary table S3.2. SNV and its effect on variant found in viral inoculum and samples collected from previously challenged vaccinated and non-vaccinated piglets with A/Swine/Spain/01/2010 (H1N1).**

**Chapter 4**

**Supplementary table S4.1. Sequenced reads obtained per sample. The total number of reads and reads mapped against reference genome after post-mapping filter application.**

**Supplementary table S4.2. SNV and its allele frequency reporter in several samples.**

**Supplementary table S4.3. SIV H3N2 single nucleotide variants detected in all samples collected from vaccinated and nonvaccinated pigs.**

**Supplementary table S4.4. HA and NA amino acid percentage identity among challenge, vaccine, and pandemic strains.**

**Chapter 5**

**Supplementary table S5.1. SIV detection in nasal swab, BALF, Lung and nasal turbinate samples collected before seeders challenge.** RT-qPCR Ct values are shown in the table.

**Supplementary table S5.2. Sequenced reads obtained per segment, subtype, and sample.** The total number reads mapped against reference genomes after post-mapping filter application are shown. The total number of reads per subtype and sample are indicated.

**Supplementary table S5.3. SIV H1N1 and H3N2 single nucleotide variants detected in all samples collected from vaccinated and nonvaccinated pigs.**

**Supplementary table S5.4. HA and NA amino acid percentage identity among challenge, and vaccine strains.**